Nagra
Nationale
Genossenschaft
für die Lagerung
radioaktiver Abfälle

Cédra
Société coopérative
nationale
pour l'entreposage
de déchets radioactifs

Cisra
Società cooperativa
nazionale
per l'immagazzinamento
di scorie radioattive

TECHNICAL REPORT 83-01

GLASSES USED IN THE SOLIDIFICATION OF HIGH LEVEL RADIOACTIVE WASTE: THEIR BEHAVIOUR IN AQUEOUS SOLUTIONS

R. GRAUER FEBRUARY 1983

SWISS FEDERAL INSTITUTE FOR REACTOR RESEARCH,
WÜRENLINGEN

Parkstrasse 23 5401 Baden/Schweiz Telephon 056/20 55 11

Nagra
Nationale
Genossenschaft
für die Lagerung
radioaktiver Abfälle

Cédra
Société coopérative
nationale
pour l'entreposage
de déchets radioactifs

Cisra
Società cooperativa
nazionale
per l'immagazzinamento
di scorie radioattive

TECHNICAL REPORT 83-01

GLASSES USED IN THE SOLIDIFICATION OF HIGH LEVEL RADIOACTIVE WASTE: THEIR BEHAVIOUR IN AQUEOUS SOLUTIONS

R. GRAUER FEBRUARY 1983

SWISS FEDERAL INSTITUTE FOR REACTOR RESEARCH,
WÜRENLINGEN

Parkstrasse 23 5401 Baden/Schweiz Telephon 056/20 55 11

Preface

The safety analysis of a final repository for high level nuclear wastes needs information on, amongst other things, the release rate of radionuclides from the glass to be used as a solidification matrix. There is such a flood of information published on this topic, that it would be difficult to summarise it all. One recently issued bibliography (40) alone gave 360 references on glass corrosion, without claiming to be comprehensive.

A simple uncritical catalogue of leaching and corrosion data would be of little value, as so many of the experiments have been carried out under unrealistic conditions. An interpretation of isolated data would also be of little use in a safety analysis, because it would fail to take into account the complex relationships and interactions within the final repository.

Examination of the literature has revealed a lack of critical evaluation of the available data. It has also shown that glass corrosion is generally treated by specialists as an isolated subject. Understanding the complex processes of glass corrosion would certainly benefit by contributions from other fields, such as dissolution mechanisms and kinetics in mineral materials, which are topics of wider interest.

This report, then, has not produced a collection of data, but rather an essay, an attempt to provide a survey of glass corrosion, by dealing with three main points:

- mechanism and kinetics of glass corrosion
- evaluation of experimental results, taking into account possible final repository conditions

- identification of gaps in current knowledge and recommendations for further investigations.

The essay does not claim to be exhaustive and by its very nature must be, to some extent, subjective.

This work is issued in parallel as a Nagra technical report and as an EIR report. This present report is translated from the original German.

Contents

Summary

Because of their amorphous structure, glasses are particularly suitable matrixes for the solidification of the mixture of radionuclides included in the high level wastes from reactor fuel reprocessing. They are not sensitive to variations in the fractions present of different waste oxides and are resistent to the effects of irradiation. In particular, borosilicate glasses have been investigated for around 25 years and the vitrification techniques have been tested on the technological scale.

The environmental conditions within a final waste repository are expected to be such that the chemical resistance of glasses to attack by groundwaters is of special interest.In the present report the corrosion behaviour is described, with emphasis being placed upon the most significant controlling parameters. Since experimental determination of corrosion rates must be done in relatively short-time experiments, the results of which can depend strongly upon the measurement methods employed, it is necessary to carry out a critical assessment of the techniques commonly used in laboratory work.

Experimental results are illustrated by means of selected examples. Particular emphasis is placed upon the effects of increased temperatures and of irradiation.

The models which have been proposed for the estimation of the long-term corrosion behaviour of glasses are not yet fully sufficient and improvements are required. Furthermore, the actual corrosion rates which are fed into such models must be replaced by values more appropriate for the actual environmental conditions to which the glasses are most likely to be exposed within high level waste repositories. It should be noted, however, that even with current conservative input data on corrosion rates, typical estimated lifetimes for vitrified waste blocks are of the order of 10^5 years.

The report concludes with recommendations concerning the most useful areas for further investigations.

Zusammenfassung

Gläser sind wegen ihrer amorphen Struktur besonders geeignet, das bei der Aufarbeitung von Reaktorbrennstoff anfallende Gemisch von hochradioaktivem Abfall zu verfestigen: sie sind unempfindlich gegen Schwankungen in der Zusammensetzung der Abfalloxide und gegen Strahlenschäden. Die dazu verwendeten Borosilikatgläser werden seit 25 Jahren untersucht, und die Abfallverglasung ist im technischen Massstab erprobt.

Im Hinblick auf mögliche Störfälle in einem Endlager ist die chemische Beständigkeit solcher Gläser gegenüber Wasser von besonderem Interesse. Dieser Bericht befasst sich mit dem Korrosionsverhalten von Gläsern, wobei die wesentlichen Einflussgrössen diskutiert werden. Die für Sicherheitsbetrachtungen benötigten Auflösungsgeschwindigkeiten müssen in relativ kurzzeitigen Experimenten bestimmt werden. Da die Art der Versuchsführung das Ergebnis in weiten Bereichen beeinflusst, ist eine kritische Beurteilung dieser Methoden erforderlich.

Experimentelle Ergebnisse werden anhand ausgewählter Beispiele dargestellt, wobei insbesondere auf die Einflüsse erhöhter Temperatur und radioaktiver Strahlung eingegangen wird.

Die Modelle zur Abschätzung des Langzeitverhaltens des verglasten Abfalls sind noch unvollkommen und bedürfen einer Verbesserung. Auch die in solche Modelle eingesetzten Auflösungsgeschwindigkeiten sollten revidiert werden: wünschbar sind Werte, die die Umgebungsbedingungen am Lagerort berücksichtigen. Es ist jedoch festzuhalten, dass schon konservative Modellannahmen mit konservativen Werten für die Auflösungsgeschwindigkeit eine "Lebensdauer" der einzulagernden Glasblöcke in der Grössenordnung von 10^5 Jahren erwarten lassen.

Dieser Bericht schliesst mit Empfehlungen für weitere Untersuchungen.

Résumé

En raison de leur structure amorphe, les verres sont particulièrement indiqués pour la solidification de la liqueur constituée par les effluents hautement radioactifs issus du traitement du combustible de réacteurs nucléaires: ils sont insensibles aux variations de la composition des oxydes contenus dans les déchets et aux dommages causés par les rayonnements. Les borosilicates utilisés dans ce but sont étudiés depuis 25 ans et la vitrification des déchets est techniquement éprouvée.

Eu égard aux événements possibles dans un dépôt de stockage définitif, la stabilité chimique de tels verres au contact avec de l'eau est d'une grande importance. Ce rapport traite du comportement des verres vis-à-vis de la corrosion, pour lequel les paramètres essentiels sont discutés. Les vitesses de dissolution prises en compte dans les analyses de sécurité ne peuvent être déterminées que dans des expériences de relativement courte durée. Comme la manière de mener ces travaux de recherche influence les résultats dans une large mesure, un jugement critique des méthodes utilisées est nécessaire.

Des données expérimentales sont présentées sur la base d'exemples choisis, pour lesquels on s'est étendu plus spécialement sur l'influence d'une température élevée et sur l'effet des rayonnements radioactifs.

Les modèles employés pour l'estimation du comportement à long terme des déchets vitrifiés sont encore imparfaits et nécessitent une amélioration.

Les vitesses de dissolution mises en jeu dans de tels modèles devraient aussi être revues: des valeurs qui tiennent compte des conditions d'environnement au lieu de stockage sont souhaitables. On peut cependant affirmer que déjà des hypothèses prudentes conduisent à une "durée de vie" des blocs de verre à stocker de l'ordre de 10^5 ans. Le rapport s'achève par des recommandations pour des investigations futures.

1. Requirements for a matrix used in the solidification of highly radioactive wastes: Why glass?

As the fuel in a nuclear power plant burns up, considerable quantities of highly radioactive fission products are formed. A 1000 MWe power plant produces annually about 1000 kg of fission material (149), consisting of a complex chemical mixture (Table 1) (124). The waste mixture contains not only the fission products, but also the remains of unseparated uranium and plutonium, transuranics and also corrosion products and some traces of chemicals from reprocessing.

Figure 1 shows the most important active elements with their decay rates. The β-and γ-radiation will have largely died out after 300 years, and the α-radiation from the decay of transuranics will then be dominant. To isolate the waste products safely from the environment they must be converted into a stable state and be isolated from the biosphere for a period of some 10'000 years. Thus the material sciences are called upon to meet extremely high demands, as completely new horizons for planning and extrapolation are opened to them.

A matrix to be used for the solidification of high level waste (HLW) must meet the following requirements:

a) good chemical stability
b) high loading capacity for the waste products
c) unaffected by variations in waste composition
d) mechanical stability
e) thermal stability (heat produced by radioactive decay)
f) unaffected by radioactive radiation (low susceptibility to structural damage)
g) availability of raw materials
h) simple, reliable and economical production technology.

	Wt %	Atom %		Wt %	Atom %
Rb_2O	0.937	0.489	Nb_2O_3	---	---
Cs_2O	6.804	2.638	MoO_3	10.798	4.099
SrO	2.476	1.305	Tc_2O_7	3.123	1.101
BaO	3.745	1.334	RuO_2	7.043	2.892
Y_2O_3	1.323	0.640	Bi_2O_3	---	---
La_2O_3	3.351	1.124	RhO_2	1.182	0.479
CeO_2	7.646	2.427	PdO	3.692	1.648
Pr_2O_3	3.166	1.049	CdO	0.219	0.093
Nd_2O_3	10.837	3.510	Ag_2O	0.156	0.073
Pm_2O_3	0.282	0.090	Sb_2O_3	0.049	0.018
Sm_2O_3	2.257	0.707	SnO_2	0.185	0.067
Eu_2O_3	0.506	0.157	U_3O_8	14.684	2.858
Gd_2O_3	0.282	0.085	NpO_2	1.216	0.247
Dy_2O_3	0.005	0.001	PuO_2	0.165	0.033
SeO_2	0.151	0.074	Am_2O_3	0.384	0.079
TeO_2	1.702	0.583	Cm_2O_3	0.107	0.022
ZrO_2	11.629	5.157	oxygen	---	64.909

Table 1: Composition of the waste from a light water reactor. Enrichment 3% U-235, burnup 30'000 MWd/tU, reprocessed 150 days after discharge. 0.5 % U and 0.5 % Pu are not separated (124).

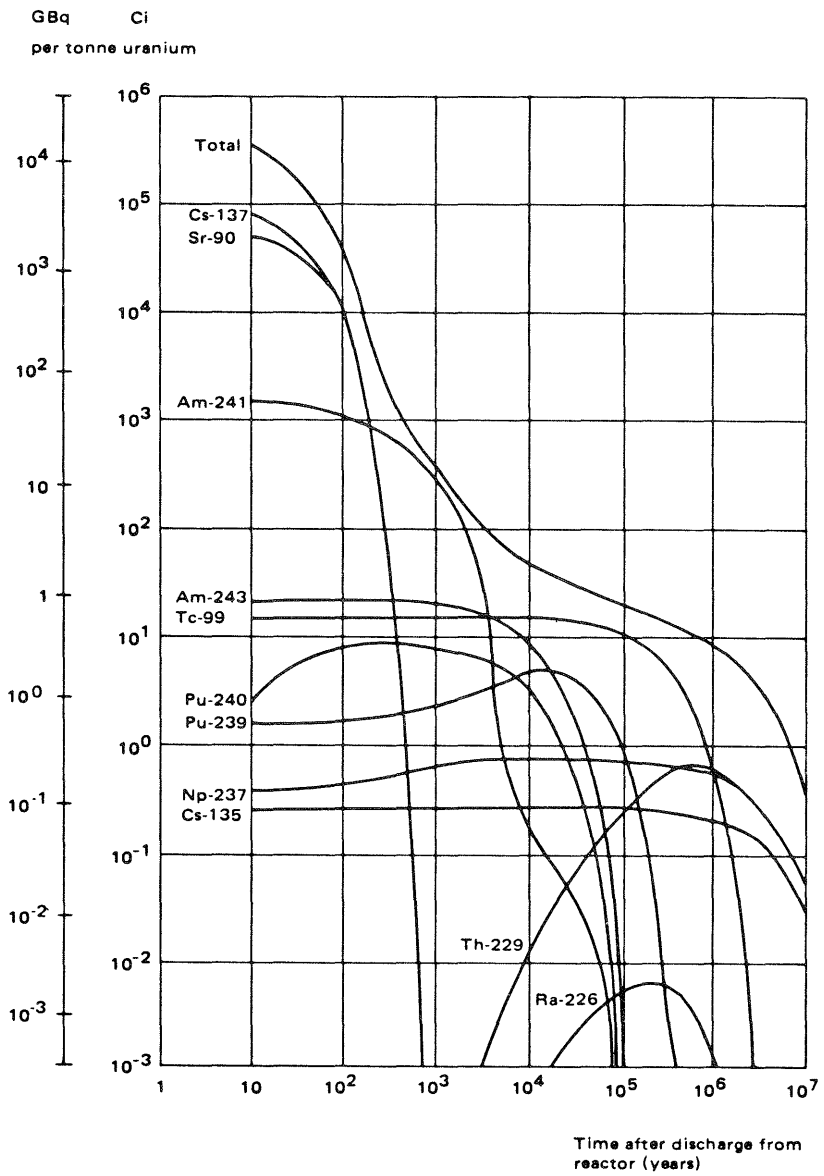

Figure 1: Radioactive decay of spent fuel. Reprocessing: 10 years after discharge. IAEA 1982.

Many materials used for the fixation of low and medium level wastes (e.g. bitumen, cement) are unsuitable for high level wastes, because of their low radiation resistance and poor thermal stability: the materials chosen for solidification must be inorganic and contain no water. Various summary works (49, 149, 207) give information about possible solidification matrices.

Glasses are particularly well suited as waste matrices (80) for several reasons. The production technology is both well-known and efficient. With their amorphous lattice structure they have a high loading capacity for oxides and are almost completely unaffected by variations in waste composition, which arise from processing.

Glasses on a phosphate basis have an advantage over silicate glasses, in that they can absorb larger quantities of sulphate and molybdate without phase separation. One objection to their use, however, is that the highly corrosive melts attack normal receptacle materials. Also, at temperatures of 400 to 500°C they form partly crystalline (devitrified) products with poor chemical resistance. Glasses with high SiO_2 content are chemically very resistant but their high melting temperatures make them unsuitable as HLW matrices: during glass production the important radionuclides cesium and ruthenium would be almost completely vaporized.

Borosilicate glasses, on the other hand, have production temperatures of 1000 to 1100°C and satisfactory chemical resistances. The last 25 years have therefore seen the intensive development of HLW glasses of this type in several countries (82, 102, 143), and in France an industrial plant for the production of active glasses has been in operation for some years (19, 20, 131, 151).

The use of a titanate ceramic (Synroc: synthetic rock) as an alternative to borosilicate glasses has been advocated, for some time, notably by A.E. Ringwood (175). Emphasis has been placed on the good leaching properties at higher temperatures (176). However, there are some drawbacks to the system (149): the production process is relatively expensive and has not yet been tested with active material on an industrial scale. The crystalline structure could also be a disadvantage. Its flexibility to cope with differing proportions of waste and with variations in waste composition still needs to be investigated. The resistance of the lattice structure to damage by α-decay of the stored transuranics also needs to be researched.

Information about further possibilities for waste storage - e.g. in the form of anhydrous oxides or "coated particles" - is given in the summary works listed.

The concept of a final repository for highly radioactive wastes envisages a diversified system of several overlapping transport barriers, the solidification matrix forms only one part of this system. The waste product, processed so as to be chemically resistant, is packed in a metal or ceramic canister (overpack). During the first phase of storage this container forms the absolute barrier against the escape of radionuclides. The material of the container should have a life of about 1000 years, even under adverse conditions. Materials such as titanium, copper or sintered aluminium oxide (133, 134) come into consideration. The container is deposited in a geologically stable rock formation, with as high an impermeability to water as possible. In Switzerland the granite found at a depth of some 600 - 1700 m below the north Mittelland could be a suitable site. As a further transport barrier the container is embedded in bentonite. This argillaceous mineral is almost totally impervious to water and is effective because of its high expansion properties and its ability to adsorb large quantities of escaping radionuclides.

The only part of this barrier system to be dealt with in this report will be the borosilicate glasses and above all their chemical resistance. But because the glass matrix is only a part of the total system, an evaluation of the resistance of the glass in the context of a safety study will not be made in isolation.

Detailed information on safety precautions and risks in the storage of radioactive wastes is given in a Nagra report (156).

2. Glass constitution and structure

As parts of this chapter will be summarising readily available text-book knowledge, not all observations are supported by references. For detailed information about the structure and properties of glasses refer to more comprehensive works (8, 59, 63, 104, 189, 212).

2.1 The glassy state

Glasses can be defined broadly as frozen, undercooled liquids. As the atomic structural units of a liquid are irregularly placed, this definition implies that glasses are amorphous. The difference between a glass and a crystalline solid can be seen from a volume/temperature diagram (figure 2). On cooling the melt, the crystalline phase is reached at a temperature T_S. In the V/T diagram this process is shown by a discontinuity. If crystallisation is prevented during cooling, e.g. by rapid cooling, then an undercooled fluid is produced whose structural elements are still free to move. Further cooling increases the viscosity until at a temperature T_G, mobility is lost and the undercooled fluid is frozen forming a glass. The characteristic V/T curve changes at this point, T_G, the slope often becoming about the same as that of the characteristic curve of the corresponding crystalline material.

T_G is the glass transformation temperature, it separates the frozen and the plastic states. Unlike the melting temperature, T_S, T_G does not have a constant value. It depends, as figure 2 shows, on the rate of cooling.

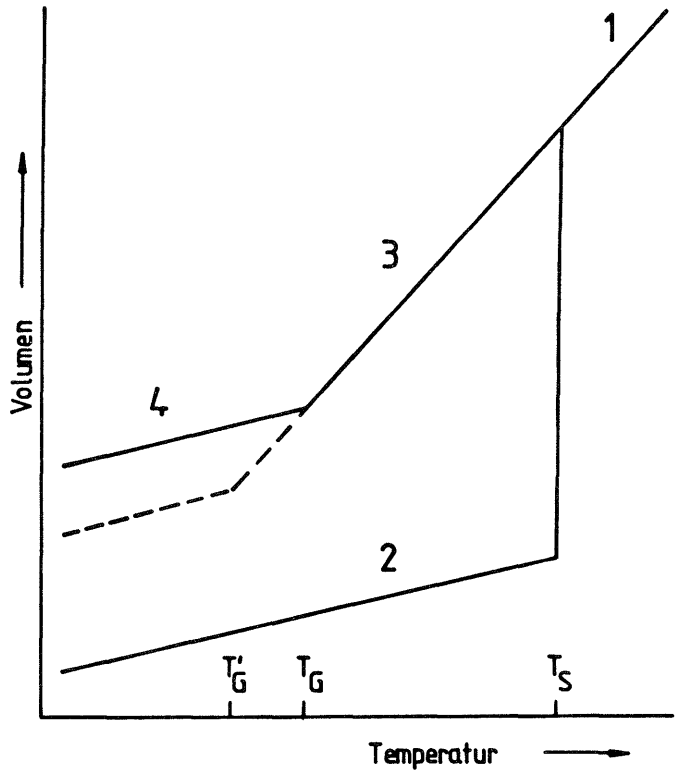

Figure 2: Relationship between volume and temperature for fluid, glassy and crystalline states. T_S: melting temperature. T_G: glass transformation temperature.

1: melt. 2: crystal. 3: undercooled fluid. 4: glass. Unlike T_S, T_G is not constant: the value of T_G is reduced by slower cooling (T'_G).

For many industrial glasses T_G lies in the range 530 to 600°C. Some values for viscosity are given here by way of illustration (104): a glass melt has a viscosity of about 10 Pa.s, processing takes place between 10^5 and 10^7 Pa.s. At the transformation point viscosity is about 10^{12} Pa.s. At room temperature it rises to 10^{19} Pa.s and the plasticity of the glass is virtually lost.

2.2 Glass structure

Whereas the co-ordination polyhedrons in a crystalline oxide are arranged in a geometrically regular pattern, those in the vitreous state form an irregular three dimensional network. Figure 3 illustrates this for crystalline and vitreous SiO_2. In both cases the SiO_4-tetrahedrons are bonded at the corners, in glass the bond-angles are slightly distorted.

If an alkali oxide, e.g. Na_2O, is added to the SiO_2-glass, the network is loosened (figure 3c) as discontinuities are produced:

$$\geqslant Si\text{-}O\text{-}Si\leqslant + Na_2O \rightarrow 2 \geqslant Si\text{-}O^- + 2\ Na^+$$

The incorporation of sodium oxide results in an increase in the density of the glass: incorporation in the loose network does not produce any substantial increase in volume. The formation of network discontinuities also reduces viscosity.

Alkaline earth ions can be incorporated in a similar fashion. Depending on the glass composition, small, high valency ions, such as aluminium, can either produce discontinuities, or be built into the network. With the radii ratio $r_{Al}3+/r_O2- = 0.43$, the aluminium ion lies on the border between four and six coordination. With the coordination number 4 - in analogy to silicates - it can replace silicon isomorphously, and is thus incorporated into the lattice. For each aluminium ion incorporated a negative charge is introduced. Aluminium can act as a network former only if this charge is neutralised by, for example, alkali metal ions. In glasses where the mol-ratio $Na_2O/Al_2O_3 > 1$, the discontinuities are closed (figure 4), so that the glass structure is re-strengthened. Such a strengthening of the glass improves, amongst other things, the chemical durability of the glass. However, if the mol-ratio is < 1, the superfluous aluminium ions are incorporated as network modifiers with a coordination number of six. Recent research has shown (114) that current ideas on the structure of aluminium-silicate glasses will have to be revised.

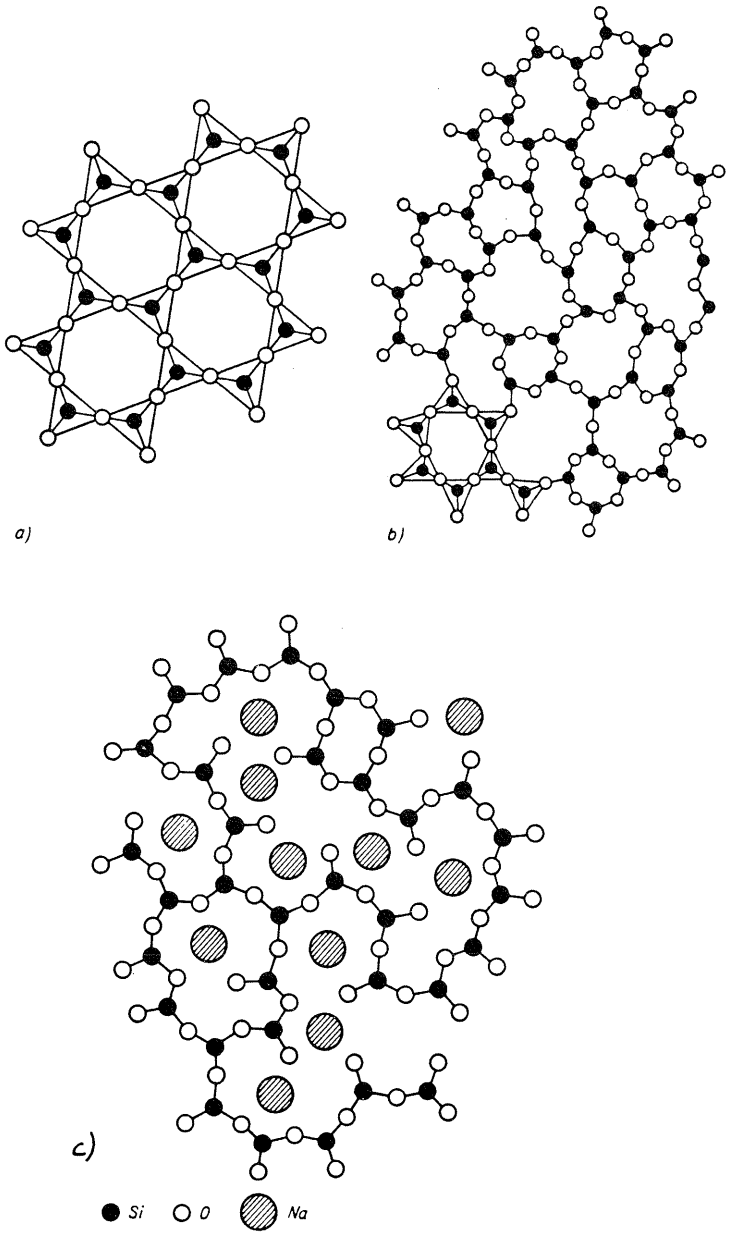

Figure 3: Schematic representation of SiO_2 and glass structures as section through the SiO_4 tetrahedron network. a) crystalline, b) vitreous SiO_2, c) sodium silicate glass.

Boron trioxide can also be incorporated into the SiO_2-network. Boron normally has a coordination number of 3. In the presence of alkali metal ions a coordination number of 4 can be adopted and the B_2O_3 can replace the SiO_2 which leads to closing of the network discontinuities (2).

As the concentration of SiO_2 and M_2O (M - metal) is reduced the proportion of boron with coordination number 3 increases (150). It is to be assumed that within the glass structure two BO_4^- tetrahedrons may not be linked directly together.

The structural principles given here can be generalised and applied to non-silicate glasses. According to the lattice theory of Zachariasen and Warren the following selection principles apply (212):

1. A compound tends to glass formation if the smallest building units are stable polyhedrons.
2. Two such polyhedrons may not have more than one common corner.
3. An anion (e.g. O^{2-}, S^{2-}, F^-) may not be shared between more than two central atoms of a polyhedron.
4. The number of corners of a polyhedron must be < 6.
5. At least three corners of a polyhedron must be bonded with neighbouring polyhedrons by anion bridges.

All the cations involved in glass formation can be divided into three groups:

1. Network formers, with coordination number 3 or 4 and largely covalent chemical bonding with oxygen (Si, B, P).
2. Network modifiers, with coordination number 6 or more, their incorporation in the glass produces network discontinuities (Na, K, Ca).
3. Intermediate oxides, with cations of coordination number 4 or 6 (Mg, Al, Zn, Nb, Be).

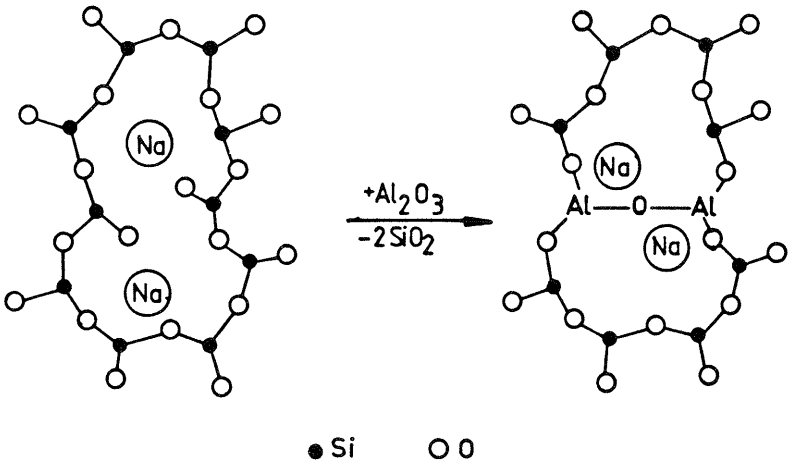

Figure 4: Schematic representation of the replacement of SiO_2 by Al_2O_3 in a sodium silicate glass. The network discontinuity is closed (189).

The intermediate oxides take an in-between position. Depending on the composition of the glass, they can either be incorporated into the network, with a coordination number 4 (network densifiers), or, with a higher coordination number, they can loosen the structure. According to Diezel (55) the three categories can be distinguished by the field strength of their ions (table 2).

Element	Valency	Ion radius (at KZ = 6)	usual coordination number	Ion spacing in Oxides	Field intensity in spacing of O^{2-}-Ions	
	Z	r [Å]	KZ	a [Å]	Z/a^2	
K	1	1,33	8	2,77	0,13	
Na	1	0,98	6	2,30	0,19	
Li	1	0,78	6	2,10	0,23	
Ba	2	1,43	8	2,86	0,24	network
Pb	2	1,32	8	2,74	0,27	modifiers $Z/a^2 \approx$
Sr	2	1,27	8	2,69	0,28	0,1 ... 0,4
Ca	2	1,06	8	2,48	0,33	
Mn	2	0,91	6	2,23	0,40	
Fe	2	0,83	6	2,15	0,43	
Mn	2	0,83	4	2,03	0,49	
Mg	2	0,78	6	2,10	0,45	
			4	1,96	0,53	
Zr	4	0,87	8	2,28	0,77	intermediate
Be	2	0,34	4	1,53	0,86	oxides
Fe	3	0,67	6	1,99	0,76	$Z/a^2 \approx$
			4	1,88	0,85	0,5 ... 1,0
Al	3	0,57	6	1,89	0,84	
			4	1,77	0,96	
Ti	4	0,64	6	1,96	1,04	
B	3	0,20	4	1,50	1,34	network
			3	1,36	1,63	formers
Si	4	0,39	4	1,60	1,57	$Z/a^2 \approx$
P	5	0,34	4	1,55	2,1	1,4 ... 2,0

Table 2: Classification of cations according to field intensity. After Diezel (55).

2.3 Crystallisation and phase separation of glasses

Devitrification

Unlike crystals or crystal mixtures of the same overall composition, undercooled melts and congealed glasses are metastable. A transition from vitreous to crystalline state (i.e. devitrification) is only possible if sufficient time is available for the formation and growth of crystal nuclei. The relevant models developed originally by Tammann (202) are still valid (figure 5). A qualitative explanation only is given here. For further details see for example (212).

In a melt at equilibrium at the melting point of a substance crystals can neither grow nor be dissolved. Cooling - corresponding to an increase in supersaturation - results in homogenous nucleation and crystal growth. Both reach a maximum and then decrease again to a negligible value.

Industrial glass melts always contain enough impurities to act as heterogeneous crystal nuclei. In HLW glasses these are present as noble metals or undissolved oxide particles. The kinetics of homogeneous nucleation is, therefore, of little importance in devitrification processes. Consequently crystal growth, which depends on supersaturation and in particular on viscosity, is more important. In many glasses the product of radial crystal growth rate, u, and viscosity, η, is proportional to the difference, ΔT, between the melting temperature and the actual temperature of the crystalline compound (58):

$$\frac{u.\eta}{\Delta T} = \text{const.}$$

Viscosity is largely temperature dependent, so that at temperatures below the transformation temperature u becomes negligible. Other sources (104) have indicated that the activation energy for crystal growth is considerably lower than that for viscous flow.

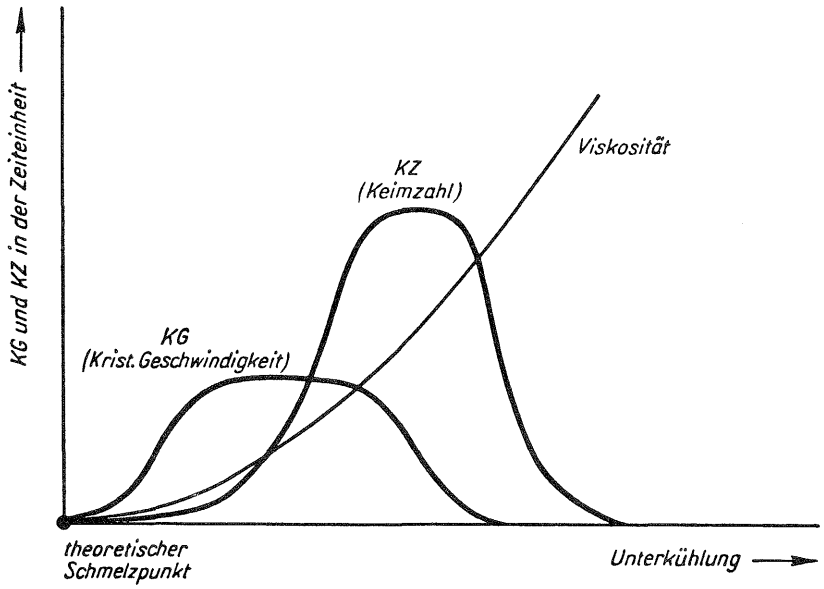

Figure 5: Dependence of homogeneous nucleation and crystal growth on the undercooling of the glass melt (Tammann).

Devitrification alters the chemical properties of the glass. The crystals which separate out often contain a higher percentage of SiO_2 than the original glass. Devitrification of window glass, with the approximate composition Na_2O . 0.7 CaO . 3.3 SiO_2 results in the formation of devitrite (Na_2O . 3 CaO . 6 SiO_2). The remaining glass has a reduced concentration of SiO_2 and calcium and, correspondingly, resistance to corrosion is reduced. The volume changes associated with crystallisation, as well as the differing thermal expansions of crystals and of glass, also produce internal stresses.

A controlled devitrification of special glasses, however, can produce crystalline material of high resistance. These glassceramics, e.g. known under the name Pyroceram, are generally based on a SiO_2-Al_2O_3-M_2O system.

Phase separation

Many liquid silicate mixtures have miscibility gaps which increase as the temperature is reduced. On cooling two distinct phases arise (figure 6). If the miscibility gap lies in the temperature range of the undercooled melt, phase separation due to high viscosity is no longer visible to the naked eye. Droplet or interwoven structures are formed, as represented schematically in figure 7.

Systematic investigations have shown that many glasses tend to form vitreous phase separations and so are not homogeneous (212). Often the phase separation structures are so fine that they can be detected only with the electron microscope.

Phase separation in sodium-borosilicate glasses has been known for a long time and is used in the production of glasses with special properties. Heat treatment of glasses of the Vycor type produces a porous structure (figure 7c) of almost pure SiO_2 and a sodium borate phase, which can be leached with acid. The remaining SiO_2 skeleton is then sintered. This process can produce, without a high melting temperature, glasses with a high chemical resistance having about 96 % SiO_2 content.

With correct processing Pyrex type glasses have no (212) phase separation structure or only a very fine one (57). Improper heat treatment coarsens the structure and this leads to a dramatic reduction in the chemical resitance of the glass (212).

Vitreous phase separation in borosilicate glasses consequently leads to a change in corrosion behaviour. Alkali and earth alkali ions accumulate in the borate phase, so that the fission products, such as cesium and strontium, can be released by preferential leaching. Particular attention should, therefore, be paid to phase separation in the development of HLW glasses.

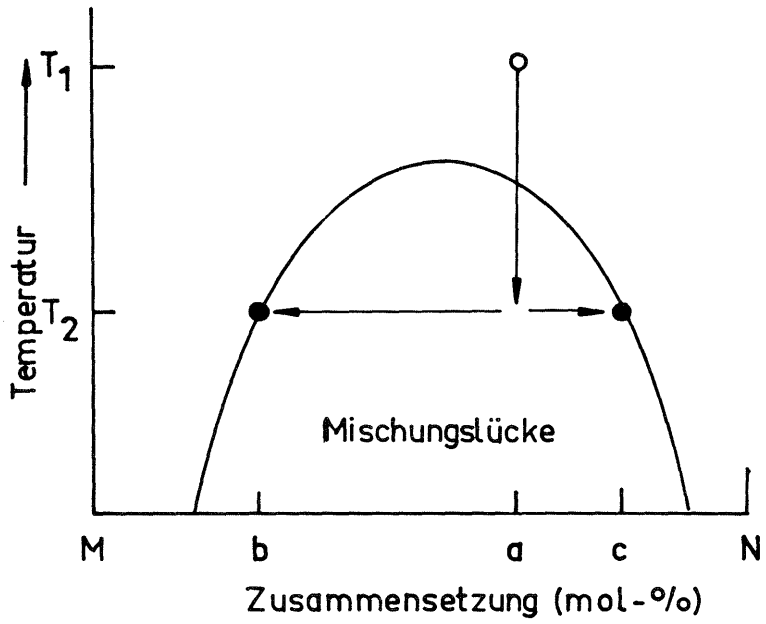

Figure 6: Hypothetical binary fluid mixture (components M and N) with a miscibility gap. On cooling from T_1 to T_2 a solution of composition, a, dissociates into two phases with composition b and c.

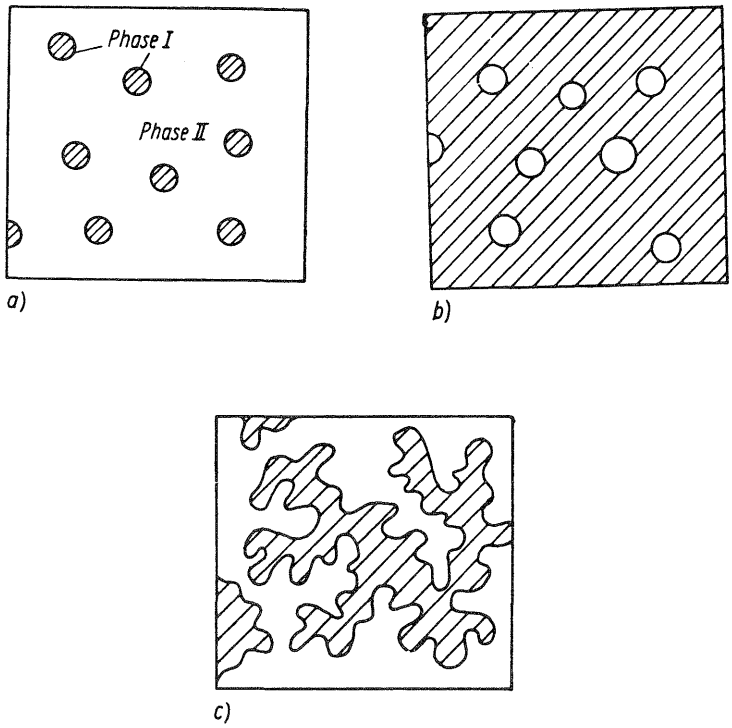

Figure 7: Schematic diagram of the structure of phase separated ternary glasses with two network formers and one network modifier (e.g. SiO_2, B_2O_3, Na_2O).

a) Low concentration of network former 1. b) High concentration of 1. c) Interwoven structure with similar concentrations of network formers 1 and 2. (63)

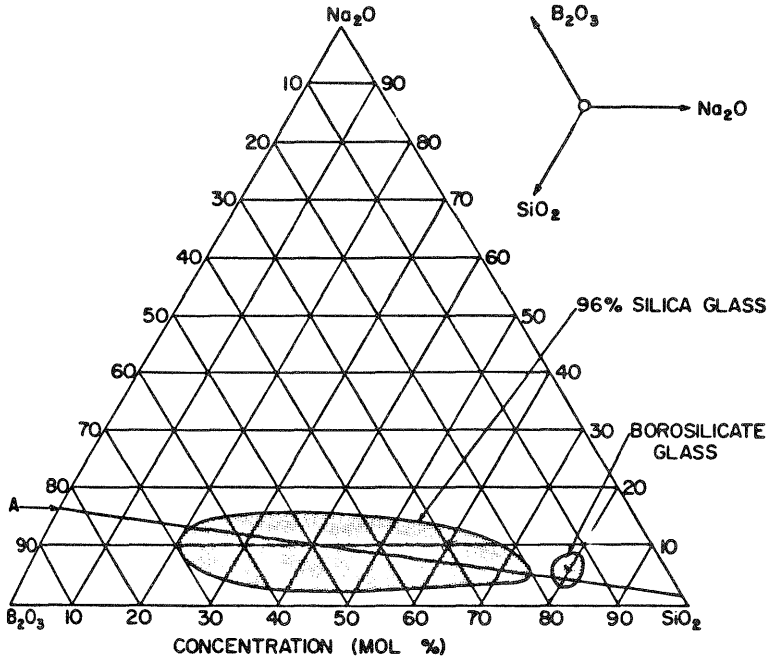

Figure 8: Phase segregation range in the ternary glass system Na_2O-B_2O_3-SiO_2 (74)

3. Chemical properties of glasses

3.1 The corrosion of mineral solids: general model concepts, nomenclature

The prediction of the chemical behaviour of HLW glasses in final repository conditions should be made as accurately as possible. The precision of such extrapolations will, of course, be improved if they are not based solely on empirical experiments but include an understanding of reaction mechanisms in formulating kinetic models.

Unlike the corrosion behaviour of metals in aquatic media (106), the dissolution behaviour of mineral solids has no sound theoretical foundation. It is currently not possible to write a textbook on this topic, even though these reactions are of such great importance in many specialised fields. Geochemists are interested in the weathering of minerals, particularly silicates (206), hydrometallurgists are interested in the dissolution behaviour of ores and material scientists are seeking theoretical principles on which to base the evaluation of the stability of ceramic materials.

The use of surface sensitive analytical methods together with surface coordination models (79) has produced some experimental and theoretical progress in the last few years. However a review of current literature shows that individual fields profit too little from advances in neighbouring fields. An interdisciplinary approach could be expected to lead to a better understanding of the surface chemistry of mineral materials.

A material of complex structure, such as silicate crystals or glass, has two basically different mechanisms for reacting with an aqueous solution (figure 9).

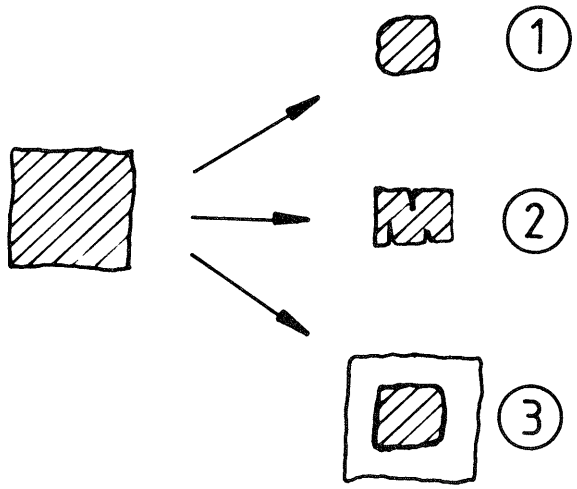

Figure 9: Types of reaction for dissolution of mineral solids.

1) stoichiometric, controlled by diffusion.
2) stoichiometric with rate determining surface reaction
3) selective dissolution.

When the components of a substance are dissolved in proportion to the chemical composition of the material, this is stoichiometric or congruent dissolution.

If one component is preferentially dissolved, then the dissolution process is selective, the original dimensions of the substance may remain unaltered.

Several authors treat incongruent dissolution as yet another special case. Here the dissolution of the solid is followed by the precipitation of a new solid. A look at the dissolution mechanism shows that this is not really a new case. Congruent or selective dissolution results in the formation of a new phase only if the solubility of that new phase is exceeded.

This can depend on several factors, for example, the flow of water through the system: if the dissolved reaction products are rapidly removed, as in an open system, then precipitation of the new phase does not occur. However, in a closed system, the new phase will be precipitated.

If the dissolution rate for a solid is controlled by diffusion, i.e. is limited by the transport processes within the solution, then, in general, the shape of the solid becomes rounded. If the rate is controlled by phase boundary reactions, the sharp edges of the solid shape are retained. Structural defects, such as screw dislocations, can produce points of preferential attack, resulting in an etched pattern. According to Berner (13), the dissolution reactions of minerals in natural conditions are usually controlled by phase boundary reactions.

Reaction kinetic formulae which describe a dissolution process must be consistent with the laws of thermodynamics. Theoretically there are two different approaches:
The net reaction rate, R, in a reversible reaction, is given by the difference between the rate of dissolution and the rate of reprecipitation on the surface:

$$R = \vec{R} - \overleftarrow{R} \quad (R \text{ e.g. in } mol.cm^{-2}.s^{-1}) \qquad I$$

A formula of this type requires a detailed knowledge of each individual reaction step. So far only very few systems can be described on this basis, e.g. the dissolution of calcite in water (169).

In the second type of formula the argument is purely thermodynamic: the relative saturation S_r is regarded as acting as a "brake" on the dissolution reaction, so that in a saturated solution, $S_r = 1$, the reaction ceases:

$$\vec{R} = \vec{R}_0 \, (1 - S_r) \qquad II$$

It is generally possible to re-express formulae of type I in terms of

type II, this can be of advantage for practical use with specific kinetic equations.

As glass can not be formed from aqueous solution, the dissolution reactions are not reversible. Also a glass does not have any thermodynamically defined solubility or saturation. The kinetic formulae of types I and II are, therefore, not strictly applicable. So fundamental problems arise in any quantitative interpretation of glass corrosion rates - thermodynamic models can strictly be applied only when no more glass is present. Also in formula I, R has no physical-chemical significance.

3.2 The dissolution of glasses

Ideally the aim would be to give the time dependence of dissolution rates at various temperatures and pressures, whilst also taking into account the effects of solvent and glass composition. However, in view of the number of possible variations here, it would be pointless to try to be comprehensive. But a qualitative survey can be made by typifying the particular processes. Any explanations should be based on systems which are not too complex. Before going on it is necessary here to give some definitions of terms used:

Corrosion is the disintegration of the glass network e.g. by congruent dissolution.

Leaching is the selective dissolution of individual glass components.

As these processes often take place simultaneously, it is not always possible to make a sharp distinction. The terms solution, dissolution process, etc., are used in a general sense.

Various detailed works (4, 63, 74, 97) and summaries (42, 51, 90-92) have been published on the chemical behaviour of glasses.

3.2.1 Network dissolution

To give a clearer understanding of the corrosion of glass, the behaviour of SiO_2 in solutions of different pH will first be discussed. The type of structure is not of primary importance, so a study of the dissolution behaviour of quartz glass can draw on experimental results for amorphous SiO_2 (silicagel) and also quartz.

Early experiments on quartz glass (60, 66) have shown that the corrosion rate over a wide pH range remains almost constant. At pH > 9 there is a rapid increase in reaction rate (figure 10). This phenomenon can be explained qualitatively by the protolytic behaviour of the dissolved silicic acid (figure 11) (200). At pH < 9, the species H_4SiO_4, acidity constant $10^{-9.5}$, is dominant, it has a low, constant solubility. At pH > 9.5 the de-protonated form is dominant and it has a higher solubility.

Rimstidt and Barnes (174) have investigated the temperature dependence of the solubility of various SiO_2 modifications in approximately neutral solutions. The following formula arose from this work:

$$R = k_+ - k_- \ (H_4SiO_4)$$

this can also be expressed in the form:

$$R = R_0(T)(1 - S_r)$$

The activation energy of k_+ is 72 and of k_- 50 kJ/mol. At temperatures below 100°C the reverse reaction is very slow, so high supersaturations are produced. At room temperature the period of time needed to reach equilibrium by precipitation is estimated at 10 years. The study also produced the important information that the rate of dissolution is practically independent of pressure up to 500 bar.

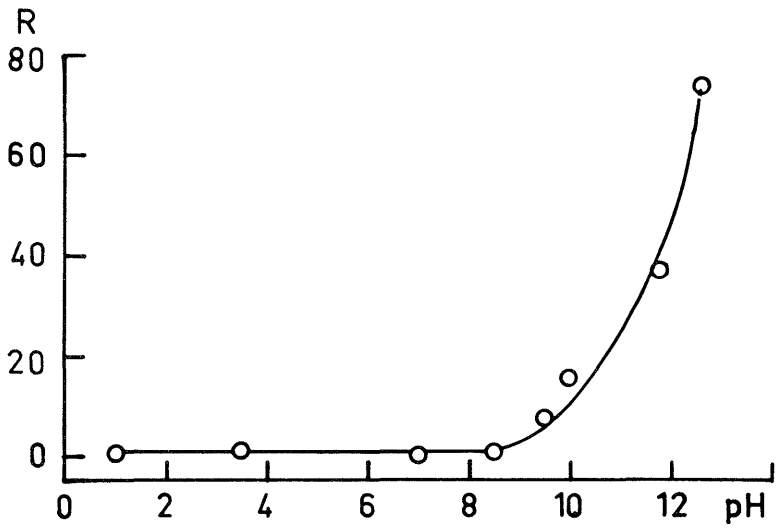

Figure 10: Effect of pH on rate of silica extraction from fused silica powder at 80°C. R in µg SiO_2/g glass.min. (60).

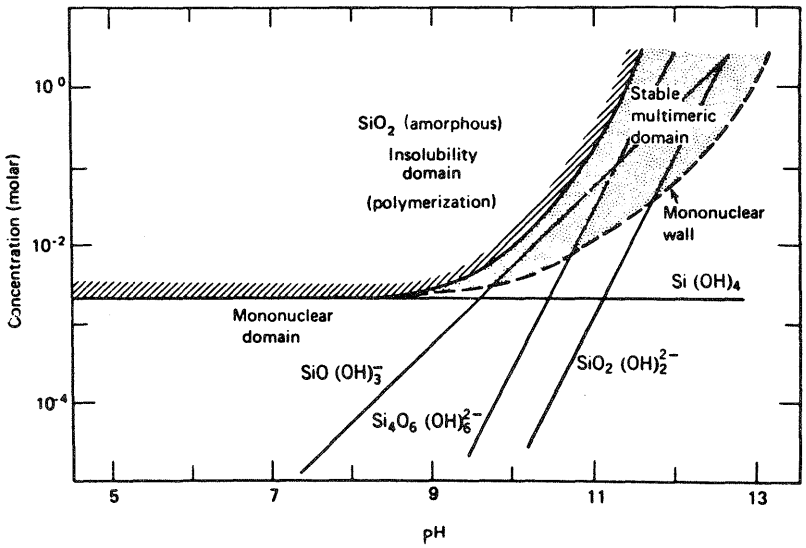

Figure 11: Solubility of amorphous silica as a function of pH
The line surrounding the shaded area gives the maximum soluble silica. The mononuclear wall represents the lower concentration limit below which multinuclear species are not stable. (200).

The results of Wirth (228) are of interest in a discussion of the reaction mechanism. Here the dissolution rate of amorphous SiO_2 at pH > 6 was found to depend on the surface charge. It should be noted in this connection that hydrated oxide surfaces are polyelectrolytes in aqueous solutions and undergo protolysis (79, 187, 200). The protolysis equilibria can be represented, using a surface acidity constant, Ka^s, thus:

$$\geqslant Si\text{-}OH_2^+ \rightleftharpoons \geqslant Si\text{-}OH + H^+$$

$$Ka_1^s = \frac{[H^+]\ \{SiOH\}}{\{SiOH_2^+\}}$$

$$\geqslant Si\text{-}OH \rightleftharpoons \geqslant Si\text{-}O^- + H^+$$

$$Ka_2^s = \frac{[H^+]\ \{SiO^-\}}{\{SiOH\}}$$

$\geqslant Si$ represents one silicon atom fixed on the surface of the solid, ( ) and { } represent molar concentration and concentration of the surface species in mol . kg^{-1} or mol . m^{-2}, respectively. For amorphous SiO_2, $pKa_1^s \approx -3$ and $pKa_2^s = 6.8$ (187). It follows from this that the SiO_2 surface does not readily protonise and that at pH > 5 the surface has a negative charge.

According to Wirth, the dissolution rate at pH < 10 is given by:

$$R = k\ \{\geqslant SiO^-\}^2\ (1 - S_r).$$

No discussion will be made here of why the square of the surface charge affects the reaction rate. However, two conclusions can be drawn from the relationship:

a) The reaction rate can be influenced by modifying the surface charge, e.g. by the adsorption of metal ions. This explains the effect of dissolution inhibitors (see section 3.3.1).

b) Surface charge is related to surface potential, which can be measured, so potential measurements can be used to investigate the corrosion of glasses (15, 36).

Various publications indicate that the solubility of SiO_2 increases slightly in an acid medium (122). According to recent kinetic studies (113), the rate of dissolution shows a marked increase only in very strong acids (pH < 0). This increase can be explained by the increased difficulty of the SiO_2 surface to be protonated (79).

The network dissolution of silicate-type multi-component glasses follows the same general principles as the dissolution of SiO_2 (figure 12) (66). The corrosion rates for glass are generally higher and are influenced to a large extent by the glass composition. The critical pH value for an increase in corrosion rate is also influenced by the composition of the glass. For commercial glasses the value is in the region pH 8.5 to 9. Below this pH value network dissolution is negligible: for window glass at pH 7 and 20°C the corrosion rate has been calculated as 1 mm in 1000 years.

Boksay and Bouquet, using electrode glass, found that at pH < 3 the corrosion rate again increased (15). At pH > 7 the same relationship between electrode potential and corrosion rate was found as for SiO_2 (228). The individual reaction steps of corrosion are not yet understood in detail. However, some models are being discussed, which take into account the charge dependency of network dissolution (15).

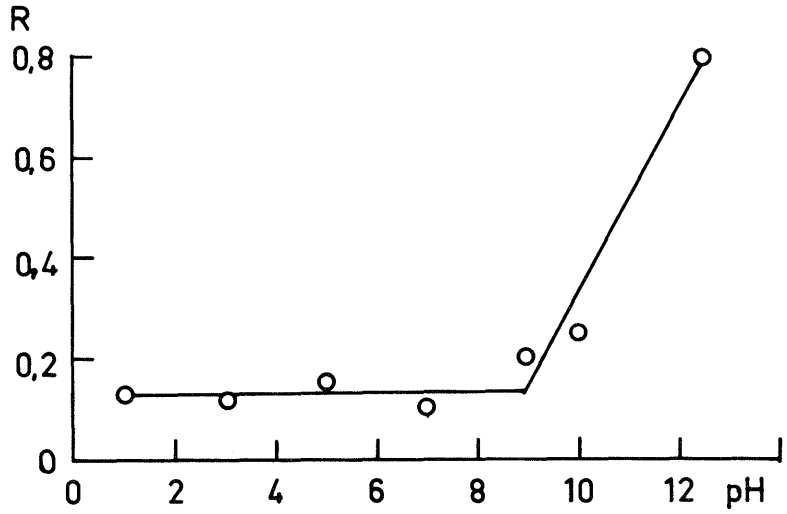

Figure 12: Effect of pH on rate of silica extraction from a Li_2O-SiO_2 glass at 35°C. R in mg/g glass in 206 min. (66).

Generally lattice dissolution shows a linear dependence on time, but it has also been found that, at low pH values, a $\sqrt{t}$ rule applies (70). It becomes linear again only in alkaline solution. As the hydrodynamic conditions were not varied in these experiments, no definite conclusions can be drawn about the reaction mechanism.

3.2.2 Glass leaching

With silicate glasses, over a fairly wide pH range, network dissolution is of less importance than the selective elimination of the network modifiers. This process can be described by an ion exchange formula:

$$\equiv Si\text{-}ONa + H^+ \longrightarrow \equiv Si\text{-}OH + Na^+, \text{ bzw.}$$

$$\equiv Si\text{-}O\text{-}Na + H_2O \longrightarrow \equiv Si\text{-}OH + Na^+ + OH^-$$

The processes are, however, considerably more complex than these simple reaction formulae suggest. The reaction mechanism still causes some controversy: on one hand it is postulated that M^+ is exchanged with H_3O^+ (115), while according to other experiments the exchange takes place with H^+ (36). Both cases are supported quantitatively by the analysis of the depth profile. Ernsberger (69) reached yet another conclusion: a non-bridging oxygen in the glass lattice reacts with water which has entered by diffusion, thus:

$$\equiv Si\text{-}O^- + H_2O \longrightarrow \equiv Si\text{-}OH + OH^-$$

This is followed by diffusion of the alkali ion and the hydroxide ion. For further details see the discussion in (189), page 266.

Without taking these discussions into account, leaching can be described by the parabolic time law which would be expected for a diffusion process:

$$Q = k.t^{1/2}$$

(Q = quantity leached). This relationship has been observed in many model glasses (60, 66). Figure 13 shows the increase with time of the thickness of the hydrated layer in window glass (115). The $\sqrt{t}$ dependence is valid for times up to 400 hours. With longer experimental times the thickness of the layer remains almost constant, as a steady state between lattice dissolution and leaching is established.

Leach rate at pH < 9 is independent of pH and is also unaffected by the M^+ concentration in the leachant (figure 14). At pH > 9 the lattice dissolution rate increases while the leach rate falls rapidly. This observation can again be explained by looking at the surface chemistry: the concentrations of H^+ and M^+ in the leachant are obviously not the deciding factors for ion exchange, but rather the surface activities of →Si-OH and →Si-OM. At pH < 9, {→SiOH} is practically constant, while at pH > 9 {→SiOM} increases, so that the ion exchange rate is reduced. In a volcanic glass, the sodium exchange with the leachant can be explained using adsorption equilibrium (222). The following findings also confirm that the surface species play a role: in a ternary electrode glass, leaching of sodium starts to decline as the pH value is reached at which the alkaline error becomes significant (66). According to recent investigations, the pH independence at pH < 9 can be explained possibly by the fact that the rate is controlled by the entry of water by diffusion (196).

Individual alkali ions have different leaching properties; with the same mol-ratio M_2O/SiO_2, the leach rate increases in the order $Li^+ < Na^+ < K^+$. In strong acids (pH < 2), the leach rate increases again as the pH value falls (66) and reaches a maximum at pH ≈ 0 (65). This pH range is not of interest in the present context, so these effects are not discussed.

If the alkali earth ions are not incorporated into the network, like beryllium or magnesium, they are leached rather like the alkali ions, but to a much smaller extent.

An interaction effect of the glass components also influences the leaching process: as an example, figure 15 shows the sodium extraction from various glasses with the same sodium content. The addition of CaO to binary glass improves resistance considerably. The small additions of other oxides to commercial glass (Al_2O_3, MgO) also improve resistance (42). Douglas et al (171) have published a systematic study of this effect using ternary glasses at various temperatures.

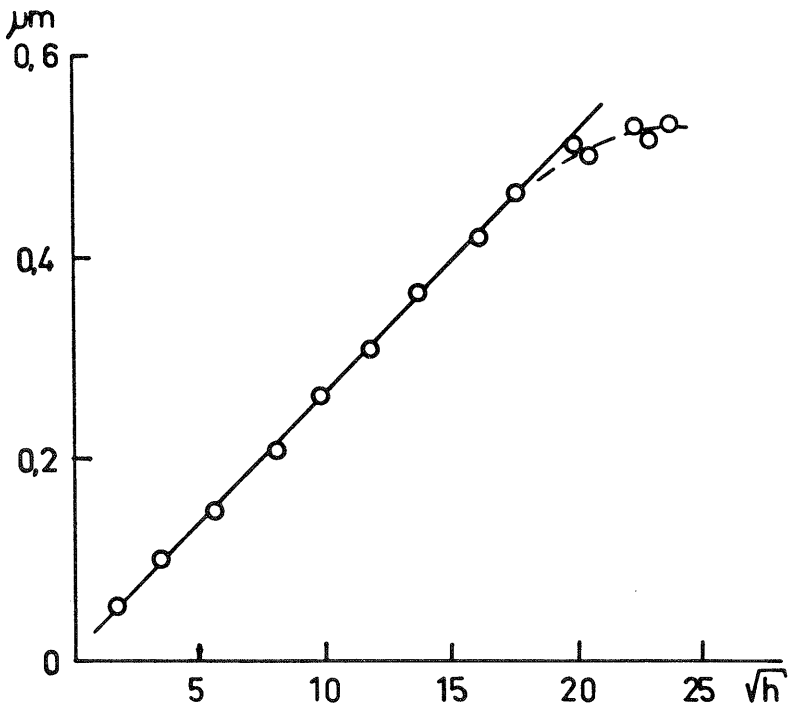

Figure 13: Depth of hydration of window glass as a function of time (115).

Leaching results in the formation of a hydrated SiO_2 rich layer which protects the glass from further attack. In glasses of complex composition, certain easily adsorbed ions may also be concentrated in this layer and so affect the process of the reaction.

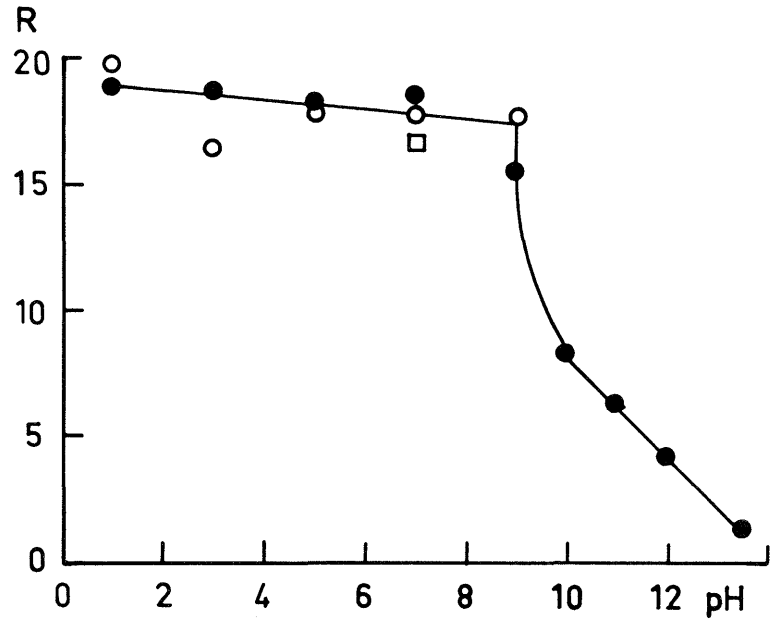

Figure 14: The pH dependence of alkali extraction for 15 K_2O: 85 SiO_2 glass. R in mg K_2O/g glass in 206 min.
● (Na^+) = 0.1 M, ○ (Na^+) = 0.0 M, □ H_2O (60)

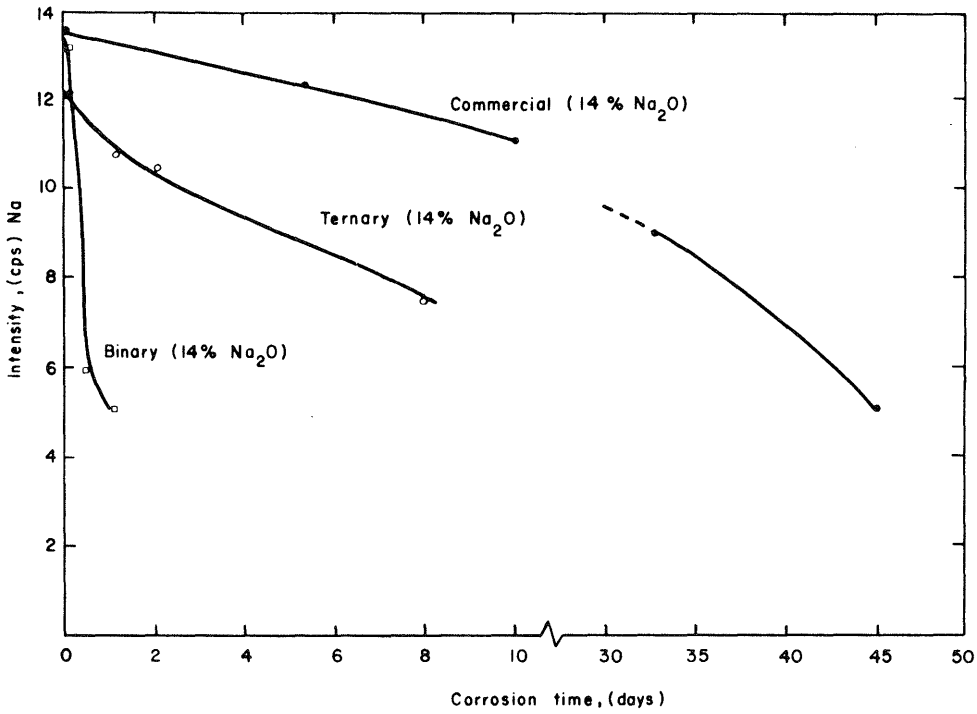

Figure 15: Sodium X-ray intensity as a function of corrosion time for three glasses containing equi-valent Na_2O (41).

3.2.3 Surface types according to Hench and Clark

According to Hench and Clark, the corroded surfaces of silicate glasses can be divided into five types (41, 90, 92). Surfaces of type 1 (figure 16) have only a thin hydrated film a few nanometres thick and show no significant changes in composition. In type 2 an SiO_2-rich layer is formed by leaching, this will act as a transport barrier. Such layers form at pH < 9.

In the reactions of glasses containing aluminium, a protective layer rich in aluminium may be formed on the surface (type 3). Similar protective films are also formed by the adsorption of inhibitors from the leachant.

Surfaces of type 4 also have a surface film rich in SiO_2. However, this film is continually being removed. Such behaviour is seen mainly in all glasses with low SiO_2 concentration and in some binary Na_2O/SiO_2 glasses, which have only moderate corrosion resistance.

Finally in surfaces of type 5, network dissolution is the dominant feature. The glass is totally dissolved by congruent dissolution. This type is represented by silicate glasses, which are subjected to a leachant of pH > 9.

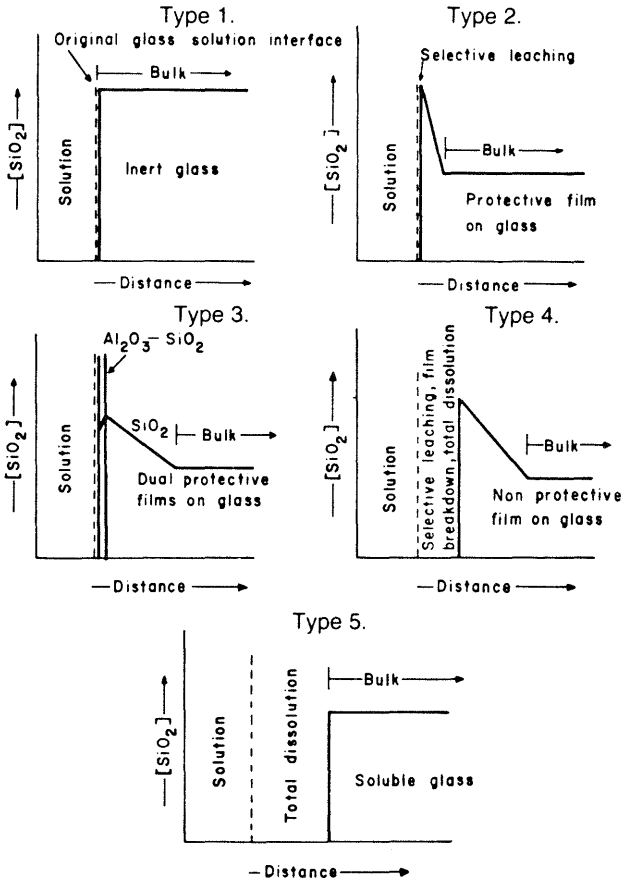

Figure 16: Five characteristic types of glass surfaces. After Hench and Clark (41).

3.3 Factors affecting glass corrosion

3.3.1 Effect of leachant composition

The composition of the leachant can affect glass corrosion in various ways: pH value determines the predominant mechanism - leaching or corrosion; the buffer capacity influences the extent of pH drift caused by the ion exchange reaction; two and higher valency cations and also phosphates inhibit network dissolution by adsorption or by phase formation at the surface; finally corrosion is affected by the silicic acid content of the leachant.

Demineralised water is a more aggressive leachant than brine (figure 17) (27). Other works also quote similar results (e.g. 107). As figure 18 shows, the leach rate of glass GP 98/12 in distilled water is about the same as in saturated rock salt solution. In a carnallite-containing quinary solution, the reaction is about 10 times slower. However, if the leach time is taken into account (figure 19), this conclusion is seen to be relative: the use of the 30 day values in figure 18 is arbitrary.These rather misleading results could be produced by the time dependent changes in leachant composition and also by surface layer formation (which is not investigated). This example also demonstrates quite clearly how the activation energies given in figures such as 17 and 18 can be misleading.

The influence of silicic acid concentration on network dissolution is observed both in pure SiO_2 (174, 228) and also in glasses: the corrosion rate of a vitreous enamel in 20% hydrochloric acid at 140°C falls from 0.2 to 0.01 mm/yr if the solution is saturated with SiO_2 (123). Table 3 shows the beneficial effect of SiO_2 on the hydrothermal reactions of a HLW glass (28).

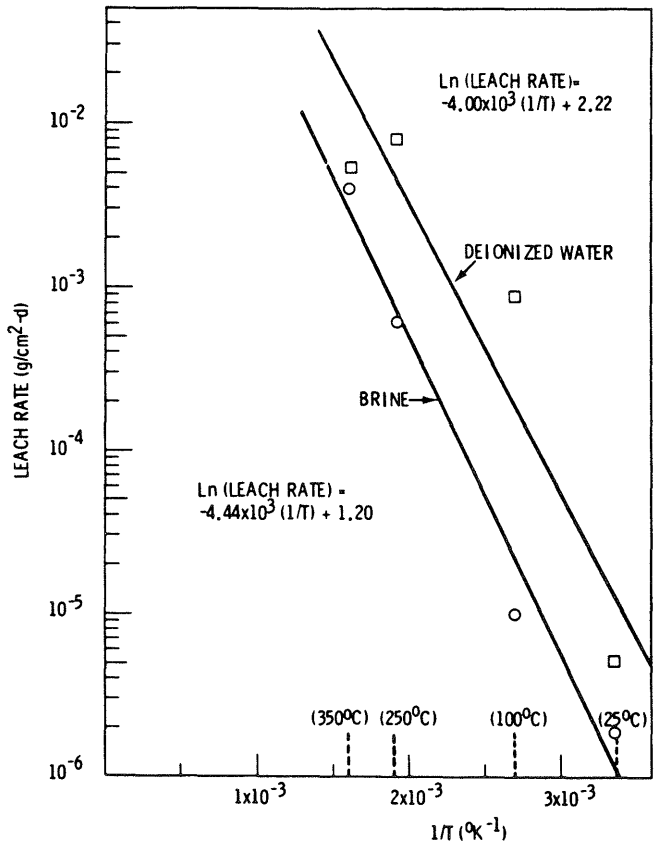

Figure 17: Leach rate of the waste glass PNL 76-68 as a function of temperature (27,221)

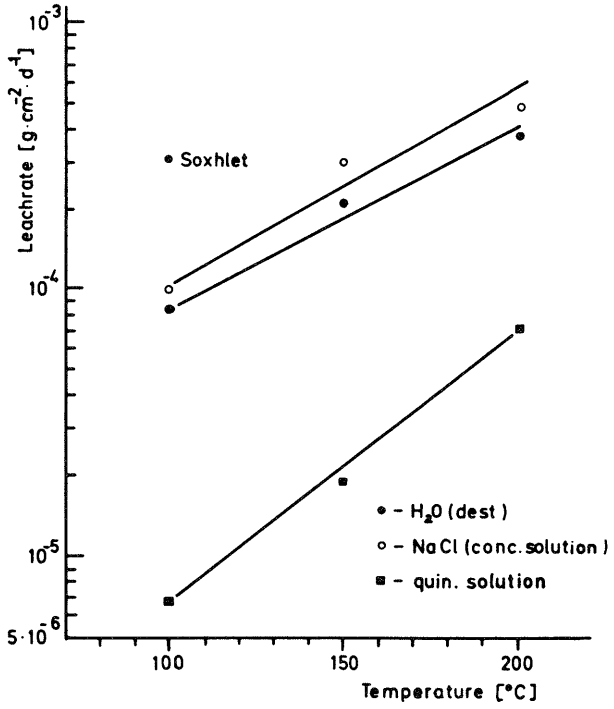

Figure 18: Glass GP 98/12: Dependence of the leach rate on temperature (pressure: 130 bars, time: 30 days) (107)

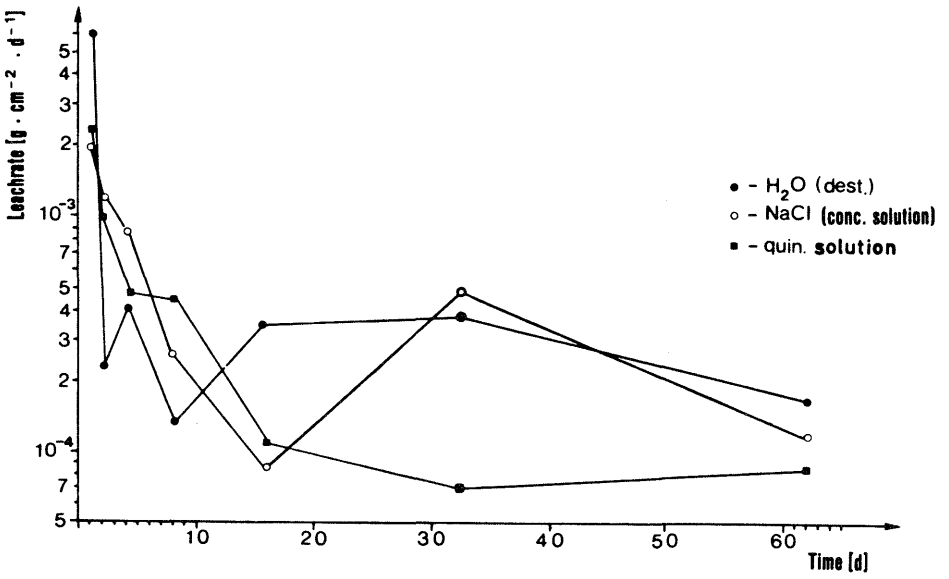

Figure 19: Leach rate of glass GP 98/12 at 200°C and 130 bars (107)

The mechanism of glass corrosion is largely determined by the pH value. For all silicate glasses at pH > 9 network dissolution predominates. Unlike normal glasses, with about 70 % SiO_2, borosilicate glasses (approx. 50 % SiO_2) show renewed increase in corrosion rate at pH values below 4 (227). This property is also observed in glasses with a significant lead, aluminium or zinc content. Figure 20 shows that the corrosion rate in acid media depends largely on the glass composition (23).

The role of the buffer capacity is also to be understood in relation to the pH effects: buffer species have a stabilising effect on pH drift caused by leach reactions. The buffering effect of not only the solvent, but also the rock and the backfill material must be taken into account, particularly at high temperatures. Differences between the leach rate in purified and in natural waters could be, at least partly, explained by the buffering effect of the CO_2/HCO_3^-.

Solvent	A/V(cm^{-1})	SiO_2 added (g/liter)	glass converted (%)	Cs in solution (%)
deionised	0,23	0,0	16,4	8,6
water	0,23	0,2	15,5	9,0
	0,23	1,0	6,0	4,6
	0,23	2,0	3,0	1,3
	$1,33 \cdot 10^{-3}$	0,0	100,0	89,5
	$1,33 \cdot 10^{-3}$	2,0	0,1	3,6
brine	0,24	0,0	6,6	0,8
brine	0,24	2,0	1,0	0,4

Table 3: The effect of the addition of SiO_2 and of the surface area/volume (A/V) ratio on the hydrothermal conversion of HLW glass (250°C, 28 days) (28)

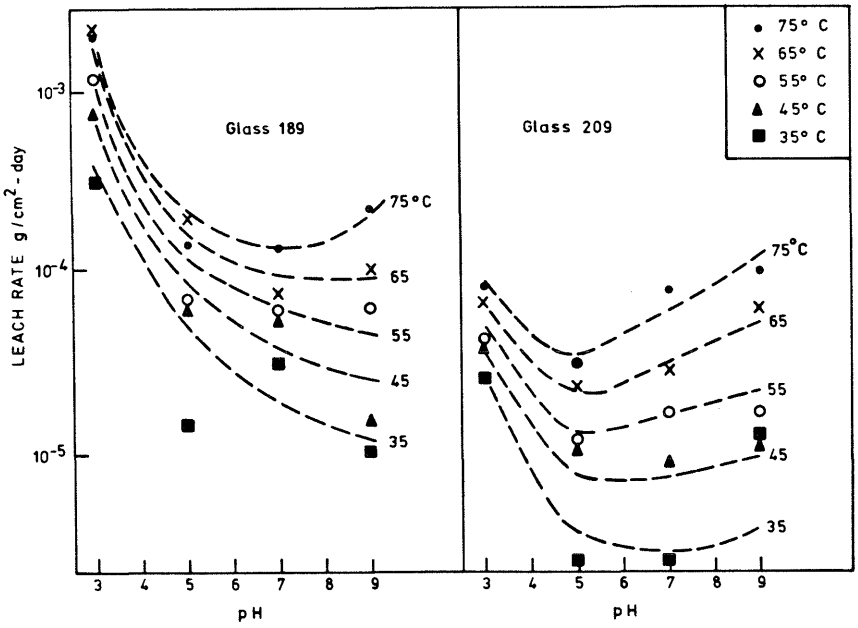

Figure 20: The effect of pH on the leach rate of glasses 189 and 209 at different temperatures. For composition see Table 7 (23)

As no redox reaction is involved in the corrosion of borosilicate glasses, the redox potential would not be expected to affect the reaction rate. The redox potential can, however, affect the adsorption onto the leached, hydrated SiO_2 surface layer of metals having several possible oxidation states.

Several investigations have shown that the dissolution rate of SiO_2 is reduced by adsorption of metal ions (100, 121). Glasses treated with various metal ions (e.g. Ca^{2+}, Zn^{2+}, Al^{3+}, Th^{4+}) showed an improved resistance in alkaline solution (91). In dilute solutions of sodium hydroxide Be^{2+} and Ca^{2+} acted as particularly effective inhibitors (165). Although this effect can be interpreted as partly due to the formation of low solubility metal-silicate films, in many cases corrosion is inhibited by metal ion adsorption, i.e. by an alteration in the surface charge.

If the reaction is inhibited by layer formation, this would imply that such layers are dense, this needs to be tested experimentally. The relatively good resistance of zinc-borosilicate glasses could be due to the inhibiting effect of re-adsorbed zinc ions (201).

Adsorption processes also play a decisive role by retaining, on the surface of the glass, the ions which have been released by the corrosion reaction (11). A leached glass surface has a layer of hydrated SiO_2 which acts as an adsorbant. The properties of this layer are comparable to those of silica gel and the adsorption properties of silica gel have been thoroughly investigated.

By means of new concepts about the solid/solution interface, metal adsorption can be understood as the formation of surface complexes and can be described quantitatively (187, 200):

$$\geq Si\text{-}OH + Me^{z+} \rightleftharpoons \geq Si\text{-}OM^{(z-1)+} + H^+$$

$$*K_1^S = \frac{[H^+]\ \{\geq SiOM^{(z-1)+}\}}{[M^{z+}]\ \{\geq SiOH\}}$$

$$2 \geq Si\text{-}OH + Me^{z+} \rightleftharpoons (\geq SiO)_2Me^{(z-2)+} + 2H^+$$

$$*\beta_2^S = \frac{[H^+]^2\ \{\geq SiO)_2Me^{(z-2)+}\}}{[Me^{z+}]\ \{\geq SiOH\}^2}$$

Figure 21, taking amorphous SiO_2 as the example, shows that a close relationship exists between the constants for surface complex formation and the more easily obtainable constants for homogeneous reactions (188).

$$Me^{z+} + H_2O \rightleftharpoons MeOH^{(z-1)+} + H^+ \qquad (*K_1)$$

$$Me^{z+} + 2H_2O \rightleftharpoons Me(OH)_2^{(z-2)+} + 2\ H^+ \qquad (*\beta_2)$$

Surface OH-groups have basically the same complexing properties as free hydroxide ions. Such correlations make it possible to estimate the tendency to adsorb metal ions. The reaction formulae show that adsorption equilibrium is dependent on pH. Figure 22 illustrates this relationship for various ions (188). Other investigations on silica gel show that, as expected, uranium IV is adsorbed more readily than uranium VI (4).

Greater effort should be made to use adsorption models to interpret the details of glass corrosion. Such models can offer a qualitative explanation, at least, of individual effects.

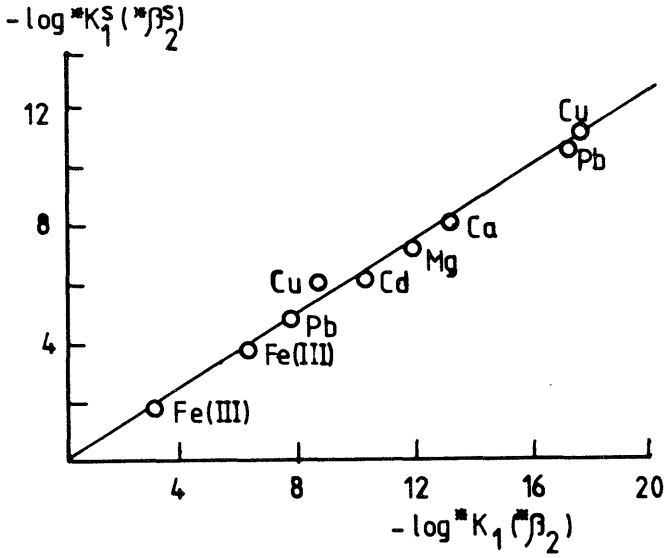

Figure 21: Correlation between the stability constants of the surface complexes ($*K_1^S$, $*\beta_2^S$) and the corresponding hydroxo complexes ($*K_1$, $*\beta_2$) (188)

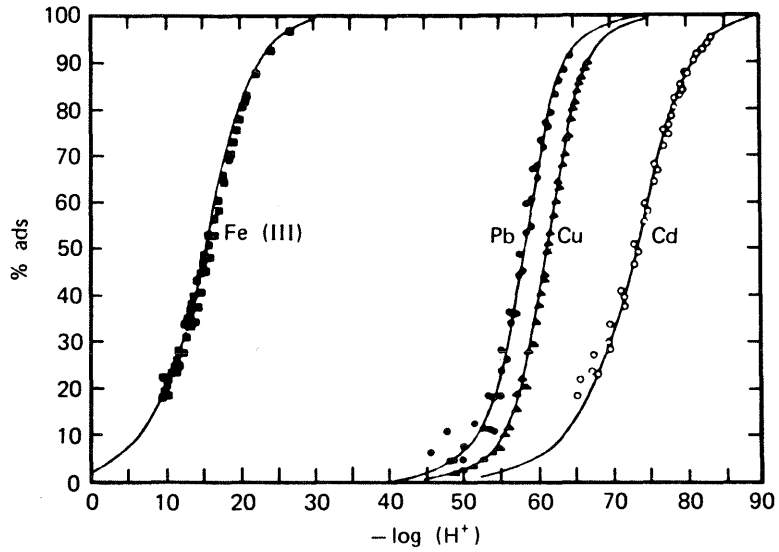

Figure 22: Adsorption of metal ions on amorphous silica as a function of pH (188)

Solvent	A/V(cm^{-1})	glass converted (%)	Cs in solution (%)
deionised	2,0	3,6	1,3
water	0,23	16,4	8,6
	0,023	70,0	38,4
	$1,33 \cdot 10^{-3}$	100,0	89,5
brine	0,24	6,6	0,8
brine	$9,2 \cdot 10^{-3}$	12,6	< 1,9

Table 4: Effect of surface area/volume ratio (A/V) on the hydrothermal conversion of HLW glass (250°C, 28 days) (28)

3.3.2 Effect of leachant supply

The ratio of glass surface, A, to solvent volume, V, has a significant influence on glass corrosion. If A/V is large, the leachant quickly becomes saturated with corrosion products and the reaction rate falls. When the solvent volume is large (A/V small) more glass will be dissolved. Table 4 illustrates this. Taking hydrothermal corrosion tests as an example, at A/V = $1.3 \times 10^{-3} cm^{-1}$, the glass is completely dissolved and 90% of the cesium originally in the glass goes into solution. At a ratio A/V = 2 cm^{-1}, other conditions being the same, only 3.6% of the glass is dissolved.

Using different experimental procedures corrosion can be speeded up by increasing the surface/volume ratio: initial ion exchanges make the solution more alkaline, until, at pH $\approx$ 9, the corrosion mechanism changes to network dissolution. The time required for this critical pH value to be reached depends on the A/V ratio. The larger the ratio, the sooner the change in corrosion mechanism takes place, increasing corrosion rate (figure 23) (70, 92).

Systematic investigations of the effect of surface/volume ratio on the corrosion of borosilicate and Na-Ca-SiO_2 glasses show that the composition of the glass and related surface film formation are also important (29).

In dynamic tests the corrosion rate is determined by the water flow. If the flow is small, then the leachant becomes saturates with corrosion products and further attack is inhibited (figure 24). With a high flow rate, however, phase boundary reactions are no longer inhibited by the saturation effect (98).

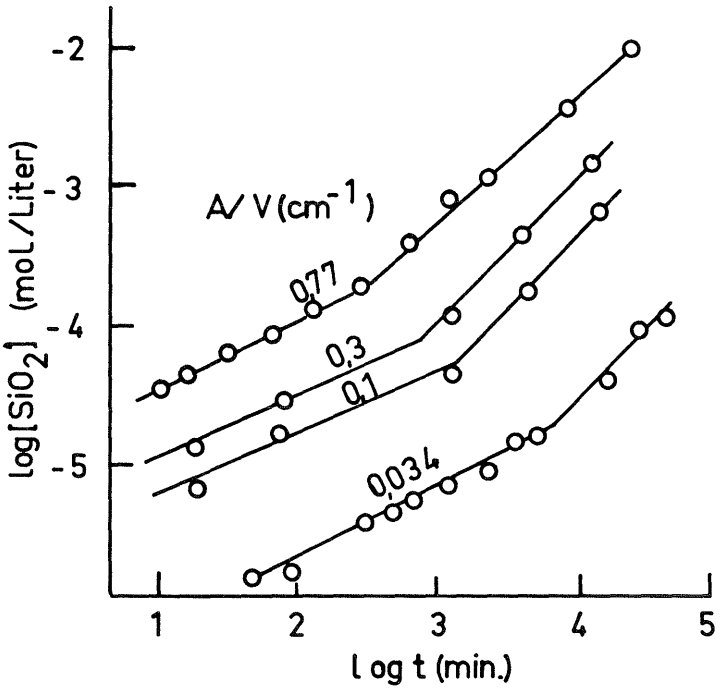

Figure 23: Concentration of silica in solution against corrosion time for polished samples at 50°C for the indicated A/V ratios (70)

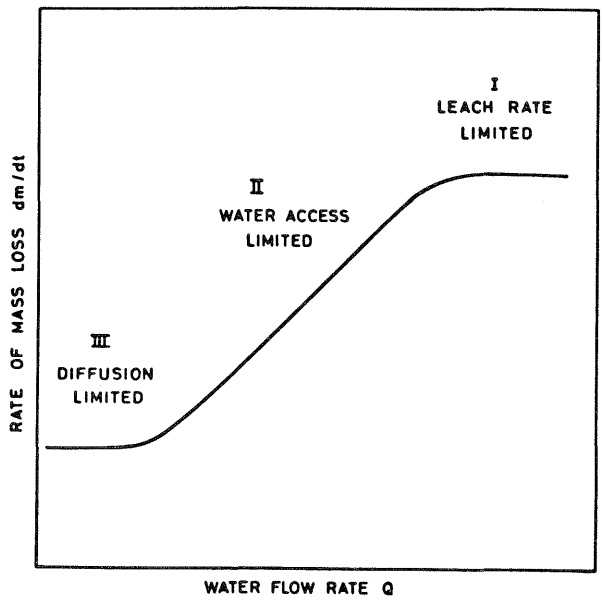

Figure 24: Schematic plot of rate of mass loss as a function of water flow rate (98)

3.3.3 The effect of pressure and temperature

The effect of pressure on the rate of dissolution has not been investigated independently, but usually in conjunction with higher temperatures. Generally it is assumed that the effect of pressure alone on glass corrosion is small. This assumption is based on the results of Rimstidt and Barnes (174), where the dissolution rate of SiO_2 up to 500 bar was practically independent of pressure. In glass, the loss of sodium and SiO_2 at room temperature was also independent of pressure up to 400 bar (47). Pressure also had no significant effect on a simulated HLW glass up to 100 bar at 90°C (224).

In hydrothermal tests on HLW glasses, where temperature and pressure were varied independently, a reduction in the reaction rate was observed with increasing pressure (33). Again, in another experiment at 150°C, a pressure increase from 600 to 1000 bar doubled the reaction rate (182).

An increase in temperature significantly accelerates both the network dissolution and the leaching. The temperature dependence of a chemical reaction rate is described, according to Arrhenius, by the formula:

$$\vec{R} \sim \exp\left(-\frac{E_a}{RT}\right)$$

E_a is the activation energy for the reaction, R is the gas constant at T the absolute temperature.

The activation energy for SiO_2 dissolution is about 70 kJ/mol. That for a depth increase of the hydrated film, shown in figure 13, is given as 79 kJ/mol (115). For leaching and corrosion of HLW glasses the value is found to be in the region 50 to 80 kJ/mol (11, 128). With an activation energy of 70 kJ/mol and a temperature increase from 25 to 100°C the reaction rate increases by a factor of 300.

It is not always easy to determine activation energy and results can become questionable if a change in the reaction mechanism is associated with the temperature increase. Vitreous enamels, for example, are leached at room temperature, but at 140°C are largely stoichiometrically dissolved (123). Surface analysis methods used on borosilicate glasses show that at 100°C congruent dissolution predominates, while at 25°C leaching of lattice modifiers is more important (139). Care should thus be taken when dealing with activation energies, particularly if the glasses involved form secondary solid phases under hydrothermal conditions.

Despite these complications the temperature dependence of glass dissolution can often be determined, at least approximately, using an Arrhenius diagram (figure 17) (27). Westsik et al (220), testing a borosilicate glass at temperatures above 200°C, did observe deviations from the ideal Arrhenius equation. These were thought to be connected with the hydrothermal phase change effects. Figure 25 (220) illustrates how complex and unpredictable the temperature dependence for the release of individual elements can be.

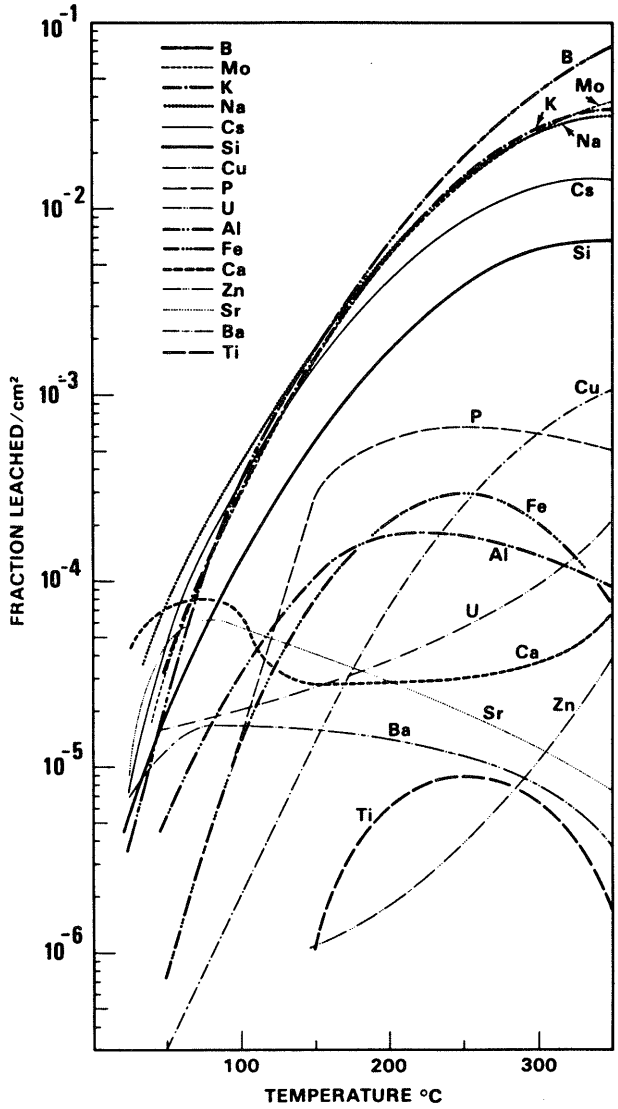

Figure 25: Elemental release from PNL 77-260 glass based on 3-day experiments (220)

3.3.4 Glass/rock and glass/backfill material interactions

Deep-seated (plutonic) rocks of magmatic origin are silicates and have a similar dissolution mechanism to that of silicate glasses. The reaction rates are generally slower.

At temperatures below 100°C the glass/rock interactions are probably limited to the influence of the rock on the leachant: the rock is in approximate equilibrium with the water flowing through it and it is the composition of this water - for example, the concentration of silicic acid - which influences glass corrosion.

If, however, the hydrothermal conditions are such that the glass and rock react rapidly with a limited solvent volume, then new solids are formed from the components of both the glass and the rock and the radioactive waste products will be redistributed between the new solids and the aqueous solution. The types of compounds formed in such reactions depend on the particular chemical, hydrological and thermal conditions in the reaction location. As a generalisation it can only be said that the presence or absence of rock does produce different results in hydrothermal investigations on HLW glasses. Rocks rich in SiO_2 usually exert a favourable influence.

The backfill material, bentonite, with its good water-bonding capacity, should protect the glass in a final repository from water intrusion and, in the event of a release of radioactivity, should bond the radionuclides escaping from the glass. Bentonites are layer silicates with ion exchange properties. These free ions (Na^+, Ca^{2+}) can be exchanged with hydrogen ions, so that the pH value of an aqueous bentonite suspension becomes significantly alkaline. This may have an adverse effect on the network dissolution of the glass.

3.3.5 The effect of radioactive decay

Radioactive radiation can influence the corrosion behaviour of a glass in two different ways:

- by alteration of the glass structure
- by modification of the solvent as a result of radiolysis.

β and γ radiation could not be responsible for any significant structural alteration. They can, however, affect the redox potential of the solvent. No estimate can be made of the extent of the effect of such short-lived radiolysis products on the dissolution mechanism.

Nitric acid is one of the products of radiolysis in aqueous solution in contact with air (105). The resulting pH reductions can accelerate the dissolution reaction in a badly buffered system.

α decay of the actinides can cause structural damage. Recoil nuclei are responsible for about 10 times more atomic displacements than α particles. With their amorphous structure glasses suffer considerably less damage than crystalline materials, which may, under certain circumstances, be converted to an amorphous state (metamictisation) (73). In glasses the volume change and related internal stresses due to radiation damage are smaller

than in crystalline materials. Depending on composition, glasses exhibit a volume change in the region ± 1 % with an α dose of 10^{19} cm^{-3}, while the values observed for crystalline materials have been over 10 % (145, 208).

3.3.6 The effect of glass composition

From the many investigations on simple models and on industrial glasses, the following general rules can be formulated:

The incorporation of Al_2O_3, ZrO_2 and TiO_2 into the glass network improves the alkali restistance of the glass (50). These oxides influence the formation of surface films (figure 16, type 3). Zirconium and titanium do not form soluble hydroxo-complexes and are thus particularly effective.

The effects of B_2O_3 additives will be discussed in more detail below. In general they reduce the diffusion coefficient of the alkali ions. The eliminated boron oxide stabilizes the pH value of the solution by neutralising the dissolved alkali oxide. The pKa value for boric acid, about 9.1, is somewhat lower than that of silicic acid (9.7).

Large additions of alkali oxides reduce corrosion resistance, particularly in a limited solvent volume: the higher the alkali content, the larger the pH increase in the solvent and so the greater the attack on the lattice. At the same alkali concentration the resistance decreases in the order Li-Na-K. The leach rate of alkali ions depends on the type of bonding: sodium, bonded to AlO_4 tetrahedrons, reacts noticably more slowly and with a different mechanism, than sodium on non-bridging oxygen (196).

If the glass contains different alkali ions, e.g. lithium and sodium, resistance is improved (22,90). The effect is greatest with a mol-ratio of about 1. The mixed alkali effect can also be observed from other properties, particularly electrical conductivity (58, 59). The cause of this behaviour has not yet been finally explained.

The addition of oxides of bivalent metals as network modifiers improves selective alkali leaching. Normally calcium oxide is added, but the oxides of Mg, Sr, Ba and Cd also act similarly. Zinc oxide improves alkali resistance, but impairs resistance to acids below pH 5.5. Lead oxide has the same qualitative effect. The stability of glasses of type $Na_2O/B_2O_3/SiO_2$ has been systematically investigated by Adams and Evans (2) in neutral solutions. The leaching of sodium was measured. The results are plotted in the phase diagram, figure 26, as lines of equal resistance. With increasing SiO_2 content, the resistance increases. With constant SiO_2 content, the resistance initially increases along the line ABC, reaches a maximum at B and then falls off again. This process could be related to the coordination of boron and the proportion of non-bridging oxygen in the lattice, the maximum chemical resistance coincides with the maximum content of BO_4 tetrahedrons. The results are generalised for a system $(R_2O + RO)B_2O_3/XO_2$. R stands for the lattice modifier, i.e. 1 and 2 valency cations, XO_2 represents all network formers except B_2O_3.

The general results of Adams and Evans have been fundamentally confirmed by the work of Harvey and Jensen (86). In glasses of $Na_2O.B_2O_3.xSiO_2$ composition, the chemical resistance at x = 4 increases dramatically (figure 27). Only if $x \geq 4$ are all boron atoms coordinated tetrahedrally via oxygen to four silica atoms.

Further systematic investigations with a much wider range of variants have been carried out at PNL (35, 142, 180). Chemical resistance was tested under various conditions (pH 4, pH 9, Soxhlet). In each case the percentage weight loss was determined. Figures 28 and 29 (35, 138) show, for example, the results of Soxhlet tests and leaching experiments at pH 4. The influence of the individual oxides corresponds in trend to the rules already given at the beginning of this section. The only contrary effect was observed with Al_2O_3 in the acidic region.

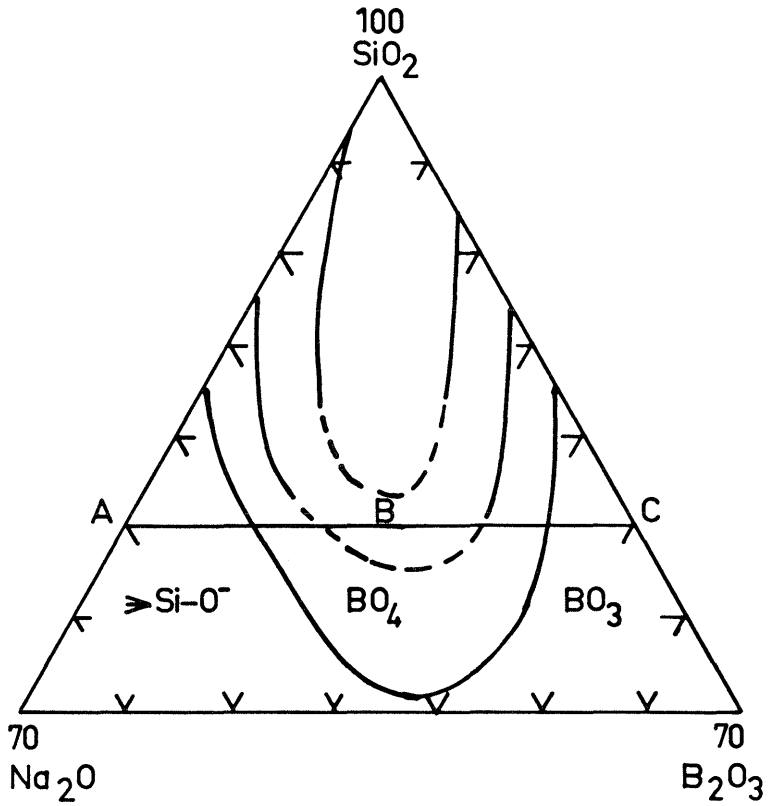

Figure 26: Lines of equal resistance (isodure) for sodium- borosilicate glasses. With constant SiO_2 content, the optimum resistance was found with maximum concentration of BO_4 tetrahedrons (2).

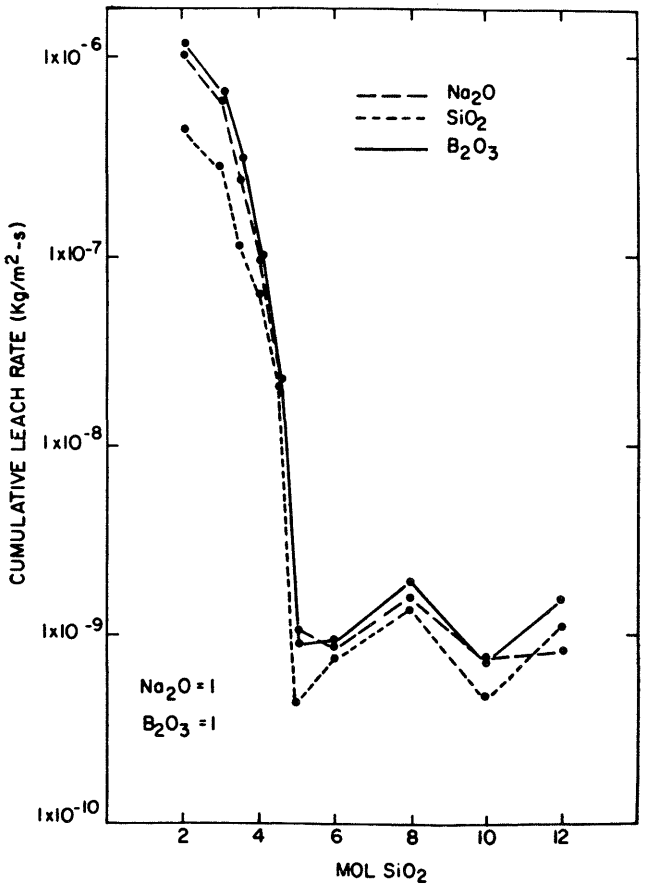

Figure 27: 30-day cumulative leach rate for glasses with the composition $Na_2O.B_2O_3.xSiO_2$, plotted as a function of silica content (86)

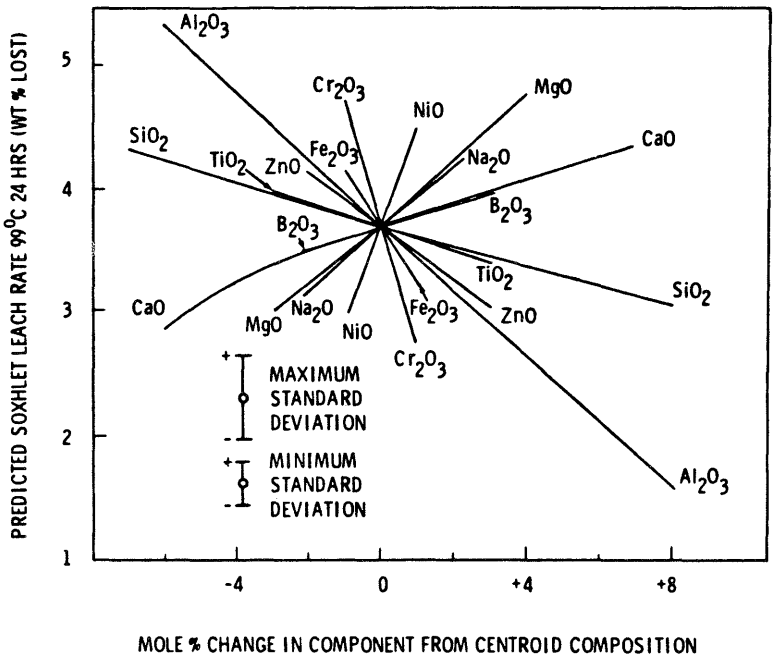

Figure 28: Soxhlet corrosion rate vs change in component from centroid PNL 11 components glass (138)

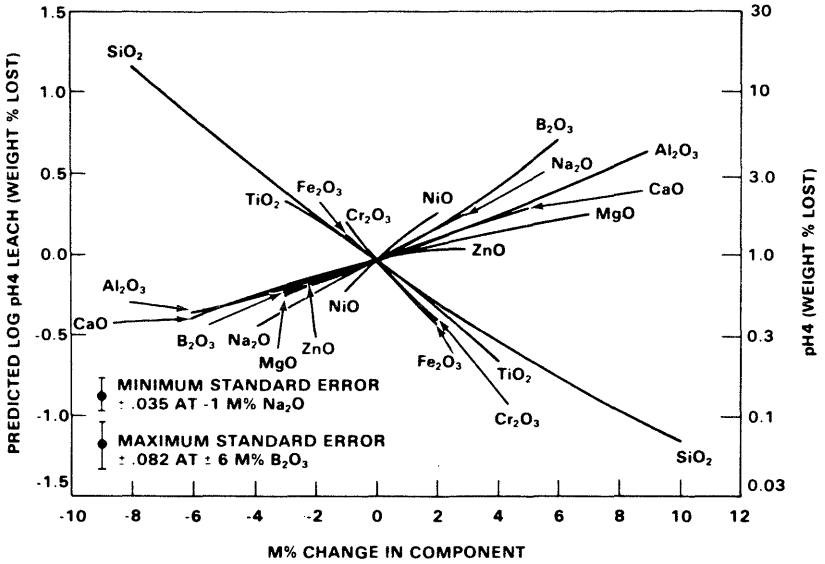

Figure 29: Corrosion rate at pH 4 vs change in component from centroid PNL 11 components glass (35)

3.4 Corrosion testing and evaluation

There are, of course, standard methods for testing materials, but these methods should not be regarded as universal. The various test methods are often rather limited in what they reveal and they should always be adapted very carefully to the problem in question. In testing the chemical resistance of glasses, the following aspects can be considered:

a) optimising product development
b) product comparison
c) quality control after manufacture
d) evaluation of long-term behaviour in final repository
e) investigation of corrosion mechanisms.

In these areas, but above all in d), corrosion tests should be continued at least until a steady state is reached. At room temperature this can take months or even years (11, 126). If the reaction is accelerated - e.g. by temperature or pH increase - then it is necessary to ensure that the change in attack conditions does not produce any undesirable change in corrosion mechanism. This can be checked by testing the glass surface, using surface sensitive methods such as SIMS or XPS.

For points a), b) and c), any standard test methods can be chosen. Some of the most common systems (42) are shown schematically in figure 30. A detailed survey is given in (3).

The aim is to cover as broad a spectrum of conditions as possible using five different standard tests (157, 198, 199). The five MCC (Material Characterisation Center) tests are described briefly below. Unless otherwise indicated, solid glass blocks were used in the tests.

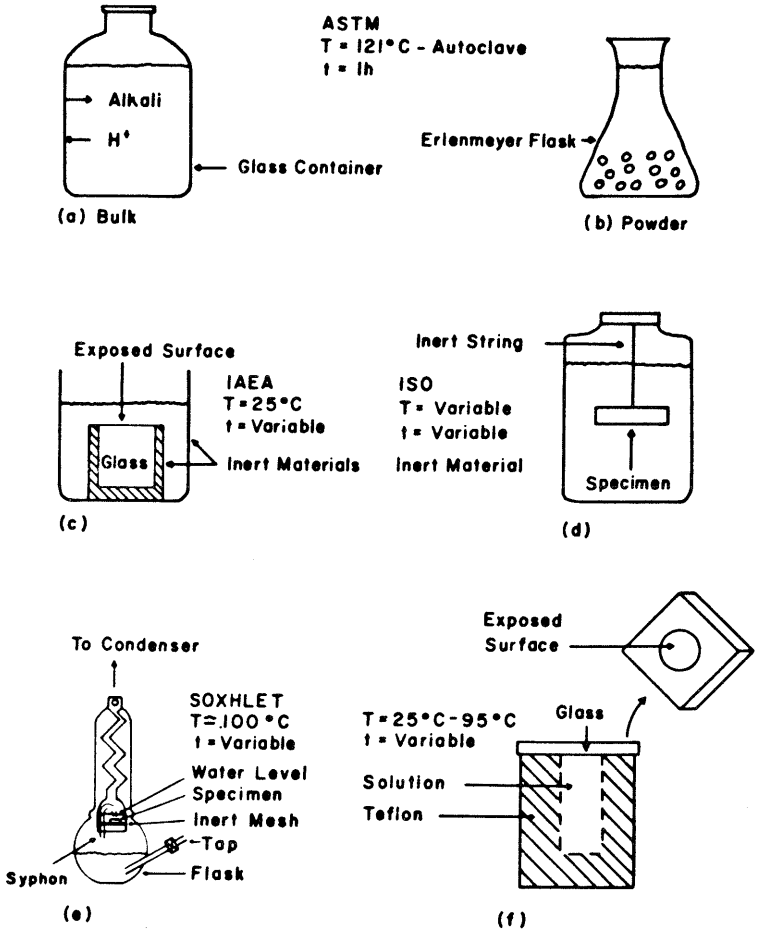

Figure 30: Tests for measuring glass corrosion (42)

MCC 1 : Static test at temperatures below 100°C
MCC 2 : Static test at temperatures above 100°C
MCC 3 : As MCC 2, but using glass powder
MCC 4 : Slow, single-pass of leachant (10^{-3} - 10^{-1} ml/min)
MCC 5 : Soxhlet test (see figure 30 e) with teflon apparatus

For MCC 1 to MCC 4, deionised water, a simulated silicate groundwater and a brine are given as standard solvents. Apart from these, water from specific locations can, of course, be used. Surface analysis tests of the corroded glass block are recommended.

The MCC tests can also be used, to a certain extent, for points d) and e). Particularly realistic conditions can be achieved with a slow, single-pass system. Parameters exerting an influence can be varied within a wide range. However, the apparatus is relatively expensive (46). A detailed discussion of what these different tests can reveal has been published by Barkatt et al (9).

The leaching equipment for active glasses at the Vulcain plant in Marcoule differs from the usual test equipment (99). A cylindrical sample is leached in a 90 second cycle: 30 s solvent sprayed in, 30 s immersion, 30 s emptying. As a rule the solvent is changed daily.

Despite every effort at standardisation, it is virtually impossible to compare the results from different laboratories. As figure 31 (36) shows, using different methods the leach rate for the same glass can vary by a factor of 10. If open or only loosely covered test vessels are used, carbon dioxide from the air can affect pH values (10) and rather misleading results can thus be obtained.

Figure 32 shows how test conditions can influence results. It summarises extensive tests on a glass of $Na_2O.B_2O_3.4SiO_2$ composition (86). If the

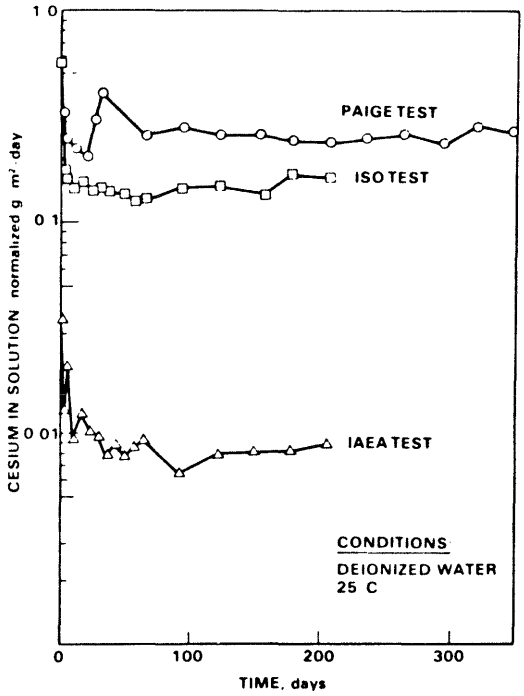

Figure 31: Comparison of three leaching techniques on radioactive waste glass (36)

test solvent is changed at short intervals, the leach rate decreases with time. This result reflects the leaching of the surface film by diffusion processes. ISO tests, where the solvent is changed daily, result in a parabolic decay of the leach rate $R \sim t^{-1/2}$ for a good 40 days. In static tests the pH value increases with time. The rapid increase in rate after 100 days may reflect arrival at the critical pH value. No explanation has been found, however, for the unexpected results with a solvent change after 30 days.

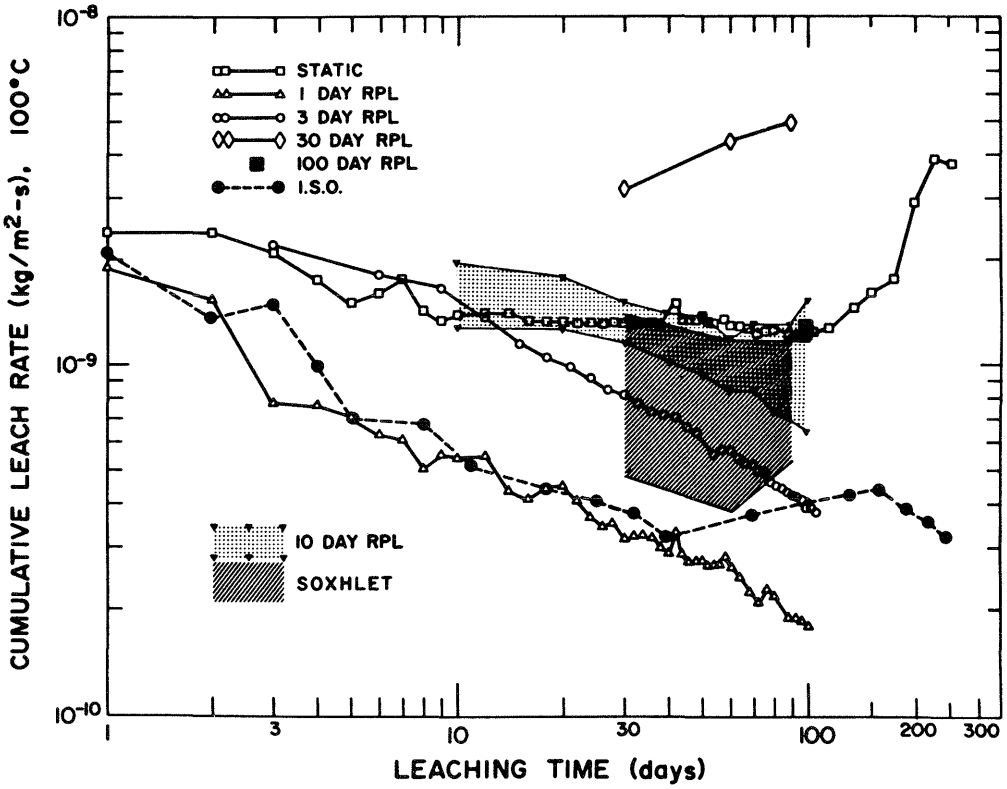

Figure 32: Leach rates for a model glass at several replenishment schedules as a function of time (86)

Another reason, why it is difficult to compare results from different sources, is because the data are often presented in different units, e.g.

- Material removed in mm/yr
- Percentage weight loss (particularly of powders)
- Weight loss per year: g/(g glass.year)

Leach rate of element, i, in $cm^{-2}.d^{-1}$, e.g. in (45):

$$R_i = \frac{M_i}{M_{i,o}} \cdot \frac{1}{\Delta t.S}$$

where M_i : mass of element, i, (activity) dissolved in time Δt

$M_{i,o}$: initial mass (activity) of i in the glass

S : surface area

- Leach rate of element, i, in g cm^{-2}. d^{-1}:

$$R_i = \frac{M_i}{M_{i,o}} \cdot \frac{W_o}{\Delta t.S}$$

where W_o is the original mass of the glass block. Irrespective of the element, i, under consideration, the units are g glass/(cm^2.d).

Conversion between the different units is only possible if the geometry and density of the test samples are known.

4. Final repository incidents and relevant corrosion tests

A final repository for highly radioactive wastes should be constructed so that the resulting individual radiation doses do not exceed 10 mrem per year (158). This value lies well within the range of natural radiation, to which we are permanently exposed.

Water is the only means by which radionuclides from a final repository, as envisaged in Switzerland, can escape into the biosphere. In a final repository, the release of radionuclides is prevented by a multiple barrier system: isolation (rock, canister), fixation (chemically resistant matrix, glass) and retention (backfill material, geological environment).

A safety study of the whole system does not lie within the scope of this report. An evaluation is simply made, based on rather summary incident scenarios, to decide which investigations are most suitable for obtaining relevant dissolution data for HLW glasses. Only the key parameters are included: waste container, temperature and pressure, water composition and availability.

Many factors which would affect the course of a possible incident are specific to the location or system. These include: dimensions of the glass cylinder, heat output during storage, packing density of the canisters in the repository, thermal conductivity of the rock, hydrological conditions.

As Switzerland, as yet, has no definite project for a final repository, values for some of these factors must be assumed or estimated. This rough basis must be used to judge the usefulness and suitability of certain laboratory and field tests against actual expected conditions.

Tables 5 and 6 list the radioactivity and heat output from vitrified waste of the type produced in France (102). These values are valid for the following conditions: 14% of fission oxides in the glass, a processed fuel of 3% ^{235}U having a burn-up of 33 GWd/t and vitrified after a one year decay period, and 92 litres of glass produced per tonne of processed fuel.

Radiation and chemical hazard potentials are time dependent (figure 33) (12). The radio-toxicity of a repository is often compared with that of a natural uranium deposit. From this viewpoint a repository would be comparable to a uranium ore of 0.2% U after about 10,000 years (144, page 60). Such statements should be treated with care. They depend very much on the toxicity index chosen and on other parameters, and so can vary very widely. These problems have been discussed at length in a work by Haug (87).

4.1 Pressure and temperature conditions in the repository

The chemical behaviour of the glass falls into three distinct periods, based on several factors: half-life of the waste components, decay time, heat output, pressure conditions. The periods are:

a) Active period of the repository (about 70 years)

The glass blocks enter the final repository only after an interim storage period of several decades. No definite value for the temperature of the glass blocks at this time can be given, it could exceed 100°C. The pressure in an open repository is 1 bar. It could increase with flooding. Radiolysis of the aqueous solution, caused by γ radiation, could affect the corrosion reactions of the canister and, to some extent, the glass.

Radiotoxicity is primarily caused by ^{90}Sr and ^{137}Cs, both of which can be selectively leached from the glass.

Cooling Period (years)	Radioactivity (Curie) per Litre Glass		
	Fission products (β,γ)	Actinides (α)	Total
1	24'000	100	24'100
10	3'450	25	3'475
100	375	3,5	379
1'000	0,17	0,87	1,04
10'000	0	0,24	0,24
50'000	0	0,042	0,042
100'000	0	0,034	0,034

Table 5: Radioactivity per litre glass as a function of time (102)

Cooling Period (years)	Watt per Litre Glass		
	Fission products (β,γ)	Actinides (α)	Total
1	110	3,47	113,5
10	11,3	0,78	12,1
100	1,14	0,11	1,25
1'000	$2 \cdot 10^{-4}$	0,025	0,025
10'000	0	0,005	0,005
50'000	0	0,0015	0,0015
100'000	0	0,0010	0,0010

Table 6: Thermal output of vitrified waste as a function of time (102)

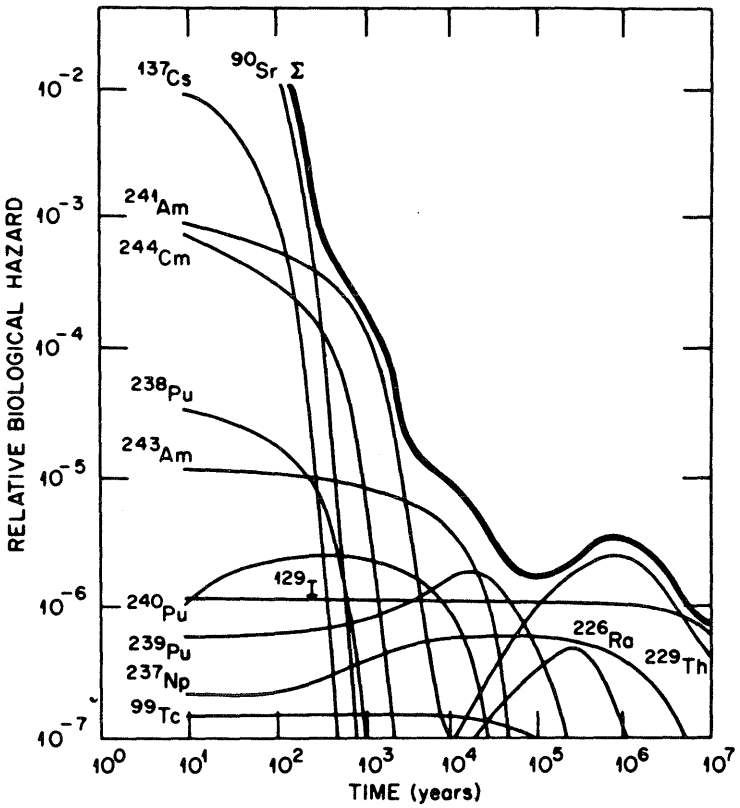

Figure 33: Relative biological hazard potentials of the more common radionuclides in high level waste. After the decay of Sr-90 and Cs-137, the activity is mainly due to α-decay of the actinides (12)

b) Sealed final repository until β and γ activity die out (about 500 years)

At the end of this period the temperature will have fallen to that of the environment (30 - 60°C). According to the evidence of a detailed final repository project, the temperature evolution with time can be calculated. The effect of radiolysis decreases with time.

After sealing the repository, the pressure builds up to that of the repository depth. If, during some incident, water penetrates the system, then hydrothermal conditions will affect glass reactions for some time. Fission products determine the toxicity during this period.

c) Long-term storage period (over 500 years)

During this phase, for some 10^5 years, toxicity is determined by the actinides and later by their decay products. Actinides are released by network dissolution. They are largely adsorbed in the backfill material. Temperature remains constant, in the region of 30 - 60°C, at the repository depth envisaged.

4.2 Hydrology and aquatic chemistry

In the geological formations proposed for the final repository, water circulation is expected to be very low. So, the subterranean waters will acquire a typical granite-water composition (200). The anticipated flow rate lies in the region 1.6×10^{-5} to 0.3 m/year (133). The water composition can be modified by interactions with the glass body, the canister and the backfill material. Also, situations could arise which result in an increased water supply. The following conditions are envisaged for the three periods described above:

a) Active period

It is difficult to make predictions for this period. At this stage it can be taken that the canister is still intact. The most probable type of incident would be the intrusion of water into the repository galleries. According to the type of repository and the pressure ratios (i.e. filling height) either hydrothermal conditions or reactions at boiling point could be expected. At these temperatures the water composition will be affected by the backfill material used. Temperature differences will produce currents in the water.

b) Decay of β and γ activity

During this period the waste matrix is warmer than the surrounding rock. Even with a limited, practically stagnant, water reservoir currents will be set up in the water by the temperature gradients: corrosion products removed from the hot matrix by the water will be redeposited in cooler locations. This transport effect prevents saturation being reached, which would in turn reduce the dissolution rate of the glass. However, it has been shown experimentally that material transport due to temperature gradients reduces the permeability of granite (154).

Corrosion is influenced primarily by water composition, and this is affected by the bentonite and dissolved glass components rather than by the colder granite, which anyway has a lower solubility rate.

c) Long-term storage period

The final repository is now approximately isothermic, so water circulation due to temperature gradients need no longer be considered. The water moves so slowly as to be virtually stagnant. But it should still be remembered that the backfill material and the glass itself do affect the water composition.

4.3 Corrosion tests for risk assessment

From the above discussion it can be seen that normal standard tests for determining dissolution rates of glasses are not always suitable for providing data for risk assessment. Care should, therefore, be taken in using such tests, as they do not always give conservative values.

Extremely complex conditions can arise during the first period of storage. Any investigations should take into account the high temperature of the glass. Such conditions could possibly be simulated by hydrothermal experiments. But few experiments have, as yet, been carried out to investigate the, quite likely, conditions of corrosion in boiling water. An isothermal test at boiling point cannot realistically simulate this case: the model must also take the heat transfer into account.

Heat transfer in austenitic chrom-nickel steels is known to impair corrosion behaviour (95). This point should be considered in corrosion tests on the canister material.

Conditions in the second period have been rather optimistically reproduced by static corrosion tests. Flow experiments are preferable and should always allow for the large influence of the backfill material on water composition.

Under hydrothermal conditions the mineral surroundings are involved in phase regeneration. Experiments which do not include backfill material and rock are, therefore, of little value. For tests at temperatures below about 100°C, it may be adequate to use water which has previously been brought to equilibrium with bentonite and granite at the test temperature. This method can also be used to simulate the conditions in the cool repository (third period). All experiments must chose realistic flow rates and surface/volume ratios.

5. Composition and properties of HLW glasses

5.1 Composition and thermal stability

The development of glasses with specific properties started with the work of Abbé and Schott (from 1880). The structure model of Zachariasen and Warren (1932/33) was another step forward: for the first time it was possible to predict, to some extent, the properties of a glass from the elementary data of the glass-forming ions.

Optimisation of a waste glass, with some 40 different elements, is a process which can hardly be done on a purely scientific basis. Formulation of a good glass composition is difficult, because the combination of properties required - e.g. low melting temperature and high chemical durability - leads to a conflict of interests: an "optimum compromise" is needed and this is currently provided by the borosilicate glasses.

5.1.1 Glass composition

Glass composition can be formulated using classical structure concepts and simple, reliable selection principles (81): this must of course be backed up by a wide range of systematic investigations. The optimisation of PNL glasses has already been mentioned in connection with corrosion behaviour (figures 28 and 29) (35, 138, 179). Other laboratories have also tested a wide range of compositions experimentally (56, 155). Some glass compositions are given in tables 7 to 11 (135). As a comparison, table 8 gives the composition of commercial glass types.

	SON 58,30,20,U2	SON 64,19,20,F3	UK 189	UK 209	VG 98/30
SiO_2	43,6	44,2	41,5	50,9	41,8
B_2O_3	19,0	17,3	21,9	11,1	10,5
Li_2O	-	-	3,7	4,0	-
Na_2O	9,4	11,5	7,7	8,3	22,3
CaO	-	-	-	-	2,3
TiO_2	-	-	-	-	3,5
Fe_2O_3	0,6	5,9	2,7	2,7	0,7
Cr_2O_3	0,2	0,5	0,5	0,6	0,2
NiO	0,1	0,2	0,4	0,4	0,2
MgO	-	-	6,2	6,3	0,4
Al_2O_3	0,1	-	5,0	5,1	1,2
Gd_2O_3	-	5,9	-	-	-
U_3O_8	3,6	0,9	0,06	0,06	1,2
Fission products	22,7	13,9	9,6	9,8	15,2

Table 7: Composition of European HLW glasses used in comparative tests (132)

	PNL 72-68	PNL 76-68	PNL 77-260	Window glass	Pyrex	Vycor
SiO_2	27,3	39,8	35,8	70	80	96
B_2O_3	11,1	9,5	9,0		11	4
Na_2O	4,1	12,5	11,1	15	5	
K_2O	4,1	-	2,0		0,5	
MgO	-	-	-	3	-	
CaO	1,5	2,0	1,0	9	1	
BaO	2,5	0,6	0,6			
ZnO	21,3	5,0	-			
Al_2O_3	-	-	2,0	1	2	
TiO_2	-	3,0	6,0			
Fe_2O_3	1,0	9,6	1,2			
MoO_3	4,0	2,3	2,0			
NiO	0,7	0,2	-			
CuO	-	-	3,0			
ZrO_2	3,1	1,8	1,5			
PdO	0,9	0,5	0,5			
RuO_2	1,9	1,1	0,9			
Cs_2O	1,8	1,1	0,8			
SrO	2,1	-	-			
U_3O_8	1,3	4,6	5,7			
SE-Oxide	7,7	4,4	14,0			

Table 8: Composition of some of the most frequently tested PNL glasses and also some commercial glasses (63, 135)

	ABS 29	ABS 39	ABS 41	Marcoule	GP 98/12	GP 98/26
SiO_2	52,0	48,5	52,0	45,6	48,2	46,1
B_2O_3	15,9	19,1	15,9	14,1	10,5	10,1
Li_2O	3,0	-	3,0	2,0	-	-
Na_2O	9,4	12,9	9,4	9,9	14,9	14,3
MgO	-	-	-	-	1,8	1,7
CaO	-	-	-	4,0	3,5	3,3
ZnO	6,0	-	3,0	2,5	-	-
TiO_2	-	-	-	-	3,9	3,7
ZrO_2	*)	*)	*)	1	*)	*)
Al_2O_3	2,5	3,1	2,5	4,9	2,2	2,1
Fe_2O_3	0,6	5,7	3,0	2,9	-	-
Cr,Ni-Oxide	-	-	-	0,9	-	-
UO_2	1,7	1,7	1,7	*)	*)	*)
Fission products	9,0	9,0	9,0	12,2	15,0	15,0
Gd_2O_3	-	-	-	-	-	3,7

Table 9: Optimised glass compositions from Sweden (67, 159), France (Nagra information) and Germany (82). *) component included with fission products.

Oxide	Wt. %	Oxide	Wt. %
MoO_3	1,63	NiO	0,37
ZrO_2	1,28	SnO	0,017
Nd_2O_8	1,21	SrO	0,26
Ce_2O_3	0,75	BaO	0,46
La_2O_3	0,71	Cs_2O	0,88
Pr_2O_3	0,35	Ag_2O	0,01
Y_2O_3	0,15	CdO	0,026
MnO_2	0,77	Sb_2O_3	0,004
CoO	0,12	Total	9,00

Table 10: Composition of simulated HLW oxides in Swedish glasses (67, 159)

Oxide	Wt. %	Oxide	Wt. %
Rb_2O	0,14	La_2O_3	0,53
SrO	0,35	CeO_2	1,08
Y_2O_3	0,22	Pr_2O_3	0,49
ZrO_2	1,78	Nd_2O_3	1,70
MoO_3	1,84	Sm_2O_3	0,36
MnO_2	0,27	Eu_2O_3	0,04
RuO_2	1,00	Gd_2O_3	0,06
Rh_2O_3	0,16	UO_2	1,08
PdO	0,58	P_2O_5	0,89
TeO_2	0,25	Fe_2O_3	0,23
Cs_2O	0,91	NiO	0,10
BaO	0,66	Cr_2O_3	0,10

Table 11: Composition of simulated HLW oxides in glasses GP 98/12 and 98/26. Enrichment 3.5% U-235, burn-up 36,000 MWd/tU, cooling period 6 years. 0.30 Tc replaced by Mn (% wt), 0.95 actinide by U, 0.08 Pm by Nd (82)

At first, attempts were made to develop a glass with as high a capacity for waste oxides as possible. Then, it was realised that heat generated by the fission products limits this capacity. A suitable limit is considered to be an output of 67 watt per litre of glass directly after processing (102). This gives a maximum content of fission material oxides of 15 %. Typical glass compositions, which take this requirement into account, are given in table 9. The range of French glass compositions, manufactured to optimise corrosion behaviour, is found in (160).

Macedo et al (125) have found an original way to combine good corrosion resistance of an SiO_2 rich glass with the advantages of low processing temperatures. They started with a Vycor type of glass (figure 7). Vitreous phase separation was induced by heat treatment and the borate phase was then leached from the powdered glass. The solution of fission products, which may also contain fine solid particles, was absorbed by the porous matrix. The powder was heated and finally sintered together inside a glass tube of high melting temperature. Such a product has better corrosion properties than a borosilicate glass. However, the process has not yet been tested on an industrial scale.

5.1.2 Crystallisation of glass

Partial crystallisation of glass can impair chemical resistance, if compounds rich in silicate are crystallised out, leaving the remaining glass deficient in SiO_2. If water soluble phases are formed, they also have an adverse effect (e.g. molybdate or pollucite: (Na, Cs) $AlSi_2O_6$). On the other hand, the formation of stable oxides (spinel, oxides of the rare earths) hardly affects chemical resistance at all. A comprehensive survey has been made by May and Turcotte (135) on the thermal stability of HLW glasses.

The devitrification tendencies of HLW glasses must be studied from two different angles:

a) Possible devitrification due to cooling immediately after production (period of days, $T > T_G$) and during the following interim storage period (some years, $200^o < T < T_G$).

b) Possible devitrification in the final repository, at temperatures below 200°C, in the course of hundreds or thousands of years.

The processes of cooling can be investigated directly, and reliable extrapolations are possible under the time-temperature conditions in the interim storage period. Such investigations are part of the glass optimisation procedure, when the loading capacity for various waste components is determined (82, 153, 214). Table 12 lists the radiographically determined phases appearing in different glasses, in the temperature range 500 to 800°C, in a period of up to 100 days (130, cf 82). They are generally SiO_2 free compounds. Figure 34, taken from the summary work (135), shows that, at storage temperatures of 600°C, no significant alteration in corrosion behaviour need be feared.

Tempering ABS glasses 39 and 41 at about 800°C for 14 days leads to an increase in the cesium leach rate (118). The corresponding value for strontium and molybdenum rates differ only slightly from those in unannealed glass (tables 13 and 14). According to tests on PNL glasses (213), the influence of glass composition is more important than that of partial devitrification. At temperatures below 500°C no crystallisation is observed even after several years. If the temperature range 600 to 800°C, which is critical for crystal formation, is quickly traversed during glass production, then devitrification during interim storage seems highly unlikely.

It is difficult to make reliable predictions of the long-term stability of glasses at final repository temperatures ($T < 200^oC$).

Phase	SON 58.30.20	VG 98/3	UK 209	UK 189
Ru_2O	x	x	x	x
Ru				x
Pd_3Te	x	x		
PdTe	x			
PdO	x			x
Pd		x		x
$CdTeO_3$	x			
$(SE)_2Te_3O_9$	x	x		
CeO_2	x	x	x	x
$(RE)_2O_3$	x		x	
$(RE)PO_4$	x		x	x
RE-Silicate				x
$(RE)MoO_6$		x	x	
$(Ba,Sr)MoO_4$	x		x	
SiO_2	x	x		
$MgSiO_3$			x	
$(Mg,Fe,Ni)Si_2O_6$			x	
$FeCr_2O_4$				x

Table 12: Possible crystalline phases in European HLW glasses (detected by X-ray diffraction) (130).
RE: Rare earth elements

Boulos et al (21) made some extrapolations for a borosilicate glass using the temperature dependence of viscosity at $T < T_G$ and theoretical formulae for crystal growth (cf also section 2.3). According to this, at 400°C, no significant crystallisation should occur for up to 10^5 years. At 100°C, the corresponding value is 10^{24} years. Terrestrial and lunar glasses of similar age (up to 4.10^9 years) support the authors' claim that glasses under environmental conditions remain stable over geological time periods.

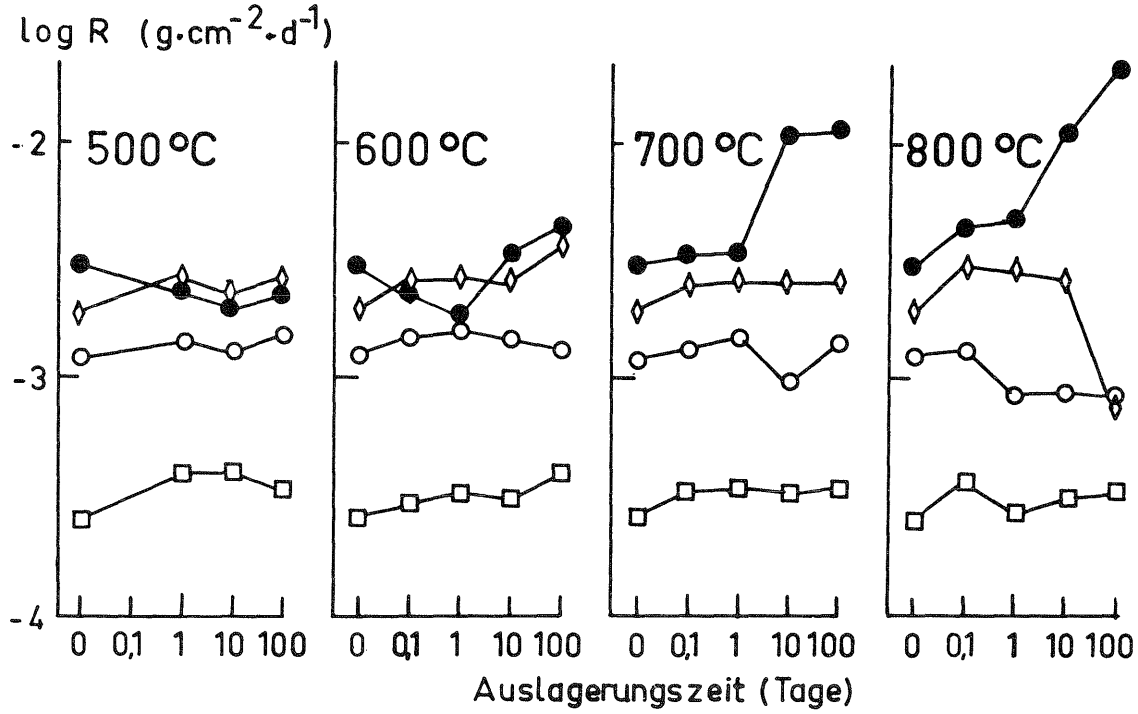

Figure 34: Soxhlet leach rate of four European borosilicate glasses as functions of heat-treatment temperature and holding time (130). □ UK 209, ○ UK 189, ● SON 58.30.20 U2, ◊ VG 98/3

Days	ABS 39. Cs	Sr	Mo	Days	ABS 41. Cs	Sr	Mo
3	2.32	3.28	6.00	3	0.41	1.84	3.07
10	1.43	1.73	3.38	10	0.23	1.21	2.26
17	1.16	1.79	2.65	17	0.24	1.64	2.58
24	0.95	1.41	2.44	24	0.24	1.28	2.37
31	1.26	1.62	3.16	31	0.23	1.28	2.17
38	0.98	2.06	1.93	39	0.20	1.17	1.73
45	0.86	1.99	1.69	45	0.27	1.42	2.08
				52	0.23	1.22	1.85
				59	0.23	2.07	2.02

Table 13: Soxhlet leach rate (in $kg.m^{-2}s^{-1} \times 10^{7}$ at 99 - 100°C) glasses ABS 39 and 41, not heat treated (118).

Days	ABS 39 Cs	Sr	Mo	Days	ABS 41. Cs	Sr	Mo
3	5.37	2.81	6.29	3	3.52	3.03	3.89
10	4.71	3.75	5.28	10	2.34	2.26	2.69
17	3.36	2.78	3.88	17	2.19	2.45	2.35
24	3.42	3.24	3.52	25	2.10	2.40	2.45
31	3.01	2.78	3.16	31	2.02	2.53	2.68
38	2.69	2.78	2.74	38	2.26	3.13	2.43
45	2.31	2.82	2.69	45	2.05	2.84	2.56
52	1.76	1.39	3.12	52	2.00	2.94	2.46

Table 14: As Table 13, but glasses are heat treated: 14 days 800°C (118).

Frequent attempts have been made to extrapolate the long term stability of glasses from empirical data (135). This is usually based on time - temperature - transformation diagrams (figure 35). Under favourable circumstances such diagrams can provide useful extrapolations. The precision of predictions could be improved by taking theoretical models into account.

5.1.3 Phase separation

Macroscopic phase separation of HLW glasses by the formation of the "yellow phase" from sulphates, molybdates, chromates and possibly chlorides, must be avoided by limiting the content of these components (82): this phase is soluble and carries with it the alkali and alkaline earth ions including the fission products cesium and strontium. The formation of a molybdate phase can be avoided by adding reducing agents, such as metallic silicium, to the melt (82). For investigations of the oxidation number of molybdenum in glasses, see (31, 162).

The characteristic tendency of borosilicate glasses to show metastable phase separation has stimulated extensive investigations on glasses ABS 39 and 41 (67). It has been verified experimentally that these glasses lie outside the 600°C phase separation boundary. The miscibility gap is influenced by various oxides, such as, Al_2O_3, Fe_2O_3 and ZnO, (67, 205) and it is made smaller by the reduction of Fe^{3+} to Fe^{2+} (205).

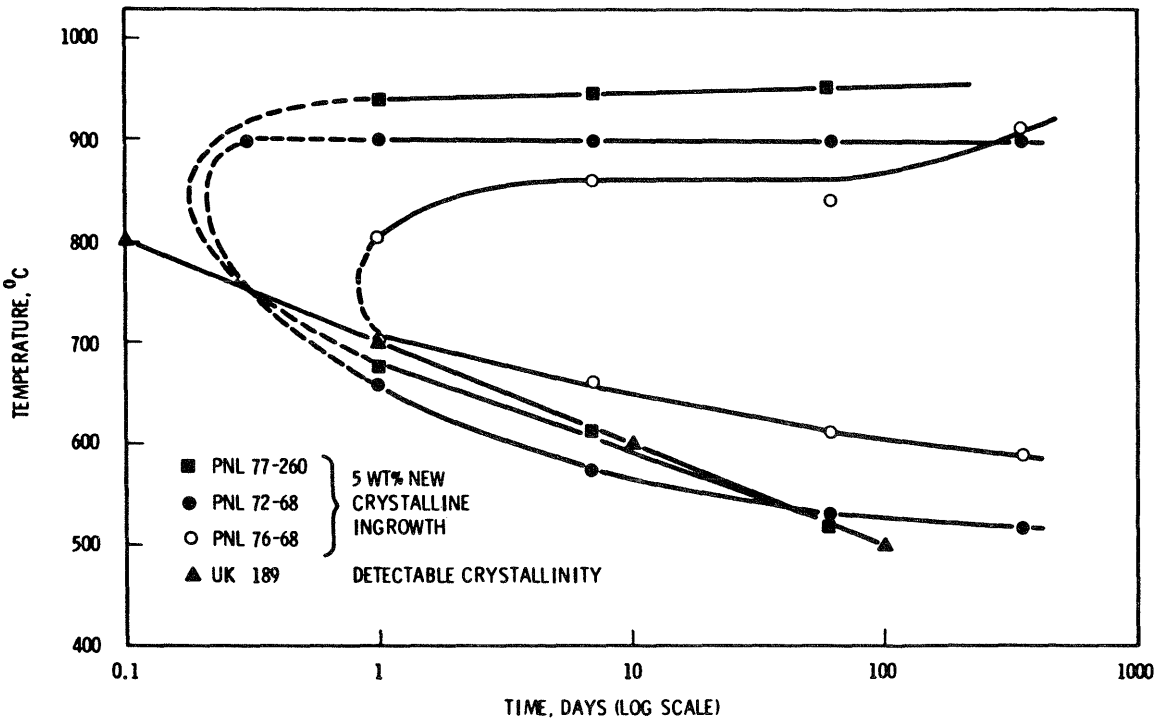

Figure 35: Time-temperature-transformation curves for HLW glasses (135, 209)

5.2 The behaviour of ancient and natural glasses

Conclusions can be drawn about the behaviour of HLW glasses under environmental conditions from tests on ancient glasses and glasses of volcanic origin.

Synthetic glass has been in use for some 3500 years, first for jewellery and luxury items, later, with the discovery of glass blowing some 2000 years ago, for everyday use. Many glass objects have survived for thousands of years, if not mechanically, then at least chemically.

Iridescent, adhesive films have been formed on ancient glasses in the earth, these films are only 0.3 to 15 µm thick (109). Sodium has largely been leached from these films. In the Middle Ages the quality of glass in general deteriorated, because sodium was replaced by potassium (84). Even if HLW glasses have a different composition to ancient glasses, the conclusion can still be drawn that glass survives thousands of years' weathering practically undamaged (48, 109).

Further evidence for the long-term stability of glass is shown by investigations on volcanic glasses, which have been exposed to weathering and the effects of water for geological time periods (72, 231). Thin, leached films are also formed on basalt glasses (45 - 54 % SiO_2) (5). According to investigations by Tombrello (204), the corrosion mechanism of obsidian is similar to that of silica glasses and can be described by the hydratisation model of Doremus (115). According to this, the time for the formation of a 20 µm thick hydrated layer at 80°C is about 100 years, at 180°C, however, only 10 weeks.

Direct comparison between HLW and natural glasses at 90°C and in Soxhlet tests shows that the borosilicate glasses are less stable than the natural products (1, 129). The better chemical stability of the natural glasses is due to their higher SiO_2 content.

The hydratisation rates of natural glasses were determined in other laboratory tests (68). Here some significant discrepancies were found between the values for laboratory samples and those obtained from tests on weathered samples.

Volcanic glasses react rapidly under hydrothermal conditions. At 300°C basalt glasses are unstable in sea water and form a mixture of crystalline phases (192). Heavy metals are released in this way; not, however, if the sea water is replaced by a 0.45 M sodium chloride solution.

5.3 Results of corrosion tests on borosilicate glasses

5.3.1 Results at temperatures up to 100°C

Before numerical values from corrosion or leaching tests can be used, they must be evaluated very critically, depending on the proposed application. In section 3.4, the influence of the test procedure was indicated using figures 31 and 32. Furthermore, the scattering of the results from individual experiments can be very significant. Figure 36 (170) serves as an example, it summarises 51 experiments which were carried out using the same glass at 200°C in brine in the autoclave. No definite functional relationship between weight loss and time can be found, because the results have such a broad scatter-band.In this connection, figures 18 and 19 (section 3.3.1) illustrate the problem of chosing representative values. Finally, figure 37 (86) shows that the dissolution behaviour of individual glasses varies enormously, the values shown are spread over a 10^5 range. A closer look, however, does show that the results for the French glasses lie in a comparatively narrow band.

Dissolution rates are generally time dependent, but this can be subject to the leach mechanism, as in the case of selective dissolution of cesium (figure 38) (223). However, irregular deviations are also observed, due to the non-homogeneous nature of the glass block and possibly also to the dissolution of surface layers. Figure 39, for example, shows the dissolution rate of americium and plutonium using a French glass (18). The same author (17) also reports on the release rate of plutonium, this increases with time (figure 40).

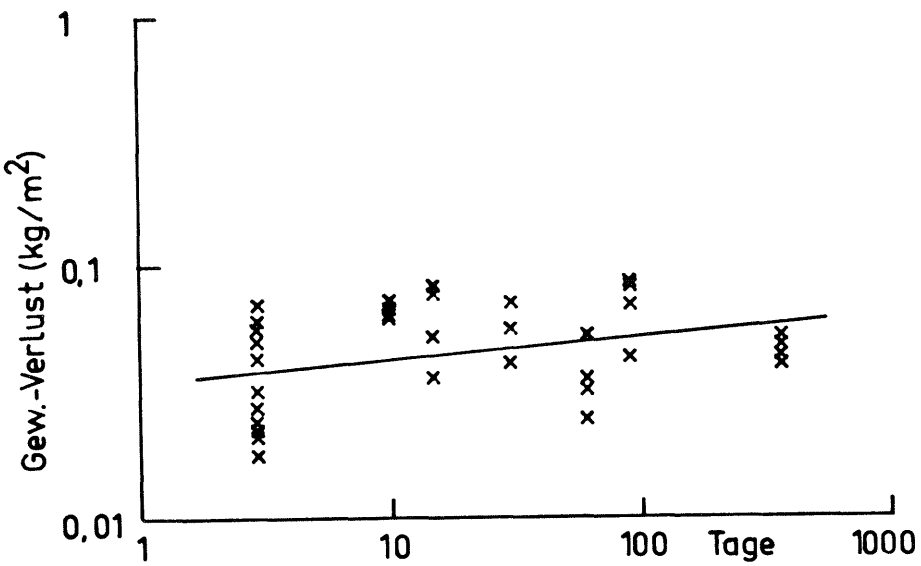

Figure 36: Specific weight loss of a borosilicate glass leached in carnallite-containing quinary solution at 200°C (170)

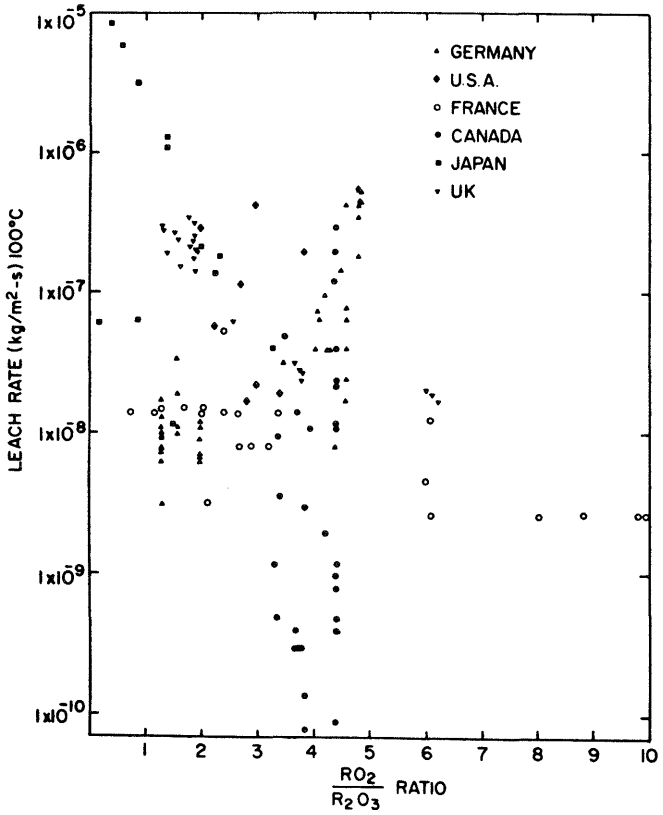

Figure 37: Leach rate plotted as a function of composition for various waste glasses developed in the national programs (86)

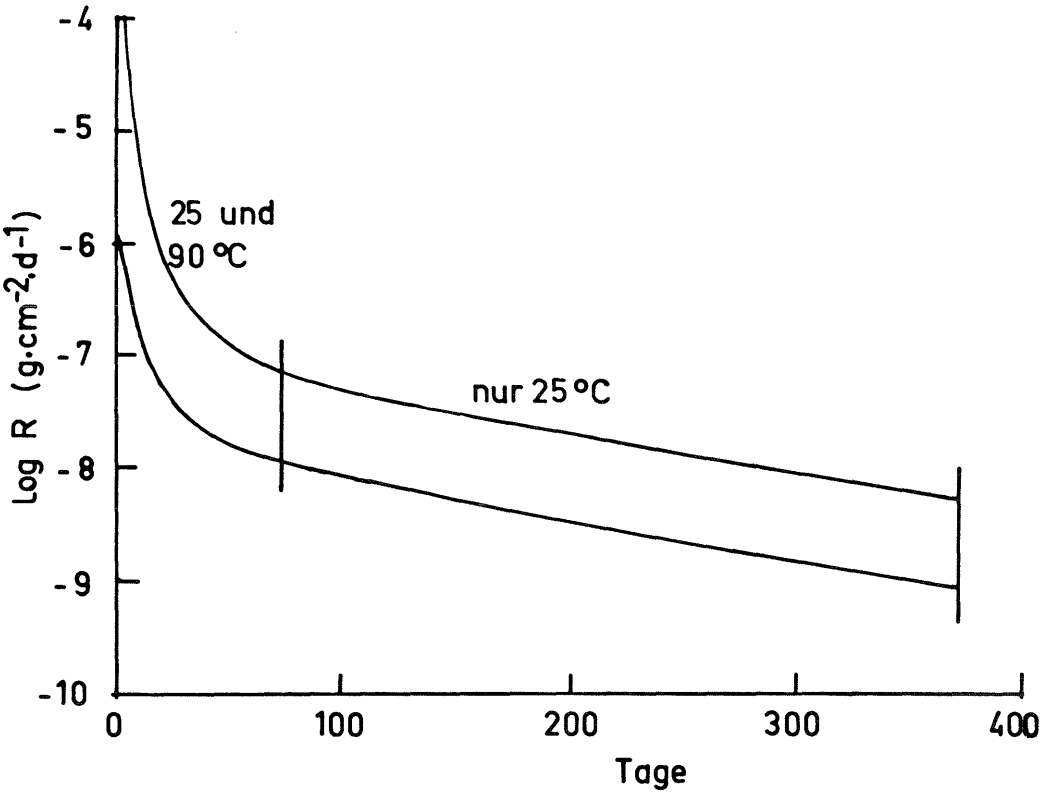

Figure 38: Band summarising all published ^{137}Cs leach rates of SRP glasses in distilled water and in salt brine (223)

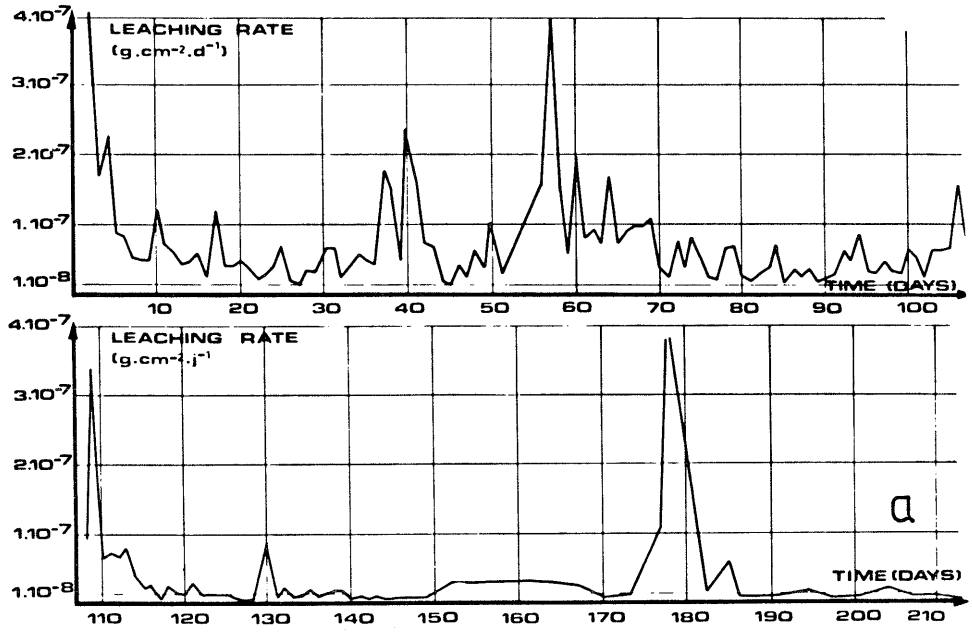

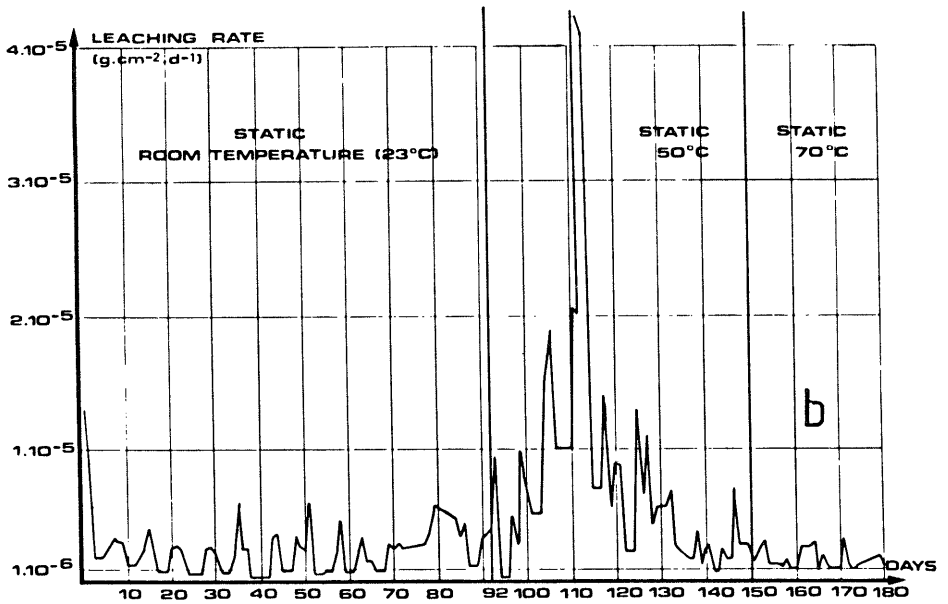

Figure 39: Long-term leaching tests of French actinide doped glasses.
a) ^{241}Am b) ^{238}Pu (18)

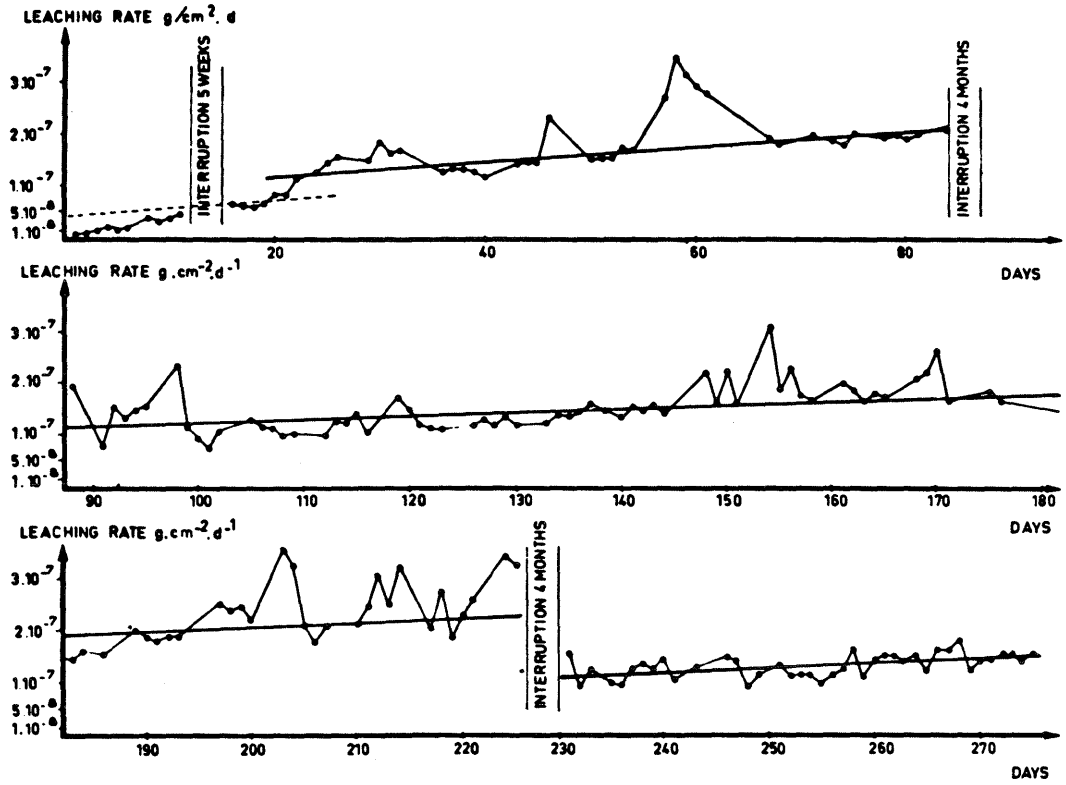

Figure 40: Leaching curve of ^{238}Pu for a French glass (17)

The results given in figure 41 (197) show how analysis of the solvent alone can give a misleading picture of glass corrosion. Whereas in brine a considerable amount of strontium is found in solution, practically no strontium is found in either of the waters. This can be explained by the different pH values: in brine pH is about 6, in both the waters about 9.6. By reacting with carbon dioxide from the air, the strontium can be precipitated as a carbonate and possibly as a silicate.

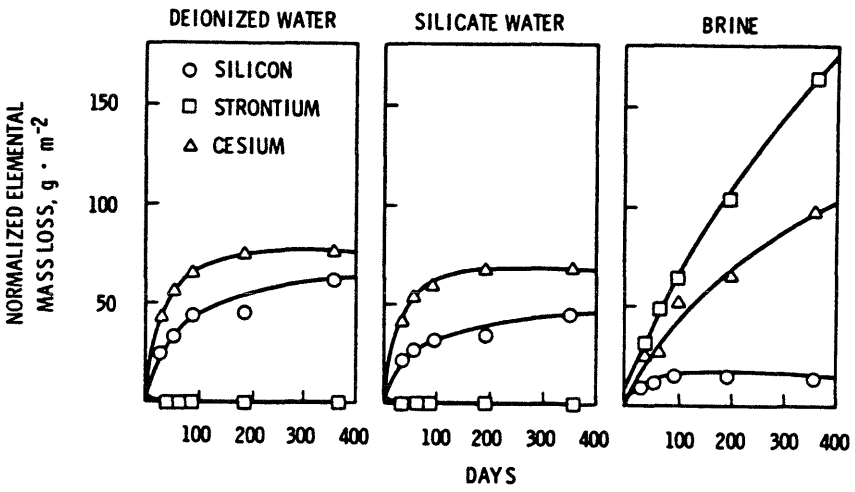

Figure 41: Leach data for PNL 76-68 glass, MCC-1 test, 90°C (197)

In view of all the unknowns and the great scattering of results due to test procedures, it would be of little use to collect and reproduce in detail the multitude of published results. It is sufficient to fall back on the more recent summaries and highlight some characteristic findings. An HMI report (210) summarises results up to the end of 1976. Other results, mostly on investigations at room temperature, are presented in an EIR report (172). PNL reports also contain comprehensive surveys. Investigations in the temperature range 20 to 100°C have recently been summarised (52). Tables 15 and 16 are taken from this work.

Glass type	Element	leach rate ($g \cdot cm^{-2} \cdot d^{-1}$)	Temp. (^oC)	Method	Time (days)	Solvent	other Variables	Ref.
PNL 76-68	Si	$5 \cdot 10^{-5}$	90	static	28	DI	A/V=0,1cm^{-1}	147
Sandia 75-32	ML	$4 \cdot 10^{-7}$-10^{-5}	boiling	Soxhlet	730	DI		112
PNL 79-417,418	Si	$4 \cdot 10^{-6}$	90	static	78	DI	A/V=0,1cm^{-1}	147
SRP	Cr,Sr,Pu	10^{-9}-10^{-8}	99	Soxhlet	100	DI silicate water		226
SRL	Cs	$6 \cdot 10^{-8}$	90	static		brine		62
	Cs,Sr	$2 \cdot 10^{-5}$-$3 \cdot 10^{-5}$	90	MCC-1	28	DI		51
SRL 211	Eu,Ce	$5 \cdot 10^{-6}$-10^{-5}	90	MCC-1	28	DI		226
	Cs,Sr	10^{-4}-$2 \cdot 10^{-3}$	90	MCC-1	40-100	DI		226
SRL (various)	ML	$4 \cdot 10^{-8}$-$5 \cdot 10^{-7}$	100	Soxhlet	28	DI		44
SRL	SiO_2	$7 \cdot 10^{-6}$	70	flow	28		5 m/ year	51
	SiO_2	$3 \cdot 10^{-5}$	70	flow	28		70 m/ year	51
TDS 211	Si	$3 \cdot 10^{-5}$	90	static	28	DI	A/V=0,1cm^{-1}	147
TDS 79-339	Si	$4 \cdot 10^{-6}$	90	static	28	DI	A/V=0,1cm^{-1}	147
RHO	Cs	10^{-5}-$4 \cdot 10^{-4}$	100	Soxhlet			Powder	181
RHO	Si	$4 \cdot 10^{-6}$	90	static	28	DI	A/V=0,1cm^{-1}	147
ICCP	Cs	$4 \cdot 10^{-4}$	95	Soxhlet	14	D		43
ICCP	Cs	$3 \cdot 10^{-5}$	95	static	28	D		43
UK 189,209	ML	10^{-4}-$2 \cdot 10^{-4}$	100	Soxhlet		D, granite water		33
VG 98	ML	10^{-4}	70	Soxhlet	15	D		83
France	Cs,Sr	$2 \cdot 10^{-5}$	100		80			17
Japan	Cs, Sr	10^{-7}-10^{-6}	94	Soxhlet	2-4	D		203

Table 15: Leach rate of representative borosilicate glasses at temperatures of 70^o to 100^{o}C (52).
DI - deionised water, D - distilled water, ML Mass loss (ML)

Glass type	Element	leach rate ($g \cdot cm^{-2} \cdot d^{-1}$)	Method	time (days)	solvent	other Variables	Ref.
PNL 72-68	Cs,Sr Pu Cm	10^{-4}-10^{-5} 10^{-6} 10^{-7}	Soxhlet	1000			181
PNL 76-68	Np	10^{-5}-10^{-7}	IAEA	420	DI		218
	Pu	10^{-6}-10^{-9}	IAEA	420	brine		44
	Cs	$2 \cdot 10^{-6}$-$8 \cdot 10^{-7}$		7	DI		75
	Eu	$3 \cdot 10^{-7}$		7	DI		75
SRL	Cs,Sr	$3 \cdot 10^{-7}$-$4 \cdot 10^{-7}$	MCC-1		DI		215
	Pu	$0,4 \cdot 10^{-5}$-$3 \cdot 10^{-5}$	MCC-1		DI	pH=4	215
SRL	Cs	10^{-9}	static	365	brine		62
	Cs	10^{-7}-10^{-8}	MCC-1	700	DI	pH 7 - 9	62
	Sr	10^{-4}-10^{-8}	MCC-1	700	DI	pH 4 - 7	62
SRP-TDS-3A/131	Pu	$5 \cdot 10^{-8}$		1000	DI	A/V=0,1 cm^{-1}	166
	Cs, Sr	$2 \cdot 10^{-7}$		1000	DI	A/V=0,1 cm^{-1}	166
France	Cs,Sr	$5 \cdot 10^{-7}$		80			17
UK 189,209	Weight loss	10^{-6}-10^{-7}	Soxhlet		granite water		33

Table 16: Leach rate of representative borosilicate glasses at room temperature (52)

DI - deionised water

In a joint operation between AERE (Harwell), HMI (Berlin) and CEA (Marcoule), 5 different borosilicate glasses were compared (table 7) (132). Two glass ceramic products and a phosphate glass were also included in the investigations. Some results are summarised in tables 17 and 18. The influence of pH value on the stability of the glass can be seen from figure 42. At 90°C a pH drift to values below 5 results in a substantial increase in corrosion rate.

The glasses were also tested in various waters and the work contains data on the change in dissolution rate due to annealing the glass at temperatures up to 800°C (cf figure 34).

Glass	corrosion rate ($g \cdot cm^{-2} \cdot d^{-1}$)		activation energy (kJ/mol)
	100°C	50°C	
UK 189	$1,3 \pm 0,2 \cdot 10^{-3}$	$5,0 \cdot 10^{-5}$	$64,8 \pm 2,5$
UK 209	$2,6 \pm 0,9 \cdot 10^{-4}$	$1,0 \cdot 10^{-5}$	$67,3 \pm 2,9$
SON 50	$3,1 \pm 0,3 \cdot 10^{-3}$	$1,1 \cdot 10^{-4}$	$80,3 \pm 2,9$
VG 98/3	$1,9 \pm 0,3 \cdot 10^{-3}$	$1,1 \cdot 10^{-4}$	$58,1 \pm 2,5$

Table 17: Mass loss (Soxhlet test) and activiation energies for various HLW glasses (132)

Isotope	Temp. °C	SON 50.30.20.U2	UK 209	SON 64.19.20.F3	VG 98/3
^{106}Ru	25	3.0×10^{-7}	1.5×10^{-6}	4.3×10^{-7}	3.4×10^{-7}
	50	1.0×10^{-7}	4.0×10^{-6}		7.7×10^{-7}
	70	1.0×10^{-7}	2.0×10^{-6}		4.1×10^{-7}
^{137}Cs	25	1.0×10^{-6}	7.0×10^{-7}	2.3×10^{-6}	2.0×10^{-6}
	50	3.0×10^{-6}	8.0×10^{-6}		2.2×10^{-5}
	70	4.5×10^{-6}	1.5×10^{-5}		4.8×10^{-5}
^{144}Ce	25	3.0×10^{-8}	1.5×10^{-8}	$< 10^{-8}$	3.6×10^{-8}
	50	1.0×10^{-8}	2.0×10^{-8}		7.0×10^{-8}
	70	2.0×10^{-9}	2.0×10^{-8}		5.8×10^{-8}
^{90}Sr	25	9.0×10^{-8}	2.5×10^{-7}	4.0×10^{-7}	1.8×10^{-6}
	50	3.5×10^{-7}	2.5×10^{-6}		1.5×10^{-5}
	70	6.0×10^{-7}	4.5×10^{-6}		3.6×10^{-5}
β Total	25	1.5×10^{-7}	2.0×10^{-7}	5.0×10^{-7}	7.6×10^{-7}
	50	5.0×10^{-7}	2.2×10^{-6}		9.9×10^{-6}
	70	7.0×10^{-7}	4.5×10^{-6}		1.8×10^{-5}

Table 18: Leach rate for specific elements ($g \cdot cm^{-2} \cdot d^{-1}$) in various European HLW glasses, using VULCAIN method (132)

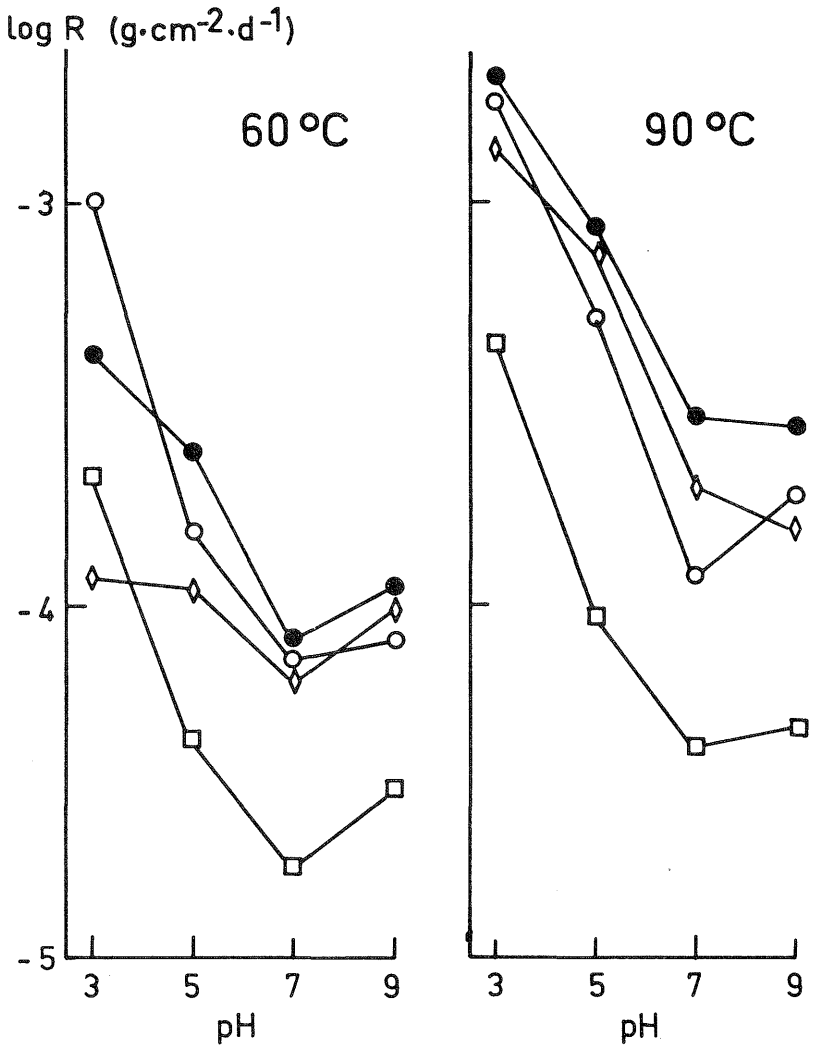

Figure 42: Durability of various European borosilicate glasses dependent on pH at 60° and 90°C.
□ UK 209, ○ UK 189, ● SON 58.30.20.U2,
◊ VG 98/3 (132)

Particularly comprehensive investigations have been carried out on the American glass PNL 76-68. The composition of this glass is given in table 8. The investigations included tests in flow equipment at temperatures of 25 and 75°C in distilled water, 0.03 M $NaHCO_3$ solution and salt brine (46). Selected results are given in figures 43 to 45. The release rate for plutonium is given in figure 46 (218). Further experimental results for the glass 76-68 are summarised by Chick et al (36).

Finally, mention should be made of some Canadian field tests using radioactive glass blocks (148). As figure 47 shows, the leach rate of ^{90}Sr decreased over the years by several orders of magnitude. Considering that the leach rates in the field tests are also influenced by sorption effects, the tests show that in practice, no surprisingly high values are obtained.

The attempt to interpret these data using a model (127) should be treated rather circumspectly; the formulae make too little allowance for the complex chemistry. (Cf also the comments on (167) in section 6).

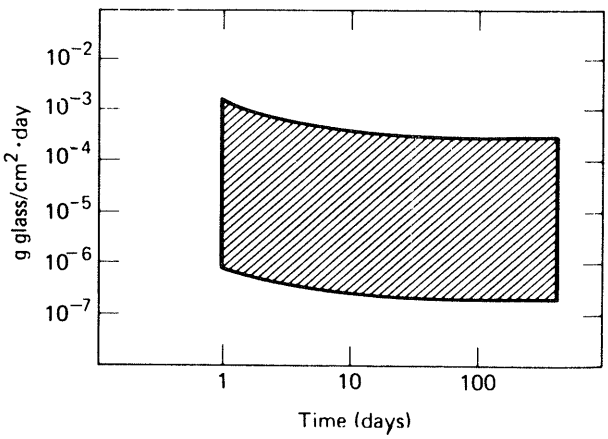

Figure 43: Summary of all leach rates (excluding Pu) for glass PNL 76-68, in three different solvents at temperatures of 25° to 70°C (46)

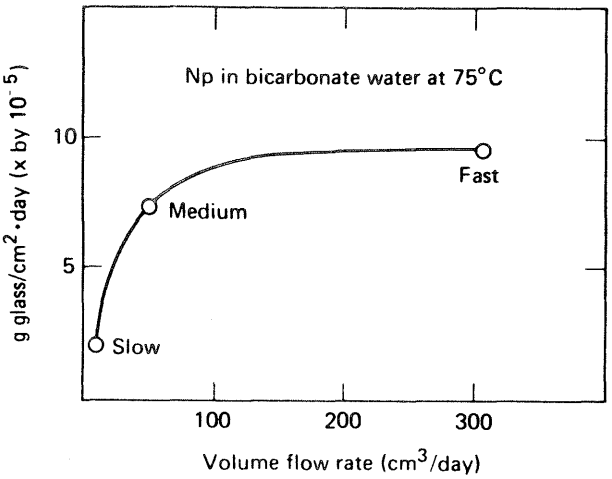

Figure 44: Effect of flow rate on the release rate of neptunium from glass PNL 76-68 in 0.03 M $NaHCO_3$ at 75°C (46)

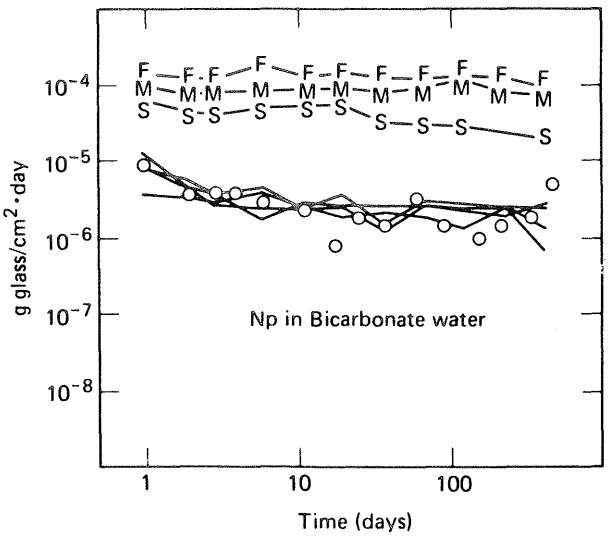

Figure 45: Leach rate of neptunium from PNL 76-68 in 0.03 M $NaHCO_3$. Upper lines show results at 75°C and the lower lines at 25°C. S - slow, M - medium, F - fast flow (cf Figure 44) (46)

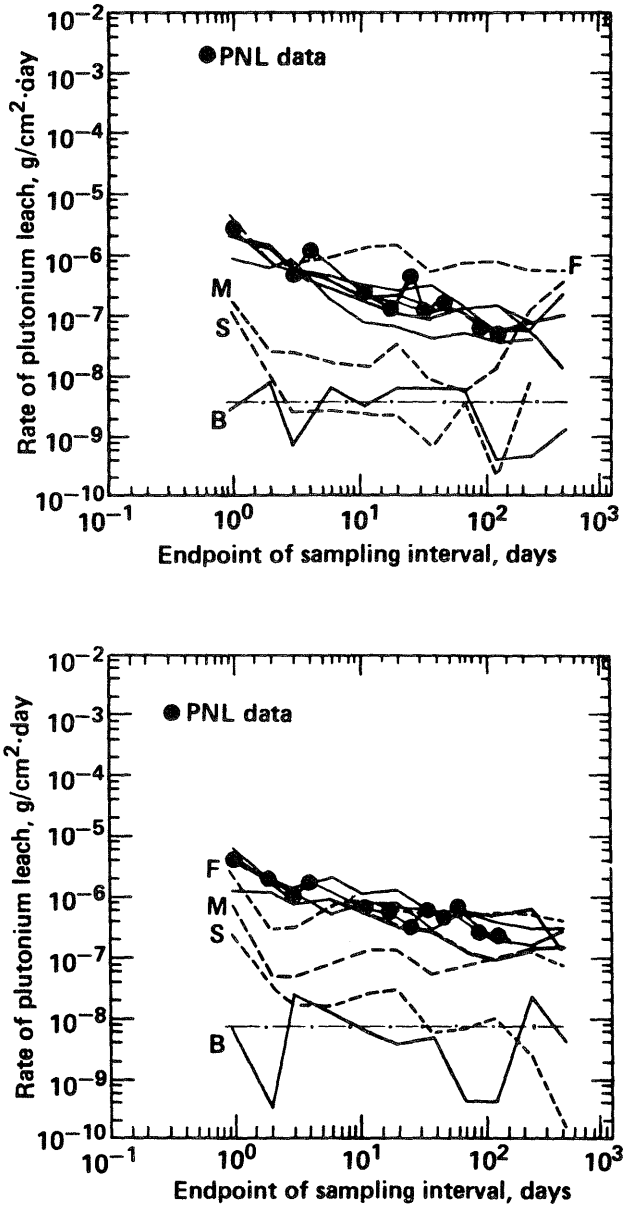

Figure 46: ^{239}Pu leach rates in distilled water (above) and in 0.03 M $NaHCO_3$ (below). Dashed lines: 75°C, solid lines: 25°C. F, M, S are fast medium and slow flow rates (see figure 44). B is the blank (218)

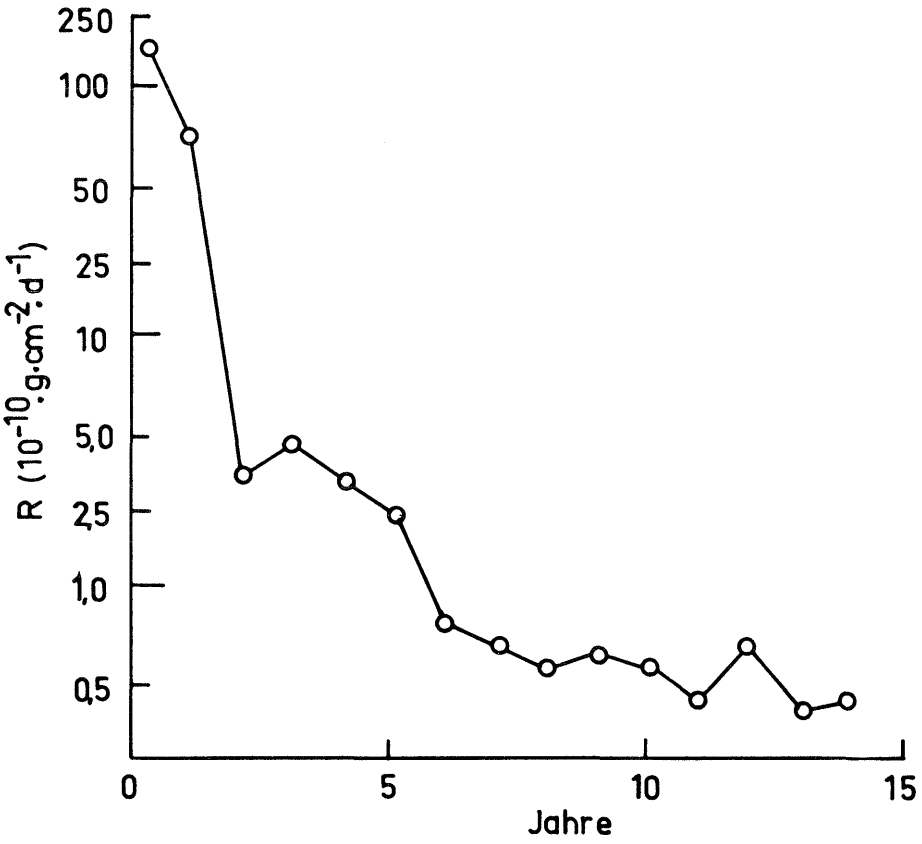

Figure 47: Experimental time dependence of leach rate based on ^{90}Sr for the Chalk River field test (127)

5.3.2 Hydrothermal conditions

Hydrothermal is here used to mean conditions in aqueous solution at temperatures over 100°C. This definition is used in chemistry for practical reasons and differs from the geological definition.

On first examination, the results of hydrothermal corrosion tests often appear contradictory: test procedures and solvent composition are largely responsible for the glass behaviour. An example of this is shown in table 19 (28). At high temperatures in static conditions, new solid phases are formed, these affect the release of the radioactive elements (221). Because the type of phase formed depends on the composition of the glass, the solvent and the mineral environment (137), it is almost impossible to generalise experimental findings. The examples used here are, therefore, given as illustrations.

The effect of test conditions is illustrated by figure 48, for example; in a flow system (0.3 ml/min) cesium is removed in the solvent, whereas in a closed system it is recombined, to some extent, to form new solids.

Recent investigations by Petit et al (168), using glass pieces of cm dimensions, show that at temperatures as low as 160°C the material reacts rapidly. The glass had the following composition (weight %): SiO_2 : 55.5, B_2O_3 : 29.3, Na_2O : 10.3, Li_2O : 4.9. The tests were carried out in the autoclave with a glass surface area/solvent volume ratio of 0.4 cm^{-1}. Figure 49 shows that new solid phases are formed when the solvent is not renewed (case 1), and that the glass disintegrates completely after about 12 days. If the solvent has previously been "equilibrated" with glass powder of the same composition, then the glass disintegrates even more quickly (case 5). It would be interesting to test glasses of specially designed composition, the hydrothermal transformation products should recombine with the radioactive waste products (110). Such investigations are still in their infancy.

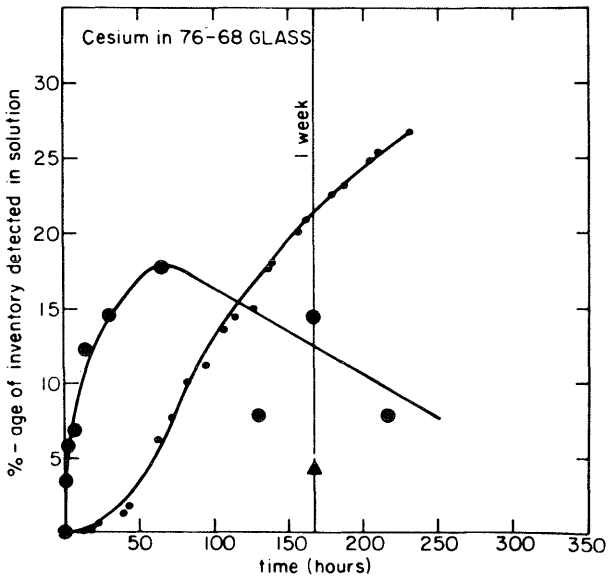

Figure 48: Effect of test conditions on the release of cesium from PNL 76-68 glass at 300°C and 30 MPa.
● rocking autoclave, ● flow system, ▲ sealed, noble metal capsule (184)

Solvent	Glass converted %	Cs in solvent %
DI water	16,4	8,6
Sea water	11,5	10,3
Brine A	6,6	0,8
Brine B	4,6	1,1
NaCl 100 g/l	3,0	1,7
NaCl 300 g/l	3,0	0,8
KCl 57 g/l + NaCl 243 g/l	2,0	0,6
$MgCl_2$ 138 g/l	15,0	5,5
$MgCl_2$ 138 g/l + NaCl 145 g/l	9,0	2,0
pH 0, H_2SO_4	100	100
pH 0, NaCl 300 g/l	25,0	8,4
pH 12, NaOH	100	84
pH 12, NaCl 300 g/l	100	29,4

Table 19: Effect of solvent composition on the hydrothermal reaction of HLW glasses (250°C, 28 days, A/V 0.2 - 0.25 cm^{-1}) (28)

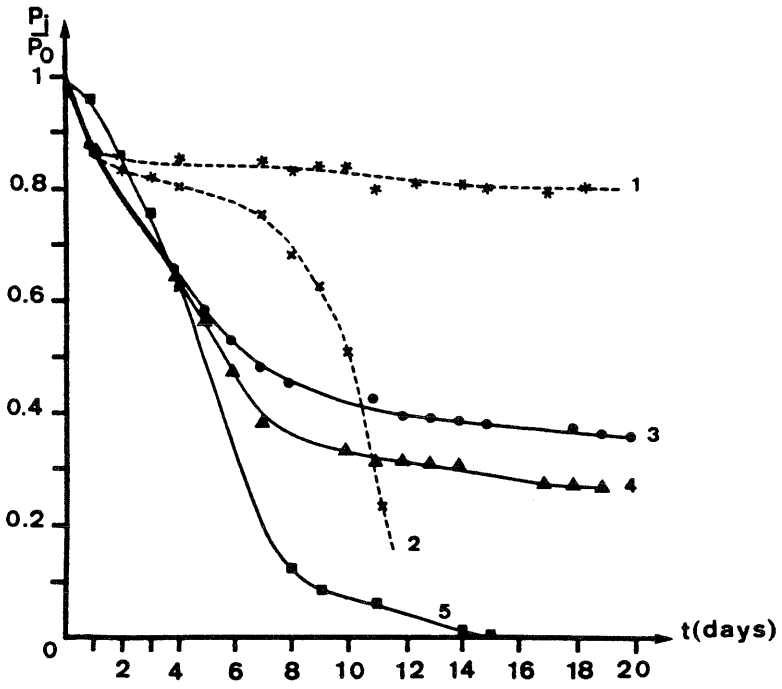

Figure 49: Variations of the ratio of weight of insoluble material (P_i) to the initial weight P_o of the glass samples with leaching time. Water at 160°C (168).

1,2: total insoluble material (1) and remaining glass only (2) for unrenewed water.

3,4: as above, with daily renewed water.

5: remaining glass for unrenewed water "pre-equilibrated" with powdered glass.

Figure 25 illustrates the extent of the investigations of Westsik et al (220). The results of more recent work are summarised in figures 50 to 52 (219). The tests were carried out with deionised water and a surface/volume ratio of 0.1 cm^{-1}. The data in figure 50 can be represented by the empirical relationship

$$Q = k \cdot t^n$$

(Q : g glass/m^2). For temperatures up to and including 150°C, n ≈ 0.7 and the activation energy up to this temperature is 53 kJ/mol (figure 51). As temperature increases, n decreases, at 250°C, n = 0.2. The test times were too short to be able to say whether the exponent, n, decreases with time at lower temperatures. As figure 52 shows, the corrosion mechanism changes at temperatures above 250°C, the corrosion rate again becoming more dependent on temperature. From figure 50 it can be seen that, at T > 50°, dissolution is almost congruent, whereas at 25 and 50° the attack is predominently selective.

Another group has tested the same glass under hydrothermal conditions (75). The release rates for different elements, based on a test period of 7 days, are given in table 20. The temperature dependence of release rate varies widely for the different elements (figure 53). Adsorption effects may be responsible for this behaviour. A long-term experiment would perhaps give a different picture.

Scanning electron microscopy has been used by Savage and Chapman (182) to enlarge on their already comprehensive corrosion tests for two simulated HLW glasses at temperatures up to 350°C. At 250°C the glass begins to disintegrate after 111 hours. At 350°C, in the same time period, the glass has already changed quite extensively into a crystalline phase. Glasses with lower B_2O_3 content have less tendency to disintegrate at 250°C (101).

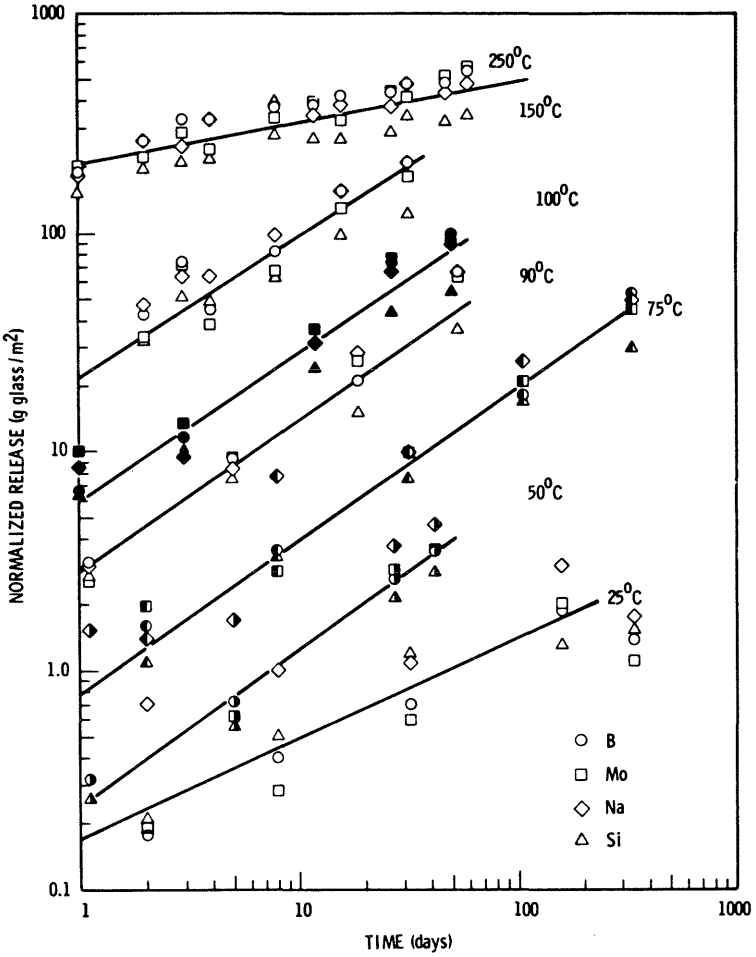

Figure 50: Time and temperature dependence of leaching for glass PNL 76-68 (219)

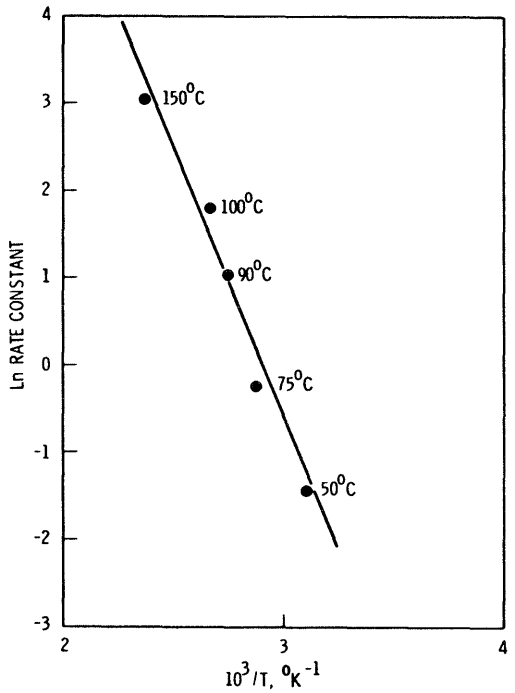

Figure 51: Kinetic constant k as a function of temperature, glass PNL 76-68 (219)

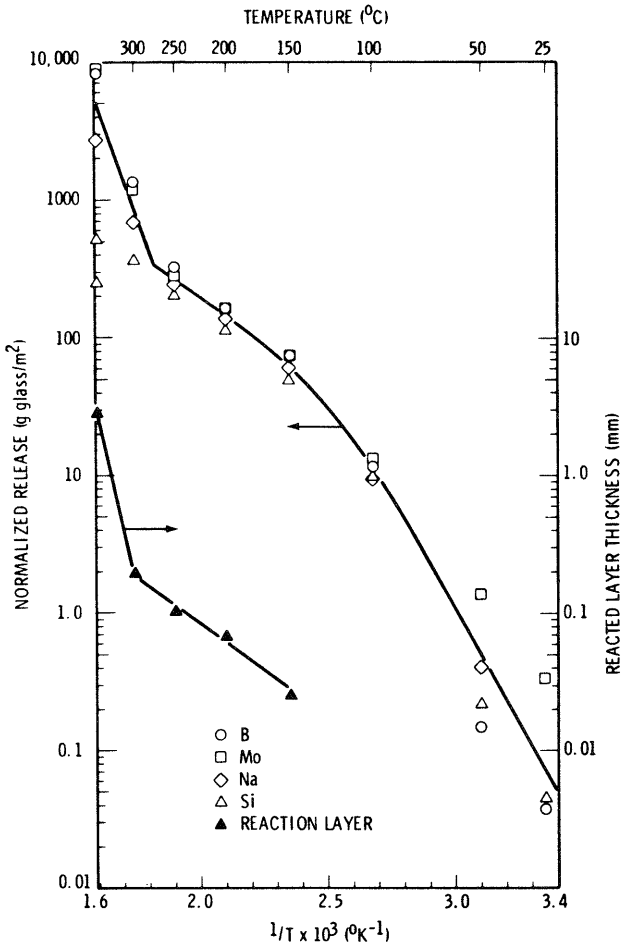

Figure 52: Temperature dependence of leach rate of various elements, glass PNL 76-68, and thickness of reacted layer after 3 days (219)

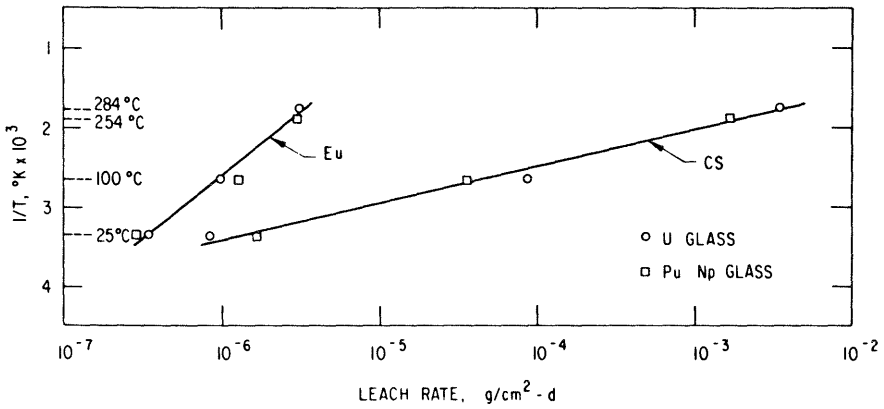

Figure 53: Effect of temperature on the leach rates of europium and cesium, PNL 76-68 (75)

Isotope	leach rate ($g \cdot m^{-2} \cdot d^{-1}$) glass doped with U			glass doped with Pu/Np		
	25 °C	100 °C	286 °C	25 °C	100 °C	254 °C
Co-60	$4,8 \cdot 10^{-6}$	$3,4 \cdot 10^{-5}$	$6,6 \cdot 10^{-5}$	$1,5 \cdot 10^{-6}$	$1,1 \cdot 10^{-5}$	$6,8 \cdot 10^{-5}$
Zn-65	$4,0 \cdot 10^{-6}$	$1,6 \cdot 10^{-5}$	$4,5 \cdot 10^{-5}$	$1,6 \cdot 10^{-6}$	$1,6 \cdot 10^{-5}$	
Zr-95	$4,5 \cdot 10^{-7}$	$2,4 \cdot 10^{-6}$	$1,1 \cdot 10^{-5}$	$1,5 \cdot 10^{-7}$	$2,8 \cdot 10^{-6}$	$1,0 \cdot 10^{-4}$
Ru-103	$1,2 \cdot 10^{-6}$	$7,4 \cdot 10^{-6}$		$1,7 \cdot 10^{-6}$	$4,8 \cdot 10^{-6}$	
Ag-110 m	$1,9 \cdot 10^{-6}$	$2,9 \cdot 10^{-5}$		$1,3 \cdot 10^{-6}$	$3,2 \cdot 10^{-5}$	
I-131	$1,5 \cdot 10^{-6}$		$1,3 \cdot 10^{-3}$	$7,1 \cdot 10^{-6}$	$3,9 \cdot 10^{-5}$	$2,6 \cdot 10^{-3}$
Cs-134	$8,4 \cdot 10^{-7}$	$8,9 \cdot 10^{-5}$	$3,5 \cdot 10^{-3}$	$1,7 \cdot 10^{-6}$	$3,6 \cdot 10^{-5}$	$1,7 \cdot 10^{-3}$
Ba-140	$1,8 \cdot 10^{-6}$	$1,5 \cdot 10^{-5}$		$5,5 \cdot 10^{-7}$	$5,9 \cdot 10^{-6}$	
Ce-141	$6,5 \cdot 10^{-7}$	$1,2 \cdot 10^{-6}$	$2,6 \cdot 10^{-6}$	$2,5 \cdot 10^{-7}$	$2,3 \cdot 10^{-6}$	
Eu-152	$3,5 \cdot 10^{-7}$	$1,0 \cdot 10^{-6}$	$3,3 \cdot 10^{-6}$	$2,9 \cdot 10^{-7}$	$1,3 \cdot 10^{-6}$	$3,2 \cdot 10^{-6}$
U-237	$5,9 \cdot 10^{-7}$			$7,2 \cdot 10^{-7}$	$3,1 \cdot 10^{-6}$	
Np-239				$7,1 \cdot 10^{-6}$	$2,4 \cdot 10^{-5}$	$2,7 \cdot 10^{-4}$

Table 20: Leach rate at various temperatures, glass PNL 76-68. Test period 7 days in distilled water. Surface/volume ratio: $2cm^{-1}$ (75).

5.3.3 The formation of sorptive surface layers

With the adsorption of heavy metals, and particularly the actinides, the release rates of the elements affected are considerably lower than the rates which arise due to network dissolution. According to a recent investigation, the release rate of neptunium is smaller by a factor of 7 (85) and of plutonium and americium by factors of 100 and 1000 respectively!

Figure 54 illustrates the retention effect exerted by the hydrated surface of a borosilicate glass which contains lanthanides (11). Na, Cs and Sr were preferentially leached and the hydrated layer grew during the whole test period. Zinc, the lanthanides and iron were, however, retained. This retention effect should be treated as a transient phenomenon and should not be allowed to lead to an over-optimistic evaluation of the actinide release rates. Long-term behaviour can be examined when steady state conditions are reached, this state had not yet been reached in the example of figure 54.

Some metals are first retained and then released again, this could be due to the saturation effect on the hydrated layer or to its dissolution. A model glass containing thorium was used to illustrate this (11), the glass had low chemical resistance. As can be seen from figure 55, at first sodium was selectively dissolved, the normalized dissolution rate of thorium being somewhat lower than that of SiO_2. Later, after a longer test time, the dissolution rates of SiO_2 and sodium were similar, and that of thorium rose.

The irregular progress of the dissolution rates in figure 56 can be explained by the formation and dissolution of the hydrated layer (111). The layers were examined using the electron microprobe. Periodic irregularities in dissolution rates have been observed for a long time (64).

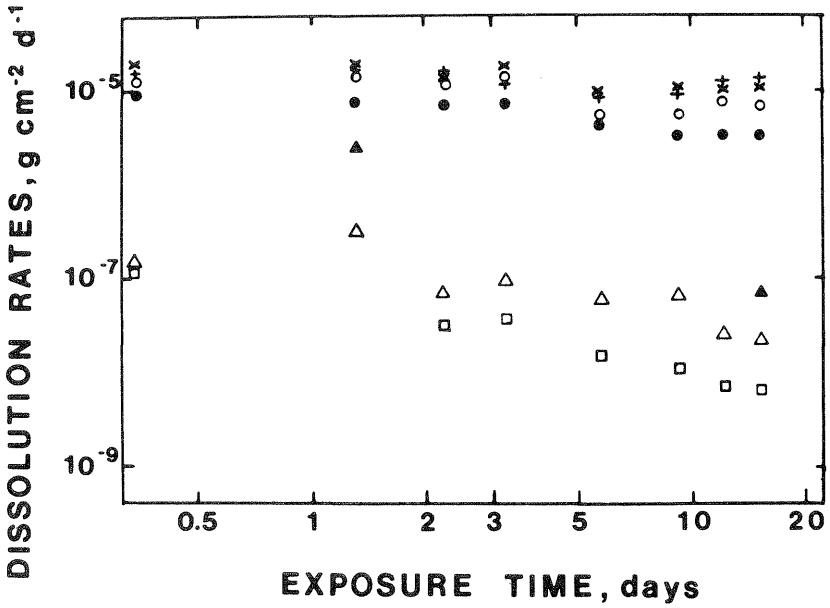

Figure 54: Dissolution rates based on individual glass components for a borosilicate glass at 70°C (11)
● SiO_2, × Na, + Cs, ○ Sr, ▲ Zn, △ RE-elements, □ Fe.

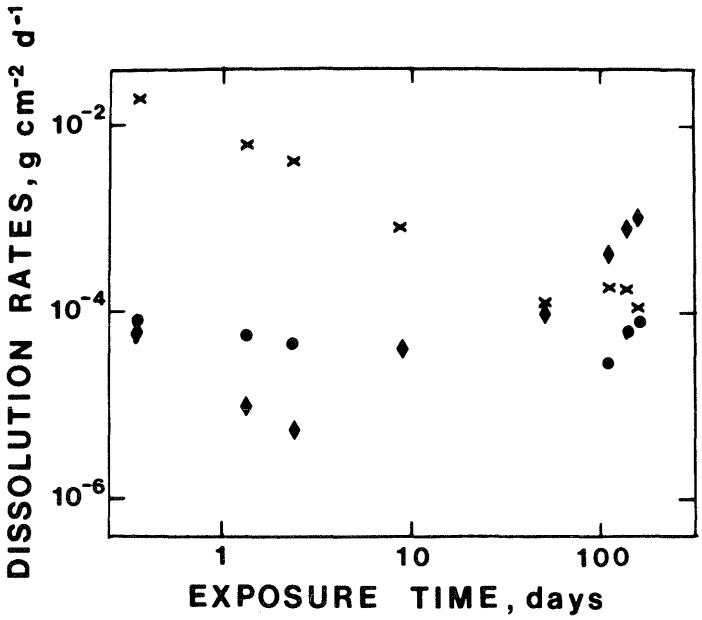

Figure 55: Dissolution rates based on individual components for a Th containing glass (55).
● SiO_2, × Na, ♦ Th.

The electronmicroprobe has also been used by another group (7) to investigate the enrichment of various elements in the surface layer. According to them, the layer structure, not the thickness, changes at 200°C over a period of 3 to 30 days. Using a simulated HLW glass it was found that, at 100 and 150°C, the layers are amorphous and contain only traces of kaolinite. At 200°C and over, the surface is covered with crystalline phases. Structural changes in the surface layer could be related to changes in the dissolution mechanism (cf section 5.3.2).

Using surface sensitive methods on borosilicate glasses containing uranium, high surface concentrations of U, Ti, Zn, Fe and rare earths were detected (108). These experiments, at 75°C, lasted for a period of up to three days only, so the results can not be used to draw long-term conclusions.

From the German investigations (186), it can be concluded that it is not possible to make any generalised predictions about the tendency to form retentive hydrated SiO_2 layers: the formation is affected not only by the glass composition but also by the solvent composition and by the temperature and by other parameters.

5.3.4 Interactions with backfill material and with rock

Up to now relatively few investigations have been carried out on glass/rock or glass/backfill material interactions in aqueous solution. Nor is it possible to generalise on individual results, because the test conditions, particularly the quantitative proportions of solids, influenced the experimental results to such a large degree (25) (cf also section 3.3.4).

The results of hydrothermal tests on glass PNL 76-68, at 300°C, in the presence of basalt, are summarised in table 21 (183). They show that cesium and, to a lesser extent, rubidium are released preferentially when

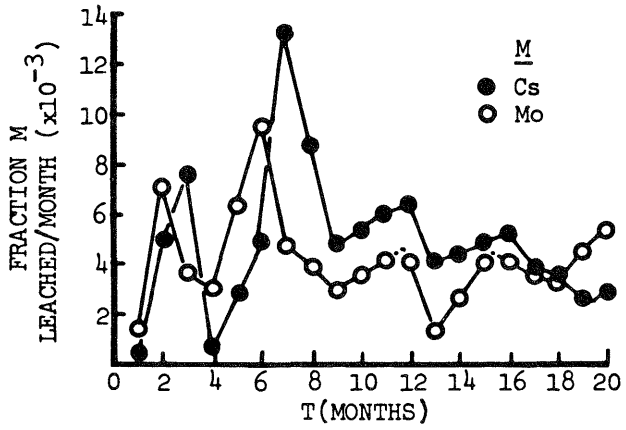

Figure 56: Soxhlet leaching of cesium and molybdenum from simulated HLW glass (111).

basalt is present. The basalt has less influence on other elements, such as molybdenum, boron and uranium. The Fe^{2+}/Fe^{3+} redox buffer from the rock determines the oxidation state of the uranium. With a smaller surface proportion of basalt, weeksite, $K_2(UO_2)_2Si_6O_{15} \cdot 4H_2O$, is formed. If the surface of basalt is proportionally higher, U^{VI} is reduced and the formation of weeksite does not take place.

The pH of water increases in contact with clay minerals. According to Belgian tests, the corrosion rate of glasses in clay water is 5 times greater than in deionised water (101).

Intensive tests on glass/bentonite/granite interactions have been carried out in Sweden both in the laboratory and on site in bore-holes (93). At 90°C, glass is attacked much more quickly in the presence of bentonite. The water content of the bentonite also plays an important role; the attack on the glass is greatest if the bentonite, instead of being in solid form, is present as a slurry. If only a little water is present, then, the bentonite, with its capacity to absorb water, can protect the glass from attack. The tests are not yet completed. Current results are reported in SKBF/KBS reports (88). Further investigations, to be carried out under the auspices of an international joint project (JSS project), with Nagra participating, will extend tests to active glasses.

Element	1 Week		4 Weeks	
	Glass	Glass+Basalt	Glass	Glass+Basalt
Cs	4,3	4,3	5,0	20,3
Rb	n	n	8,7	14,0
Na	46	38	45	38
Sr	0,6	n	0,15	n
Ba	1,5	n	0,1	n
Ca	0,5	n	1,2	n
Mo	72	78	72	85
B	84	87	93	91
Si	2,7	1,3	4,6	1,0
U	0,15	0,06	0,03	0,05

Table 21: Percentage release of elements from glass PNL 76-68 at 300°C, with and without the addition of basalt (183). n : not detected.

As glass corrosion can be inhibited by phosphates and other materials, studies have also been made of bentonite additives. An industrial by-product, i.e. a phosphate slime, calcium hydrogen phosphate and vanadium pentoxide appear suitable (39, 89).

The backfill material can not just be thought of as a simple retentive medium. It is largely responsible for the water chemistry (e.g. the H_4SiO_4 content), which, with the inhibiting additives, will influence glass corrosion. The addition of redox buffers could influence both the corrosion behaviour of the metal canister material and the mobility of released actinides.

5.3.5 Radiation effects

The possible influences of radioactivity on glass corrosion have been treated in section 3.3.5. For detailed discussions see the comprehensive surveys (3, 52, 116, 178, 217). Table 22 summarises the radiation influences to which a HLW glass is exposed (3). Most of the β and γ radiation will have decayed after about 1000 years and need only be considered in "short-term" predictions. Long-term, only damage due to α radiation and recoil nuclei plays a role. Cumulative atomic displacements reach the order of 0.1 mol/cm^3 after 10^6 years (figure 57) (177).

The principal effect of β and γ radiation is ionisation, so, rather than altering the solids, this effect is seen in reactions with aqueous solution. To determine the effect of the radiolysis products formed, corrosion tests have been carried out using external radiation sources.

Irradiation from a ^{60}Co source, with a dose rate of 2.4 Mrad/h, produced about double the weight loss at 50° and 90°C. For some elements the leach rate was considerably higher (140, 141). In these experiments the effect of nitric acid, formed from water and nitrogen in the air, was also noticeably felt: in comparison to tests where air was excluded, the pH value dropped noticeably, and this was connected with the increase in dissolution rate. Control experiments in nitric acid, without irradiation, clearly showed that both hydrogen ions and radiolysis products must take part in the dissolution reactions.

In contrast to the above findings, a similar experiment with 10 Mrad/h for 79 days (28) showed that the cesium and uranium release was hardly affected by irradiation. This was also the case for electron irradiated samples in drinking water (120).

Radiation	Range (mm)	Dose after 10^6 years	Percentage in 1000 yrs	Effects
α	$2{,}5 \cdot 10^{-2}$	$10^{19}/cm^3$	10 %	- approx. 150 atom displacements per decay - Ionisation - Helium formation
recoil nuclei	10^{-5}	$10^{19}/cm^3$	10 %	- approx 2000 atom displacements per decay
β	1	$2 \cdot 10^{20}/cm^3$	>90 %	- approx 0.13 atom displacements per decay - Ionisation - charge transfer - heating
γ		10^{11}-10^{12}rad	>90 %	- Ionisation - charge transfer - heating

Table 22: Radiation doses and their effect on solidified radioactive waste after (3).

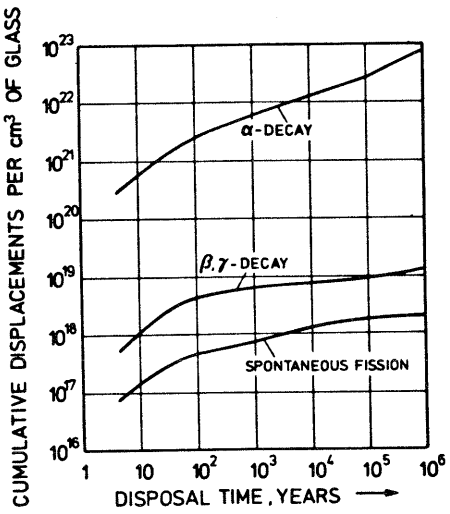

Figure 57: Cumulative atomic displacements in commercial HLW solids (177).

Concentration calculations for radiolysis products formed under realistic final repository conditions (30) lead to the conclusion that radiolysis does not greatly affect the chemical behaviour of glasses. It should be remembered that the accelerated reaction rates observed are, at least partly, due to pH reduction by nitric acid. The buffering effect of the backfill material should offset this effect. In any case it is anticipated that the canister will protect the glass from any water during the radiolysis period.

There appears to be no reason for assuming that the chemical resistance of glasses will be impaired dramatically by β and γ radiation. However, further investigations, particularly at higher temperatures, would seem advisable.

In laboratory tests where active glasses are used in Teflon containers, it should be remembered that hydrofluoric acid can be formed by radiolysis. This acid is extremely aggressive against SiO_2 and so experimental results will not be realistic.

It is less easy to simulate α radiation damage. In 1980 two investigations caused rather a stir by showing that external irradiation of glasses, using lead or argon ions, accelerates glass corrosion quite dramatically (61, 95). These experiments have subsequently been severely criticised (30, 164, 208). It has been pointed out, that surface irradiation with heavy ions in no way simulates the processes which occur during α decay within the glass. By incorporating short-lived α emitters into the glass (^{241}Am, ^{238}Pu, ^{242}Cm, ^{244}Cm), α radiation doses can be generated within a few years, which correspond to a HLW glass age of over 10^5 years. Various groups have investigated the leaching behaviour of such glasses. Table 23, which is taken from the summary work by Turcotte (208), gives some results: the leach rate changes only very slightly - and that in both directions. Drastic effects, as postulated in works (61, 95), were not found in any of the tests. Another critical summary (116) also reached the same conclusions. Investigations on French HLW glasses (103, 211) using α doses up to $8 \cdot 10^{17}$ decays per cm^3 showed no significant change in chemical behaviour.

However, glass can be damaged by radiation, as was observed by Otto Hönigschmid while determining the atomic weight of radium. Using small quartz flasks in experiments with 3 curie radium, scales flaked off the flasks (190).

During radioactive decay, elements are formed which have different ionic radii and different oxidation states. It is possible that such transmutations could alter the properties of a solid. As the proportion of transmuted elements lies in the region of 1 - 2 atom-%, it can be assumed that the amorphous glass structure will not be affected (116). Investigations on Cs → Ba transmutations are in progress (208).

Glass	Method	leach rate R_o ($g \cdot cm^{-2} \cdot d^{-1}$)	dose $\cdot 10^{-18}$ (α- decay $/cm^3$)	R_D/R_o	Ref.
PNL 77-260	Soxhlet	$3,2 \cdot 10^{-4}$	4,5	0,9	216
	static (pH 9)	$8 \cdot 10^{-5}$	4,5	0,1	216
PNL 77-260 (devitrified)	Soxhlet	$1,8 \cdot 10^{-4}$	4,5	0,6	216
	static (pH 9)	$1,8 \cdot 10^{-5}$	4,5	4,0	216
PNL 72-68	static (K)	$1,6 \cdot 10^{-5}$	$\sim$ 3	0,6	146
	static (Cm)	$7 \cdot 10^{-8}$	$\sim$ 3	1,4	
UK 189	Soxhlet	$1,5 \cdot 10^{-3}$	$\sim$ 8	1,6	23
	Soxhlet	$1,3 \cdot 10^{-3}$	3,3	1,5	130
UK 209	Soxhlet	$2,1 \cdot 10^{-4}$	3,3	1,1	130
SRL (SRP)	static (Cm)	$1,6 \cdot 10^{-8}$	1,1	3,0	14
Glass 98	Period. renewal of leachant (Cm)	$\sim 5 \cdot 10^{-7}$	4,0	1,0	185
VG 98/3	Soxhlet	$2,2 \cdot 10^{-3}$	3,3	1,3	130
SON 58.30.20.U2	Soxhlet	$2,2 \cdot 10^{-3}$	3,3	3,1	130

Table 23: Changes in leach rate in HLW glasses generated by α decay
R_o: initial leach rate, R_D leach rate at maximum dose (208)

6. Models for long-term extrapolations

The glass dissolution models so far available, for calculating the release rate of nuclides, differ widely in quality and usefulness. Herrnberger (94) gives a critical discussion of model concepts which are based on the theory of material transport. See also the works of Godbee et al (77, 78).

The best developed models are diffusion models, they cover practically all existing geometries and also permit the evaluation of temperature and species dependence. But, as pure diffusion processes prevail for only a limited time in glass corrosion, long-term extrapolations of dissolution tend to be under-estimated. Models, which take into account not only diffusion but also corrosion and other processes, such as phase regeneration, are less well developed.

Recently Claassen (38) discussed various model concepts and tried to tie in information from the evolution of groundwater, and also from experiments on volcanic glass. According to him, under realistic final repository conditions, the precipitation of new phases and the sorption processes should limit the passage of material into solution.

A comprehensive glass dissolution model must be able to take into account at least the following effects:

- temperature and pressure
- solvent composition and its alteration with time (e.g. pH, silicic acid concentration, buffer capacity)
- solvent supply (flow rate, glass surface area/solvent volume)
- formation and dissolution of surface layers rich in SiO_2 and their adsorption properties
- formation of new solid phases (also adsorbed substances and mixed phases, such as $Ca_{1-x}Sr_xCO_3$)
- geometry of samples and the alteration of surface area with time.

So far no models fulfil all these conditions, but it should not be forgotten that some fundamental problems do arise (see section 3.1). The main difficulty in formulating a physico-chemical model for glass dissolution is that the chemical processes of the reaction do not remain constant with time. The various stages, arising at different times, are summarised schematically in figure 58 (193). In practice, these problems are surmounted by using empirical or semi-empirical relationships. Thus, for example, Hench et al (230) propose a simple, but not unproblematical, extrapolation process, based on laboratory experiments, field tests and experience with natural glasses.

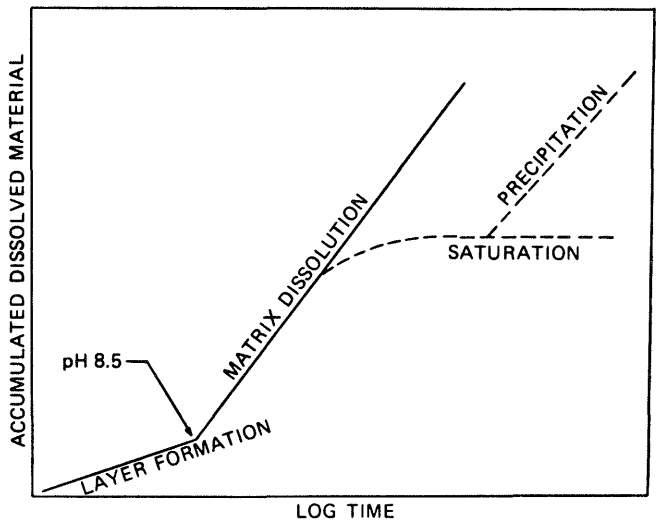

Figure 58: Model showing the effect of accumulation of corrosion products followed by saturation effects and precipitation (193).

The starting point for many models is that glass dissolution can be described as a combination of a diffusion controlled release with phase boundary reactions (section 3.2). This can be expressed as:

$$Q = a \cdot t^{1/2} + b \cdot t, \quad \text{or}$$

$$R = 1/2a \cdot t^{-1/2} + b.$$

Sometimes a further constant is introduced:

$$Q = a \cdot t^{1/2} + b \cdot t + c,$$

where c represents the mass dissolved due to rapid surface-ion exchange, or to rapid reactions at particularly active surface sites. Richardson (173) applied this type of model to the release of silicon from HLW glasses. The experiment, which ran for 577 days, agreed well with theory. Lanza and Parnisari (117) described their long-term tests (8000 hrs) between 30° and 100°C, with a similar equation (cf also 85). A similar equation forms the basis of Wiley's model (225).

As the constants a, b and c are found experimentally, extrapolation over hundreds or thousands of years gives rather dubious results. However, such test evaluations can be used to estimate the tendency of a glass to form reaction inhibiting layers. As an evaluation criterion, a time, t', is chosen, at which diffusion and corrosion take place at the same rate:

$$t' = \frac{a^2}{b^2}$$

By using an Arrhenius term, such equations can be employed to study temperature dependence. It should be noted that diffusion and corrosion have different activation energies ($E_{act}(diff) < E_{act}(corr)$).

Ewest (71) discusses three different models which can be used for long-term extrapolation:

a) Constant rate corrosion

$$F_1 = \frac{M}{M_o} = 2\left[\left(\frac{1}{p} + 1\right)\tau - \left(\frac{2}{p} + \frac{1}{2}\right)\tau^2 + \frac{1}{p} \cdot \tau^3\right]$$

where F : fraction dissolved
M : dissolved mass
M_o: total mass of sample
p = L/r, cylinder length/radius

$\tau = \frac{R(t - t_0)}{g \cdot r}$ dimensionless time parameter, where

R : dissolution rate
t : time
t_0 : start of leach process
g : density of glass

b) Diffusion*)

$$F_2 = \frac{S}{M_0} \cdot 2C_0 \left(\frac{D}{\pi}\right)^{1/2} (t - t_0)^{1/2} = \frac{S}{M_0 \cdot S_S} a_1 (t - t_0)^{1/2}$$

where S : surface area of the glass block
S_S : specific surface area at start of leaching
C_0 : concentration of the diffusive component
(in case of homogeneous dissolution: density of glass)
D : diffusion coefficient
a_1 : constant with dimension $t^{-1/2}$

c) Simultaneous corrosion and diffusion*). This case is described by an empirical relationship derived from experiments:

$$F_3 = \frac{M}{M_0} = \frac{S}{M_0 \cdot S_S} \cdot a_2 (t - t_0)^x$$

Here a_2 is a constant of dimensions t^{-x}, and x an exponent in the range $0.5 \leq x \leq 1$.

---

*) Some dimensions given in the original paper are not consistent with dimensionless fractions F.

The following values were obtained from corrosion experiments at pH 4 and room temperature over 150 days:

$a_1 = 0.478 \ (year)^{-1/2}$ $\quad S_s = 1236 \ cm^2/g$

$a_2 = 0.613 \ (year)^{-2/3}$ $\quad D = 5.8 \times 10^{-16} \ cm^2/s$

$x = 2/3$ $\quad R = 1.87 \times 10^{-6} \ g \cdot cm^{-2} \cdot d^{-1}$.

As figures 59 shows, these three equations produce very different results. With constant corrosion rate, the cylinder is completely dissolved after about 10^4 years. According to the empirical relationship, which is taken to be the most accurate, only about 1% of the block is dissolved in this time period.

The empirical model of Ewest has been extended by Altenhein (6) by taking into account the temperature dependence of corrosion:

$$R(t,T) = n(T_o) \cdot A \cdot \exp\left(-\frac{E_{akt}}{RT}\right) \cdot t^{n(T_o)-1}$$

where n, A and the activation energy are given experimentally. The exponent, n, is temperature dependent (219) (see section 5.3.2).

The release of radioactivity into the solvent, should water penetrate the final repository, can also be calculated, based on experimental results with conservative suppositions (170). The results reproduced in figure 60 refer to a glass block of 75 litres. The initial temperature was taken as 200°C. The temperature evolution with time for a final repository in salt was taken from the work of Deslisle (53).

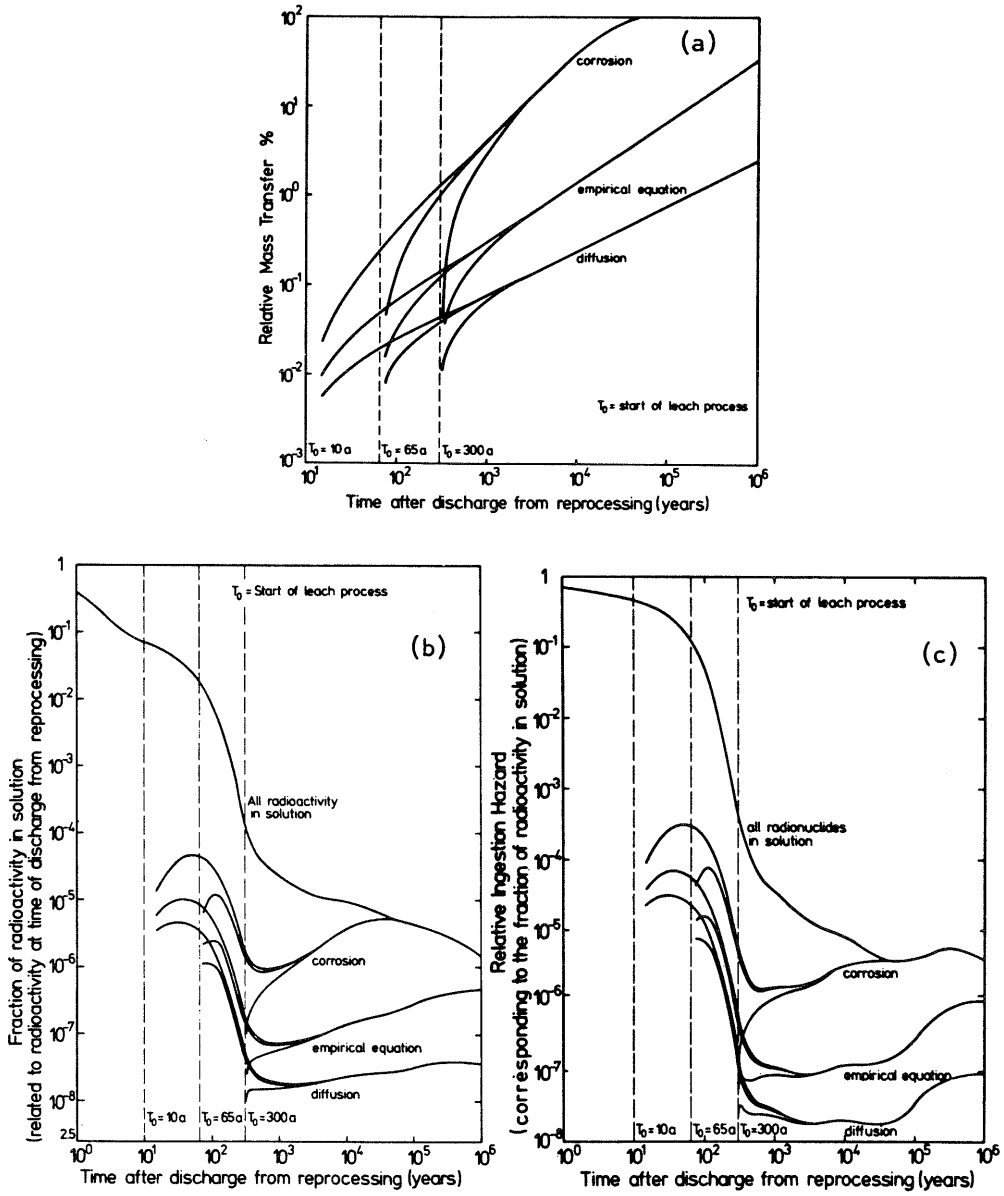

Figure 59: Leaching calculations for a 70 litre glass cylinder (71).

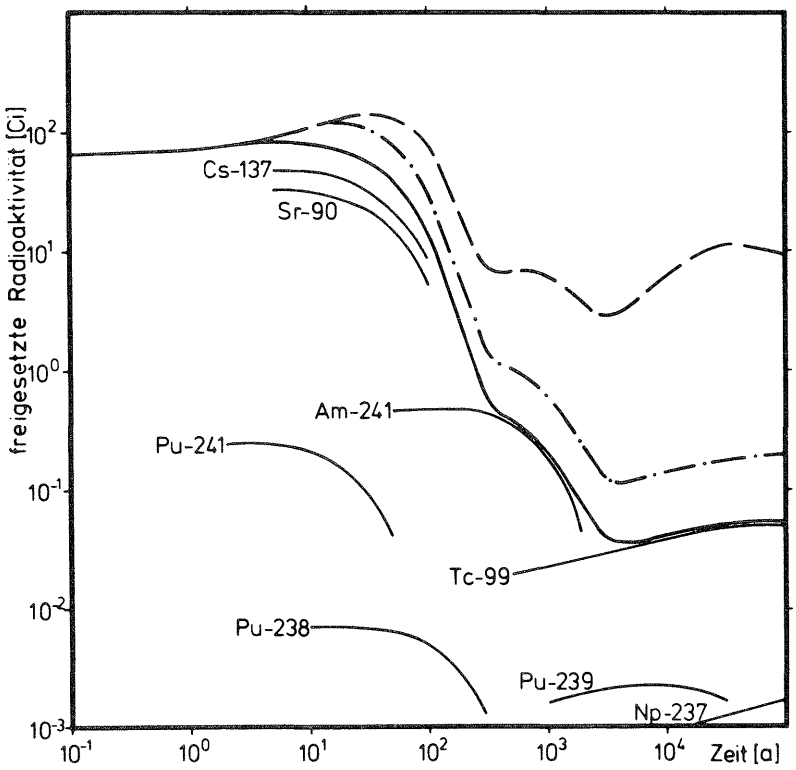

Figure 60: Release of radioactivity from a glass block under various conditions (170).

---- Constant release rate, regular dissolution, T = 200°C

____ Temperature dependent release rate, regular dissolution

-.-.- Temperature dependent release rate, periodic dissolution.

With a constant dissolution rate and constant temperature the glass block would be dissolved after 4.10^4 years. If cooling is taken into account, then the dissolution rate falls noticeably after some 300 years. If, in addition, it is assumed that a reaction retarding layer is periodically formed and dissolved on the glass surface, a slightly higher release of radioactivity occurs. In figure 60, a period of three years (corresponding to the longest test time) is assumed. An increase in the time period has a levelling effect. If the period is longer than ten years, then it makes little difference if the layer is periodically unstable or if it remains stable.

Whether a fixed period of time can be assumed for the formation and removal of layers, is debatable to say the least. The dissolution of a layer from the surface of a monolithic glass block can hardly be compared with the shedding of a snake's skin. The attack is irregular, so the process fluctuates with time and location, and will not take place simultaneously over the whole glass body.

Model calculations usually assume monolithic glass blocks. As such blocks may crack during cooling, this assumption leads to rather too optimistic evaluations. Figure 61 shows the results of American investigations (195): with realistic cooling rates, surface area can increase by up to a factor of 10. See also the relevant French investigations (119), the results have not yet been published in detail.

Hughes et al (98) have tried to forecast realistic dissolution rates for final repository conditions. These are based on the assumption that corrosion rate falls with reduced flow rate (see figure 24, section 3.2.2). In this case, if rate is assumed dependent on the diffusion of reaction products in almost stagnant solution, or in water-retaining rock, then the Soxhlet leach rate results from laboratory tests are reduced by about

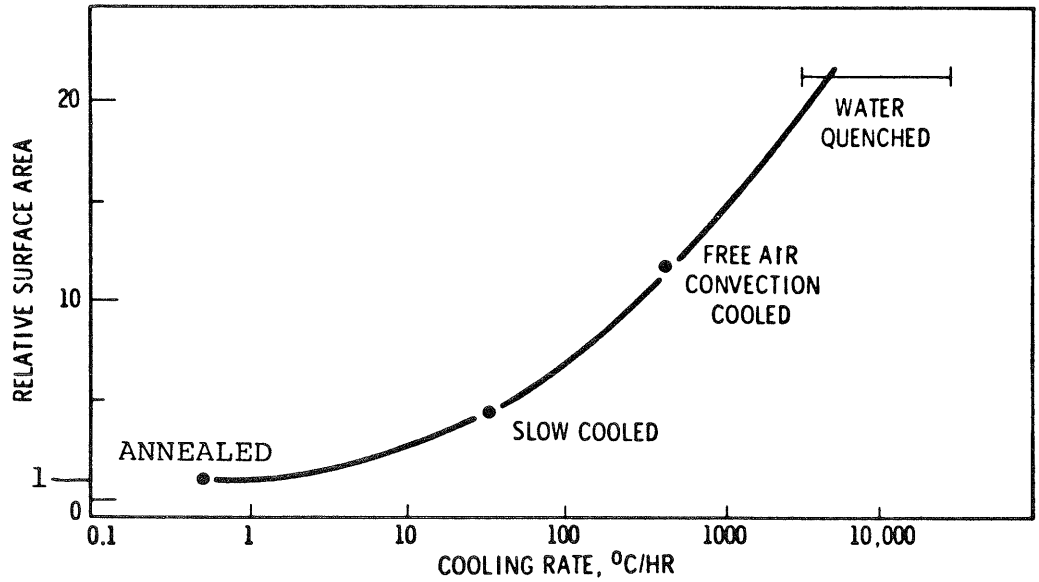

Figure 61: Thermal shock-increased surface area of glass cylinders (diam. 15 cm, length 150 cm) (195).

$\sim 10^{-5}$ $g \cdot cm^{-2} \cdot d^{-1}$ to $1{\cdot}7 \times 10^{-8}$ with no backfill, and to $1{\cdot}7 \times 10^{-12}$ $g \cdot cm^{-2} \cdot d^{-1}$ with backfill in the repository. Similar reasoning has been proposed by other authors (34).

These forecasts are likely to be very optimistic as the model does not consider pH increase during the reaction. Also, the model uses a badly defined "saturation concentration of glass". If the model were to take temperature dependence into account, then the activation energy of glass dissolution may not be used, even for the border-line case of diffusion-controlled reaction.

According to the experimental work of Macedo et al (126), the relationship assumed above between dissolution rate and water flow is not appropriate: maximum attack occurs with medium flow rates and is caused by a pH increase resulting from the reaction. At high flow rates the attack is slower because the reaction products are carried away, at low flow rates the saturation effect inhibites attack.

Recently Macedo et al (126) published a model theory, which takes into account the influence of flow rate, pH drift and silicic acid concentration. The model calculations follow from laboratory experiments with differing flow rates. Temperature dependence is not currently being considered. The first data are available for glass 76-68. Future developments and improvements in the model will be reported in later publications.

A recently published leach model (167) contains a striking discrepancy between the mathematics and the underlying chemical assumptions: network dissolution is not considered and leaching is assumed to be reversible. Carried to a logical conclusion, these suppositions would produce chemically unsound statements: the glass is leached until the block is converted into a pudding of hydrated SiO_2. Then, the addition of aqueous solutions of network modifiers reconstitutes the glass block.

Further developments in dissolution models should certainly try to make use of information on the dissolution kinetics of silicate minerals. In this connection reference may be made to the summary by Tournay (206) and also the theoretical work of Dibble and Tiller (54).

7. Conclusions and recommendations

7.1 Conclusions

Corrosion mechanisms: The development and optimisation of HLW glasses have given considerable fresh impetus to fundamental investigations of glass corrosion. Although the basic mechanisms of glass dissolution are now well understood, there are still many individual areas, not always unimportant ones, which are unclear. These include, the large increase in corrosion rate of HLW glasses at low pH values, also, the formation and stability of SiO_2-rich surface layers. A related problem is raised by the low release rates of actinides compared with network dissolution: it is not clear whether these effects are due to adsorption at the glass surface or to precipitation reactions. On the other hand, preferential leaching of alkali ions is understood.

The question also arises, whether the basic information available will be applied in practice. Furthermore, progress remains to be made in the optimisation of backfill material (e.g. by addition of inhibitors).

Chemical stability of the glasses: At room temperature the dissolution rate of HLW glasses lies in the range

$$10^{-4} \text{ to } 10^{-7} \text{ g}\cdot\text{cm}^{-2}.\text{d}^{-1}$$

This corresponds to the conversion of a 1 cm thick glass layer in 77 to 77,000 years (density of the glass: 2.7 $\text{g}.\text{cm}^{-3}$). The data are confusing; the high dissolution rates of the order 10^{-4} $\text{g}\cdot\text{cm}^{-2}.\text{d}^{-1}$ seem to contradict practical experimental results, and the findings from ancient and natural glasses. As has often been pointed out, the experimental conditions have a great influence on the dissolution rates.

At 90 to 100°C the dissolution rates still fluctuate in the range 10^{-4} to 10^{-7} $g.cm^{-2}.d^{-1}$ (table 16), due to poor quality experimental data. Values of 50 to 80 $kJ.mol^{-1}$ are given for the activation energy of glass dissolution. A temperature increase of 25° to 100°C results in a reaction acceleration by a factor of 55 to 635.

At temperatures above 150°C the reaction rates increase so greatly that the glass would be completely converted very rapidly (figure 62). For this reason the temperature in a final repository, where conditions allow the glass to come into contact with water, should never be much over 100°C.

Resistance to radioactive radiation: The influence of α decay on the corrosion behaviour of the glass has been extensively investigated. There is no reason to fear that the chemical properties of a HLW glass will be impaired by radiation with the proposed actinide content. On the other hand, there is still not enough information on the effects of radiolysis on water at high temperatures.

Data for safety studies: The choice of data for long-term models of corrosion rates is a serious problem. Figure 63 shows schematically some extrapolation possibilities (193). Model 4, which deals with the short-term selective leaching of alkali metals, gives values which are too conservative, because, in reality the diffusion processes quickly fade. Model 1 is based on a supposition, which is correct in the long-term, that glasses dissolve congruently in steady state conditions. But this model gives values which are too optimistic, if corrosion is related to a periodic formation and dissolution of surface layers rich in SiO_2. This conditions is taken into account in models 2 and 3.

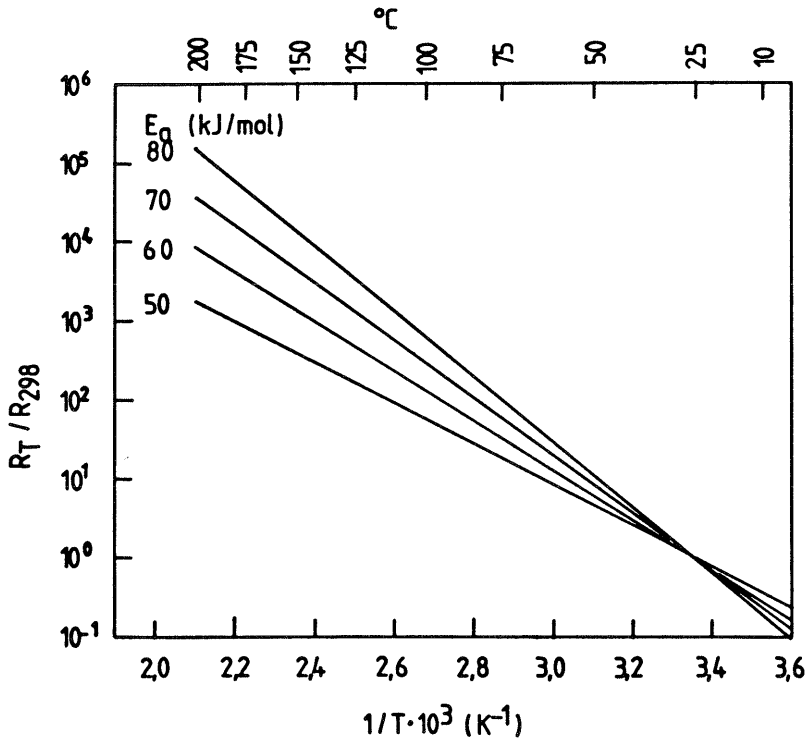

Figure 62: Temperature dependence of reaction rate, R, for different activation energies E_a. (1 kJ $\simeq$ 0.239 kcal)

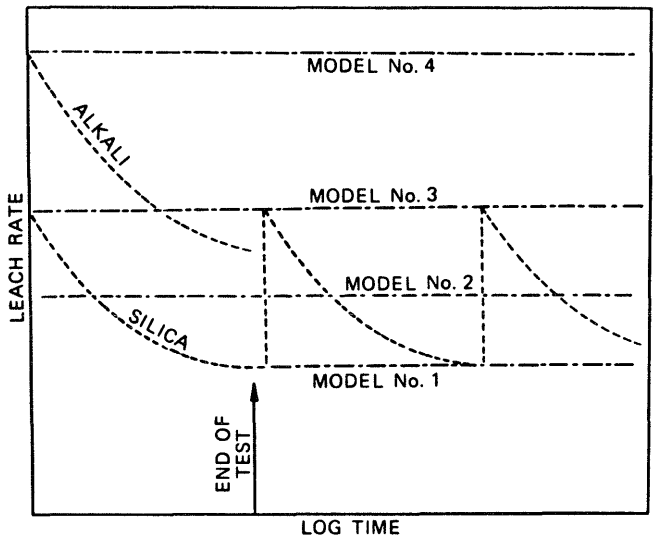

Figure 63: Four extrapolation models for glass corrosion (193).

One particular problem lies in the fact that much data have been obtained under far from realistic conditions. Particular mention must be made here of the ratio glass surface area/solvent volume (or flow rate) and the influence of backfill material on aquatic chemistry.

In calculating release rates at different temperatures, great care must be taken because only the apparent activation energies are known. Activation energies from short-term experiments in low temperature ranges will generally be too low, because under such conditions, diffusion processes determine the release rate.

7.2 Recommendations for further work

More explanations and investigations are required to contribute to a better evaluation of the durability of HLW glasses under final repository conditions. Some recommendations for further work are summarised in the following (some of these have already been taken into account in the JSS joint project).

The determination of dissolution rates for safety analyses:

A steady state must be reached in all dissolution experiments. This rules out short-term experiments and experiments at room temperature. Temperatures between 50^{o} and $90^{o}C$ seem both suitable and realistic.

Particular attention must be given to the modification of the aquatic chemistry by the backfill and canister material. The water supply must be kept within realistic limits. The buffer capacity of the test system must not be influenced by CO_2 in the air.

Not only the solvent, but also, if possible, the corroded glass surface and perhaps also the newly formed solid phases should be analysed.

In hydrothermal experiments with a limited solvent supply, new solid phases are formed. These may immobilize some of the glass components again. Such experiments are to be carried out with particular reference to real conditions, because, not only the glass but also the backfill material, the rock and the water (and also the relative amounts) determine the chemical identity of the new solids formed.

Models for long-term extrapolation should be developed and improved. Amongst other things, the complex influence of flow rate on corrosion must be described quantitatively.

The behaviour of glasses in wet/dry cycles: Under such conditions the corrosion behaviour is determined by the formation and subsequent shrinking of SiO_2-rich surface layers. It is not known how serious the effect of such cycles is, nor how likely they are to occur. As layer formation is a complex process, dependent on many parameters, realistic test conditions are desirable.

Mechanism of actinide release: The low release of actinides compared with network dissolution ($R_{Act} < R_{SiO_2}$) could arise from sorption or precipitation effects.For any long-term forecasts it is important to understand the chemistry of this phenomenon.

Radiolysis effects: Whether alterations of the water, as a result of radiolysis, affect the corrosion of glass has not, so far, been sufficiently investigated at high temperatures. A fundamental understanding of the radiolysis effects on glass corrosion is also lacking. Both experiments to simulate the behaviour of HLW glasses under location-specific conditions, and also investigations of the underlying principles, are required.

Corrosion of hot glass ($T > 100^{o}C$) at atmospheric pressure: These conditions could arise during an early incident in an unsealed repository. No experimental results are available for glass corrosion under heat transfer conditions. These conditions could be more important for the canister than for the glass. The effects of radiolysis should be taken into consideration here.

Optimising backfill material: The proposed backfill material, bentonite, could be improved by the addition of corrosion inhibitors (for both the glass and the canister material) and possibly also of pH and redox buffers.

The possibilities presenting themselves do not yet seem to have been systematically clarified and critically evaluated. It is necessary to continue and intensify the experimental work already begun on this topic.

8. References

1. P.B. Adams: in (37), page 233.

2. P.B. Adams, D.L. Evans: in Borate Glasses (Eds. D. Pye, V.D. Fréchette, N.J. Kreidl) page 525, Plenum Press (1978). P.B. Adams, D.L. Evans: Materials Sci. Res. 12 (1978) 525.

3. T.M. Ahn et al.: Nuclear Waste Management, Technical Support in the Development of Nuclear Waste Form Criteria for the NRC, Task 4: Test Development Review. NUREG/CR-2333, Vol 4, BNL-NUREG-51458 (1982).

4. S. Ahrland, I. Grenthe, B. Norén: Acta Chem. Scand. 14 (1960) 1059; 1077.

5. C.C. Allen: in (191), Abstract II/3.

6. F.K. Altenhein, W. Lutze: in (191), Abstract II/5.

7. F.K. Altenhein, W. Lutze, G. Malow: in (152), page 363.

8. P. Balta, E. Balta: Introduction to the Physical Chemistry of the Vitreous State. Abacus Press, Turnbridge Wells (GB) (1976).

9. A. Barkatt: Nucl. Chem. Waste Manage. 2 (1981) 151.

10. A. Barkatt et al.: Nucl. Technol. 56 (1982) 271.

11. A. Barkatt, J.H. Simmons, P.B. Macedo: Nucl. Chem. Waste Manage. 2 (1981) 3; Phys. Chem. Glasses 22 (1981) 73.

12. G.W. Beall: in (16), page 262.

13. R.A. Berner: Amer. J. of Science 278 (1978) 1235.

14. N.E. Bibler, J.A. Kelley: Effect of Internal α-Radiation on Borosilicate Glasses Containing Savannah River Plant Wastes. DP 1482, E.I. DuPont de Nemours & Co (SRL) (1978).

15. Z. Boksay, G. Bouquet: Phys. Chem. Glasses 21 (1980) 110.

16. L.A. Boatner, G.C. Battle (Eds.): Alternate Nuclear Waste Forms and Interactions in Geologic Media. Proc. Workshop in Gatlinburg, Tenn. US Dept. of Commerce, Springfield VA. CONF-8005107 (1980).

17. R.A. Bonniaud et al.: in (37), page 57.

18. R.A. Bonniaud, N.R. Jaquet-Francillon, G.C. Sombret: in (161), page 117.

19. R. Bonniaud, A. Jouan, C. Sombret: in (32), page 155.

20. R. Bonniaud, C. Sombret: in Borate Glasses (Eds. D. Pye, V.D. Fréchette, N.J. Kreidl), page 597. Plenum Press (1978).

21. E.N. Boulos et al.: J. Amer. Ceram. Soc. 63 (1980) 496.

22. K.A. Boult: AERE-R-9188 (1978).

23. K.A. Boult et al.: in (37), page 248.

24. D.J. Bradley, C.O. Harvey, R.P. Turcotte: Leaching of Actinides and Technetium from Simulated HLW Glass. PNL-3152 (1979).

25. D.J. Bradley, G.L. McVay, D.G. Coles: Leach Test Methodology for the Waste/Rock Interactions Technology Program. PNL-3326 (1980).

26. D.J. Bradley: Leaching of Fully Radioactive HLW Glass. PNL-2664 (1978). In Radioactive Waste in Geologic Storage (S. Fried, Ed.), Seite 75. ACS Symposium Series Vol. 100 (1979).

27. J. Bradley: Nucl. Technol. 51 (1980) 111.

28. J.W. Braithwaite: in (161), page 199.

29. C.Q. Buckwalter, L.R. Pederson, G.L. McVay: J. Non-Cryst. Solids 49 (1982) 397.

30. W.G. Burns et al.: Nature 295 (1982) 130; AERE-R-10189 (1981).

31. C. Camara, W. Lutze, J. Lux: in (161), page 93.

32. L.A. Casey (Ed.): Proc. Conf. on High Level Radioactive Solid Waste Forms, Denver. SCS Engineers, Reston VA. NUREG-CP-0005 (1979).

33. N.A. Chapman, D.A. Savage: in (161), page 183.

34. H. Cheung, D.D. Jackson, M.A. Revelli: UCRL-53188-80 (1981).

35. L.A. Chick et al.: in (161), page 175.

36. L.A. Chick et al.: PNL-3465 (1980).

37. T.D. Chikalla, J.E. Mendel (Eds.): Ceramics in Nuclear Waste Management. Proc. Symp. in Cincinnati. Techn. Information Center, US Dept. of Energy.
CONF-790420 (1979).

38. H.C. Claassen: Nucl. Chem. Waste Manage. 2 (1981) 307.

39. D.E. Clark, C.A. Maurer: in (191), Abstract II/7.

40. D.E. Clark, A.R. Jurgensen, L.L. Hench: A Bibliography of High Level Nuclear Wastes. Ceramics Division, Dept. of Materials Science and Engineering. University of Florida, Gainsville, Florida 32611 (1982).

41. D.E. Clark, C.G. Pantano, L.L. Hench: Corrosion of Glass. Books for Industry and the Glass Industry. New York (1979).

42. D.E. Clark, E.L. Yen-Bower: Surface Sci. 100 (1980) 53.

43. W.R. Corman: Composite Quarterly Technical Report, Long Term HLW Technology, July-September 1980. DP-80-157-3 (1981).

44. W.R. Corman: as (43), October-December 1980. DP-80-157-4 (1981).

45. D.G. Coles et al.: in Radioactive Waste in Geologic Storgae (Ed. S. Fried) page 93. ACS Symposium Series Vol. 100 (1979).

46. D.G. Coles: Nucl. Chem. Waste Manage. 2 (1981) 245.

47. R. Cousens et al.: in (191), Abstract A-14.

48. C.A. Cox, A.M. Pollard: Archeometry 19 (1977) 45.

49. J.L. Crandall: in (161), page 39.

50. C.R. Das: Glass and Ceram. Res. Bull. 26 (1979) 11;
J. Amer. Ceram. Soc. 64 (1981) 188.

51. M.S. Davis, D.G. Schweitzer: Review of DOE Waste Package Program, Subtask 1.1: National Waste Package Program. NUREG/CR-2482 Vol. 1. BNL-NUREG-51494 (1982).

52. R. Dayal et al.: Nuclear Waste Management, Technical Support in the Development of Nuclear Waste Form Criteria for the NRC, Task 1: Waste Package Overview. NUREG/CR-2333, Vol. 1, BNL-NUREG-51458.

53. G. Deslisle: Zt. dt. Geol. Ges. 131 (1980) 461.

54. W.E. Dibble, W.A. Tiller: Geochim. Cosmochim. Acta 45 (1981) 79.

55. E. Diezel: Z. Elektrochem. 48 (1942) 9; Glastechn. Berichte 22 (1948/49) 212.

56. T. Dippel, L. Kahl, J. Saidl: Atomwirtschaft 25 (1980) 81.

57. R.H. Doremus, A.M. Turkalo: Science 164 (1969) 418.

58. R.H. Doremus: Structure of Inorganic Glasses. In Annual Rev. of Materials Sci. Vol. 2 (Ed. R. Higgins) page 93-120. Annual Reviews Inc., Palo Alto (1972).

59. R.H. Doremus: Glass Science. J. Wiley & Sons (1973).

60. R.W. Douglas, T.M. El-Shamy: J. Amer. Ceram. Soc. 50 (1967) 1.

61. J.C. Dran, M. Meurette, J.C. Petit: Science 209 (1980) 1518.

62. M.D. Dukes et al.: in (161), page 231.

63. H.H. Dunken: Physikalische Chemie der Glasoberfläche. VEB Deutscher Verlag für Grundstoffindustrie. Leipzig (1981).

64. M.N. Elliot, D.B. Auty: Glass Technol. 9 (1968) 5.

65. E.T. El-Shamy et al.: J. Non-Cryst. Solids 19 (1975) 241.

66. E.T. El-Shamy, J. Lewins, R.W. Douglas: Glass Technol. 13 (1972) 81.

67. J. Engell et al.: Investigation of Metastable Immiscibility in Borate Waste Glasses. SKBF/KBS-TR-81-14 (1981).

68. J.E. Ericson: in (152), page 283.

69. F.M. Ernsberger: Phys. Chem. Glasses 21 (1980) 146.

70. E.C. Ethridge, D.E. Clark, L.L. Hench: Phys. Chem. Glasses 20 (1979) 35.

71. E. Ewest: in (136), page 161.

72. R.C. Ewing: in (136), page 57.

73. R.C. Ewing, R.F. Hacker: Nucl. Chem. Waste Manage. 1 (1980) 51.

74. A.M. Filbert, M.L. Hair: Surface Chemistry and Corrosion of Glass. In Advances in Corrosion Science and Technology (M.G. Fontana, R.W. Staehle, Eds.) Vol. 5, page 1-54. Plenum Press (1976).

75. K.F. Flynn, L.J. Jardine, M.J. Steindler: in (161), page 103.

76. G. Gliemeroth, G. Müller: Glas und Glaskeramik. In Ullmanns Encykolpädie der technischen Chemie 4. Aufl., Band 12, Seite 317. Verlag Chemie (1976).

77. W.H. Godbee, D.S. Joy: ORNL-TM-4333 (Pt. 1) (1974).

78. W.H. Godbee: Nucl. Chem. Waste Manage. 1 (1980) 29.

79. R. Grauer, W. Stumm: Colloid and Polymer Science 260 (1982) 959.

80. J.R. Grover: Radioactive Waste Management 1 (1980) 1.

81. F.R. Grover, B.E. Chidley: J. Nucl. Energy, Pt. A/B 16 (1962) 405.

82. F. Guber et al.: Charakterisierung eines verbesserten Borosilikatglases zur Verfestigung von hochaktiven Spaltprodukten, Teil 1. KfK-2721 (1979). L. Kahl et al.: Teil 2. KfK-3251 (1982). J. Saidl, L. Kahl: in (163), page 621.

83. W. Guber et al.: in (161), page 37.

84. G. Günther, H. Löffler, H.A. Weyl: Glas . In Ullmanns Encyklopädie der technischen Chemie, 3. Aufl., Band 8, Seite 133. Urban & Schwarzenberg, München (1957).

85. A.R. Hall, A. Hough, J.A.C. Marples: in (191), Abstract II/8.

86. K.B. Harvey, C.D. Jensen: Nucl. Chem. Waste Manage. 3 (1982) 43.

87. H.O. Haug: Zerfallsrechnungen verschiedener mittelaktiver und aktinidenhaltiger Abfälle des LWR-Brennstoffkreislaufes. Teil II: Radiotoxizitätsvergleich. KfK-3222 (1981).

88. L.L. Hench: SKBF/KBS Arbeitsrapport AR 81-03; 81-05; 81-11; 81-15; 82-16 (1981, 1982).

89. L.L. Hench: SKBF/KBS Arbeitsrapport AR 81-13; 81-14 (1981).

90. L.L. Hench, D.E. Clark: J. Non-Cryst. Solids 28 (1978) 83.

91. L.L. Hench, D.E. Clark, E.L. Yen-Bower: in (32), page 199. L.L. Hench: J. Non-Cryst. Solids 25 (1977) 343.

92. L.L. Hench, D.E. Clark, E.L. Yen-Bower: Nucl. Chem. Waste Manage. 1 (1980) 59.

93. L.L. Hench, L. Werme: in (191), Abstract A-3.

94. V. Herrnberger: Die mathematische Modellierung der Auslaugung verfestigter Abfälle. NAGRA- Report NTB-80-08 and EIR- Report Nr. 416 (1980). For details see EIR- internal Report TM-PH-833 (1979).

95. E.H. Hirsch: Science 209 (1980) 1520.

96. G. Herbsleb, W. Schwenk: in Korrosion in Kalt- und Warmwassersystemen der Hausinstallation. Berichte der Tagung in Bad Nauheim, page 82. Dt. Ges. für Metallkunde, Oberursel, Taunus (1974).

97. L. Holland: The Properties of Glass Surfaces. Chapmann and Hall, London (1964).

98. A.E. Hughes, J.A.C. Marples, A.M. Stoneham: AERE-R-10190 (1981).

99. IAEA, T.R. Series No. 187: Characterisation of HLW-Products (1979). I.C. Imbert, F. Pacaud, CEA-R-4550 (1974).

100. K. Iler: J. Coll. Interface Sci. 43 (1973) 399.

101. P. van Isegem, W. Timmermans, R. de Batist: in (163), page 829.

102. N. Jaquet-Francillon, R. Bonniaud, C. Sombret: Radiochim. Acta 25 (1978) 231.

103. N. Jaquet-Francillon, E. Vernaz: Internat. Symp. on Scientific Bases for Nuclear Waste Management. Boston (1981).

104. G.O. Jones: Glass. 2nd. Ed. Chapman and Hall (1971).

105. R.A. Jones: Radiation Research 10 (1959) 655.

106. H. Kaesche: Die Korrosion der Metalle. 2. Aufl. Springer (1979).

107. L. Kahl: Nucl. Chem. Waste Manage. 2 (1981) 143.

108. D. Karim et al.: in (152), page 397.

109. M.F. Kaplan: in (161), page 85.

110. S.N. Karkhanis et al.: in (152), page 115.

111. B.T. Kenna, K.D. Murphy: in (136), page 157 and in (161), page 191.

112. B.T. Kenna, K.D. Murphy: in (16).

113. W.E. Kline, H.S. Fogler: J. Coll. Interface Sci. 82 (1981) 93.

114. D.J. Lam, A.P. Paulikas, B.W. Veal: J. Non-Cryst. Solids 42 (1980) 41. R. Brückner et al.: ibid. 42 (1980) 49.

115. W.A. Lanford et al.: J. Non-Cryst. Solids 33 (1979) 249. R.H. Doremus: ibid. 19 (1975) 137. R.H. Doremus: Nucl. Chem. Waste Manage. 2 (1981) 119.

116. F. Lanza et al.: in (163), page 733.

117. F. Lanza, E. Parnisari: Nucl. Chem. Waste Manage. 2 (1981) 131.

118. T. Latakos: Soxhlet Leach Test on two HLW Glasses: ABS 39 and ABS 41. SKBF/KBS-AR 82-03 (1982).

119. F. Laude, E. Vernaz, M. Saint-Gaudens: in (191), Abstract A-5.

120. F. Laude: Risk Analysis and Geologic Modelling. OECD-CEC. Ispra (1977).

121. J.C. Lewin: Geochim. Cosmochim. Acta 21 (1961) 182.

122. L. Lidström: in Surface Chemistry (Ed. P. Ekwall et al.), Seite 42. Munksgaard, Kopenhagen (1965).

123. R. Lorentz: Werkstoffe und Korrosion 33 (1982) 247.

124. W. Lutze, R. Borchardt, A.K. Dé: in (136), page 69.

125. P.B. Macedo et al.: in (16), page 317 and in (37), page 321. J.H. Simmons et al.: Nature 278 (1979) 729.

126. P.B. Macedo, A. Barkatt, J.H. Simmons: Nucl. Chem. Waste Manage. 2 (1981) 151; in (191), Abstract II/6.

127. A.J. Machiels: in (16), page 70.

128. G. Malow: in (163), page 430.

129. G. Malow, R.C. Ewing: in (152), page 315.

130. G. Malow, J.A.C. Marples, C. Sombret: in (194), page 341.

131. Mamelle, Merlin, Sombret: CEA-CONF-5540 (1980).

132. J.A.C. Marples, W. Lutze, C. Sombret: in (194), page 307.

133. C.P. Marsh: Nucl. Energy 21 (1982) 253.

134. E. Mattson: in (136), page 271.

135. R.P. May, R.P. Turcotte: Thermal Phase Stability. In J.E. Mendel et al.: PNL-3802 (1981).

136. G.J. McCarthy (Ed.): Scientific Basis for Nuclear Waste Management, Vol. 1. Plenum Press (1979).

137. G.J. McCarthy et al.: in (136), page 329.

138. J.L. McElroy: PNL-3050-2 (1979).

139. N.S. McIntyre, G.G. Strathee, B.F. Philipps: Surface Sci. 100 (1980) 71.

140. G.L. McVay, C.Q. Buckwalter: Nucl. Technol. 51 (1980) 123. G.L. McVay, L.R. Pederson: J. Amer. Ceram. Soc. 64 (1981) 154.

141. G.L. McVay, W.J. Weber, L.R. Pederson: Nucl. Chem. Waste Manage. 2 (1981) 103.

142. G.B. Mellinger, L.A. Chick: in (37), page 213.

143. J.E. Mendel: Nucl. Technol. 32 (1977) 72.

144. J.E. Mendel: PNL-2764 (1978).

145. J.E. Mendel et al.: Nucl. Chem. Waste Manage 1 (1980) 17.

146. J.E. Mendel et al.: in Management of Radioactive Wastes from the Nuclear Fuel Cycle Seite 49. IAEA-SM-207/100, Vol. 2. (1976).

147. J.E. Mendel, J.H. Westsik, D.E. Clark: PNL-3802 (1981).

148. W.F. Merrit: Nucl. Technol. 32 (1977) 88.

149. E. Merz: in (163), page 570; Atomwirtschaft 24 (1979) 409.

150. M. Milberg et al.: Phys. Chem. Glasses 13 (1972) 79.

151. J.P. Moncouyoux, P. Hugony, A. Pieraggi: in (163), page 12.

152. J.G. Moore (Ed.): Scientific Basis for Nuclear Waste Management Vol. 3. Plenum Press (1981).

153. M. Morlevat, M. Uny, N. Jaquet-Francillon: in (163), page 657.

154. C. Morrow et al.: J. Geophys. Res. 86, No B4 (1981) 3002.

155. J. Mukerji, A.S. Sanyal: Ann. Nucl. Energy 3 (1976) 253.

156. Nagra: Technischer Bericht NTB 81-08: Vergleichende Uebersicht der Gefahren, Schutzmassnahmen und Risiken einer Endlagerung radioaktiver Abfälle. (Elektrowatt Ingenieurunternehmung AG) (1981).

157. R.D. Nelson, J.E. Mendel, R.P- Turcotte: in (163), page 507.

158. U. Niederer: in Waste Management '81 (R.G. Post, Ed.), Seite 53. Arizona Board of Regents (1981). Cf also the references quoted therein.

159. J.L. Nogues, L.L. Hench: KBS-TR-81-15.

160. J.L. Nogues, L.L. Hench, J. Zarzycki: in (191), Abstract A-22.

161. C.J.M. Northrup (Ed.): Scientific Basis for Nuclear Waste Management, Vol. 2. Plenum Press (1980).

162. R. Nyholm, L.O. Werme: in (152), page 101.

163. R. Odoj, E. Merz (Eds.): Proc. on the International Seminar on Chemistry and Process Engineering for High-Level Liquid Waste Solidification (Jülich). Jül-Conf-42 (Vol. 1+2) (1981).

164. P. Offermann, H. Matzke: Atomwirtschaft 26 (1981) 350.

165. Y. Oka, M. Tomozawa: J. Non-Cryst. Solids 42 (1980) 535.

166. L.M. Papouchado: Use of Borosilicate Glasses for Immobilisation of Savannah River Plant Radioactive Waste. Vortrag (1981). Cited by (52).

167. C. Pescatore, A.J. Machiels: J. Non-Cryst. Solids 49 (1982) 379.

168. J.C. Petit et al.: in (191), Abstract A-21.

169. L.N. Plummer, T.M. Wigley, D.L. Parkhurst: Amer. J. of Science 278 (1978) 179.

170. PSE, Projekt Sicherheitsstudie Entsorgung. Zusammenfassender Zwischenbericht. Berlin, Oktober 1981.

171. M.A. Rana, R.W. Douglas: Phys. Chem. Glasses 2 (1961) 196. C.R. Das, R.W. Douglas: ibid. 8 (1967) 178.

172. A. Ray, M. Güntensperger: EIR-internal Report TM-33-80-5 (1980).

173. G.L. Richardson: Nucl. Chem. Waste Manage. 2 (181) 237.

174. J.D. Rimstidt, H.L. Barnes: Geochim. Cosmochim. Acta 44 (1980) 1683.

175. A.E. Ringwood et al.: Nucl. Chem. Waste Manage. 2 (1981) 287. Ted Ringwood: Amer. Scientist 70 (1982) 201.

176. A.E. Ringwood, V.M. Oversby, S.E. Kesson: in (163), page 495. Cf also C.R. Kennedy et al.: Nucl. Technol. 56 (1982) 278.

177. F.P. Roberts, G.H. Jenks, C.D. Bopp: BNWL-1944 (1976).

178. F.P. Roberts, R.P. Turcotte, W.J. Weber: PNL-3588 (1981).

179. W.A. Ross: PNL-2481 (1978).

180. W.A. Ross, J.E. Mendel: PNL-3060 (1979).

181. J.M. Rusin: PNL-3035 (1980).

182. D.A. Savage, N.A. Chapman: Geochemical Factors Controlling the Nuclide Release Source-Term in Garantie: Dissolution of the Waste Form. Institute of Geological Sciences. Natural Environment Research Council Report No. ENPU-80-12. Cf also (33).

183. B.E. Scheetz et al.: in (161), page 207.

184. B.E. Scheetz et al.: Nucl. Chem. Waste Manage. 2 (1981) 229.

185. K. Scheffler, U. Riege: KFK-2422 (1976).

186. K. Scheffler et al.: KFK-2456 (1977).

187. P.W. Schindler: Surface Complexes at Oxide-Water Interfaces. In Adsorption of Inorganics at Solid-Liquid Interface (Eds. M.A. Anderson, A.J. Rubin), page 1. Ann Arbor Science (1981).

188. P.W. Schindler et al.: J. Colloid Interface Sci. 55 (1976) 469.

189. H. Scholze: Glas - Natur, Struktur und Eigenschaften. 2. Aufl. Springer (1977).

190. R. Schwanker: Chemie in unserer Zeit 15 (1981) 163.

191. Scientific Basis for Nuclear Waste Management, Berlin 1982, Abstracts. The lectures appear as vol. 5 in the series Scientific Basis for Nuclear Waste Management. North-Holland.

192. W.E. Seyfried, J.L. Bischoff: Geochim. Cosmochim. Acta 45 (1981) 135, W.E. Seyfried, M.J. Mottl: ibid. 46 (1982) 985.

193. J.H. Simmons, A. Barkatt, P.B. Macedo: Nucl. Technol. 56 (1982) 265.

194. R. Simon, S. Orlowski (Eds.): Radioactive Waste Management and Disposal. Harwood Academic Publishers (1980).

195. S.C. Slate: Stress and Cracking in HLW-Glass. In (32), page 393.

196. B.M. Smets, T.P.A. Lommen: Phys. Chem. Glasses 23 (1982) 83.

197. D.M. Strachan, B.O. Barnes: in (191), Abstract A-18.

198. D.M. Strachan, R.O. Barnes, R.P. Turcotte: PNL-SA-8712 (1980); CONF-801124-46.

199. D.M. Strachan, R.P. Turcotte, B.O. Barnes: Nucl. Technol. 56 (1982) 306; in (152), page 347.

200. W. Stumm, J.J. Morgan: Aquatic Chemistry, 2nd. Ed. Wiley & Sons (1981).

201. J.C. Tait, C.D. Jensen: J. Non-Cryst. Solids 49 (1982) 363.

202. G. Tammann: Der Glaszustand. Voss, Leipzig (1933).

203. R. Terai, K. Eguchi, H. Yamanaka: in (37), page 248.

204. T.A. Tombrello: in (32).

205. M. Tomozawa et al.: in (37), page 193.

206. J.C. Touray: La Dissolution des Minéraux. Masson, Paris (1979).

207. R.L. Treat: in Waste Management '80 (Ed. R.E. Post), Vol. 2, page 503. Arizona Board of Regents (1980). Cf also PNL-SA-8280.

208. R.P. Turcotte: Radiactive Waste Managemet 2 (1981) 169.

209. R.P. Turcotte, J.W. Wald, R.P. May: in (161), page 141.

210. S. Tymochowicz: HMI-B241 (1977).

211. E. Vernaz, N. Jaquet-Francillon, R. Bonniaud: Echos CEA, Spécial 1982, page 38.

212. W. Vogel: Struktur und Kristallisation der Gläser. 2. Aufl. VEB Deutscher Verlag für Grundstoffindustrie, Leipzig (1971).

213. J.W. Wald, J.H. Westsik: in (37), page 277.

214. C.T. Walker, U. Riege: in (37), page 198.

215. D.D. Walker et al.: Leach Rate Studies on Glass Containing Actual Radioactive Waste. In ORNL Conf. on the Leachability of Radioactive Solids. Gatlinburg (1980).

216. W.J. Weber: in (37), page 248.

217. W.J. Weber, F.P. Roberts: Radiation Effects. In J.E. Mendel et al.: PNL-3802 (1981).

218. H.C. Weed et al.: in (161), page 167.

219. J.H. Westsik: R.D. Peters: in (152), page 355; PNL-SA-9054 (1981).

220. J.H. Westsik, J.W. Shade, G.L. McVay: in (161), page 239.

221. J.H. Westsik. T.M. Turcotte: PNL-2759 (1978).

222. A.F. White, H.C. Claassen: Chem. Geology 28 (1980) 91.

223. G. Wicks: in Waste Management '81 (Ed. R.G. Post), page 321. Arizona Board of Regents (1981).

224. G.G. Wicks et al.: J. Non-Cryst. Solids 49 (1982) 413.

225. J.R. Wiley: Nucl. Technol. 43 (1979) 268.

226. J.R. Wiley et al.: Glass as a Matrix for SRP High-Level Defense Waste. DP-ST-79-294 (1980).

227. J.W. Wiley, S.M. Plodinec: ONWI-212, page 110 (1980).

228. G.S. Wirth: The Heterogeneous Kinetics of Silica Dissolution in Aqueous Media. PhD-Thesis, Scripps Institution of Oceanography (1980).

229. R. Wollast, Ch. van Damme, A. Jolli: The Corrosion of Glass by Aqueous Solutions. OEDC-Rep. DAS/SP3/ 71.35, Seite 188-231. Paris (1971).

230. E.L. Yen-Bower, D.E. Clark, L.L. Hench: in (37), page 41.

231. R.A. Zielinski: Nucl. Technol. 51 (1980) 197.

9. List of abbreviations

AERE	Atomic Energy Research Establishment, Harwell (GB)
BNL	Brookhaven National Laboratorium
BNWL	Battelle Northwest Laboratories
CEA	Commisariat à l'Energie Atomique (F)
DP	E.I. DuPont de Nemours & Co. Aiken, South Carolina
HMI	Hahn-Meitner-Institut für Kernforschung, Berlin
IAEA	International Atomic Energy Agency, Wien
KFA	Kernforschungsanlage Jülich
KfK	Kernforschungszentrum Karlsruhe
KFK	Gesellschaft für Kernforschung m.b.H., Karlsruhe
NUREG	US Nuclear Regulatory Comission
OECD	Organisation for Economic Cooperation and Development, Paris
ONWI	Office of Nuclear Waste Isolation, Battelle Memorial Institute, Columbus, Ohio
ORNL	Oak Ridge National Laboratory, Oak Ridge, Tenn.
PNL	Pacific Northwest Laboratories (Battelle), Richland, Washington
SKBF/ KBS	Svensk Kärnbränsleförsörjning AB/ Projekt Kärnbränsle-säkerhet
SRL	Savannah River Laborytory
UCRL	Lawrence Livermore Laboratory, University of California, Livermore, Calif.